Process Monitoring with Multivariate Data: Varying Sample Sizes and Linear Profiles

Keunpyo Kim

Dissertation submitted to the Faculty of the
Virginia Polytechnic Institute and State University
in partial fulfillment of the requirements for the degree of

Doctor of Philosophy
in
Statistics

Marion R. Reynolds, Jr., Co-Chairman
William H. Woodall, Co-Chairman
Eric P. Smith
G. Geoffrey Vining
Christine Anderson-Cook

November 17, 2003
Blacksburg, Virginia

Keywords: Statistical Process Control, Statistical Quality Control, MEWMA, Variable Sampling Rate, Sequential Sampling, Double Sampling, Calibration, EWMA, Average Run Length

Process Monitoring with Multivariate Data: Varying Sample Sizes and Linear Profiles

Keunpyo Kim

(ABSTRACT)

Multivariate control charts are used to monitor a process when more than one quality variable associated with the process is being observed. The multivariate exponentially weighted moving average (MEWMA) control chart is one of the most commonly recommended tools for multivariate process monitoring. The standard practice, when using the MEWMA control chart, is to take samples of fixed size at regular sampling intervals for each variable. In the first part of this dissertation, MEWMA control charts based on sequential sampling schemes with two possible stages are investigated. When sequential sampling with two possible stages is used, observations at a sampling point are taken in two groups, and the number of groups actually taken is a random variable that depends on the data. The basic idea is that sampling starts with a small initial group of observations, and no additional sampling is done at this point if there is no indication of a problem with the process. But if there is some indication of a problem with the process then an additional group of observations is taken at this sampling point. The performance of the sequential sampling (SS) MEWMA control chart is compared to the performance of standard control charts. It is shown that that the SS MEWMA chart is substantially more efficient in detecting changes in the process mean vector than standard control charts that do not use sequential sampling. Also the situation is considered where different variables may have different measurement costs. MEWMA control charts with unequal sample sizes based on differing measurement costs are investigated in order to improve the performance of process monitoring. Sequential sampling plans are applied to MEWMA control charts with unequal sample sizes and compared to the standard MEWMA control charts with a fixed sample size. The steady-state average time to signal (SSATS) is computed using simulation and compared for some selected sets of sample sizes. When different variables have significantly different measurement costs, using

unequal sample sizes can be more cost effective than using the same fixed sample size for each variable.

In the second part of this dissertation, control chart methods are proposed for process monitoring when the quality of a process or product is characterized by a linear function. In the historical analysis of Phase I data, methods including the use of a bivariate T^2 chart to check for stability of the regression coefficients in conjunction with a univariate Shewhart chart to check for stability of the variation about the regression line are recommended. The use of three univariate control charts in Phase II is recommended. These three charts are used to monitor the Y-intercept, the slope, and the variance of the deviations about the regression line, respectively. A simulation study shows that this type of Phase II method can detect sustained shifts in the parameters better than competing methods in terms of average run length (ARL) performance. The monitoring of linear profiles is also related to the control charting of regression-adjusted variables and other methods.

Dedication

To my parents, my wife Hyunsun, and my daughter Yubin

Acknowledgments

I would like to thank all those who have contributed to the completion of my dissertation.

I would like to sincerely thank my co-advisors, Dr. Marion R. Reynolds, Jr. and Dr. William Woodall for sharing their knowledge and directing my research. The years that I have spent with both professors are an invaluable experience for me.

I would also like to thank my committee members, Dr. Eric Smith, Dr. Geoffrey Vining, and Dr. Christine Anderson-Cook for their helpful suggestions and comments on the dissertation.

I would like to thank Dr. Changsoon Park for helping me experience the wonderful educational environment at Virginia Tech.

I would like to thank my parents and parents-in-law for their support and concern. Also my thanks goes to my brother and sisters-in-law for their encouragement and concern.

Finally, my special thanks goes to my wife, Hyunsun, and my daughter, Yubin, for their love and support during the past years in Blacksburg.

Contents

List of Figures

List of Tables

Acronyms and Abbreviations

ANOS	Average Number of Observations to Signal
AGS	Average Group Size
ANGS	Average Number of Groups to Signal
ANSS	Average Number of Samples to Signal
ARL	Average Run Length
ATS	Average Time to Signal
CUSUM	Cumulative Sum
δ	Non-centrality Parameter
DS	Double Sampling
DSVSI	Double Sampling and Variable Sampling Interval
EWMA	Exponentially Weighted Moving Average
FSR	Fixed Sampling Rate
g	Control Limit
h	Control Limit
LCL	Lower Control Limit

MEWMA	Multivariate Exponentially Weighted Moving Average
n	Sample Size
p	Number of Variable
r	Smoothing Parameter
SPC	Statistical Process Control
SPRT	Sequential Probability Ratio Test
SS	Sequential Sampling
SSATS	Steady-State Average Time to Signal
τ	Maximum Total Sample Size Possible at a Sampling Point
UCL	Upper Control Limit
UG	Unequal Group Size
UGSS	Unequal Group Size Sequential Sampling
VSI	Variable Sampling Interval
VSR	Variable Sampling Rate
VSS	Variable Sample Size

Chapter 1

Introduction

1.1 Brief Description of Process Monitoring Problems and Control Charts

Statistical Process Control (SPC) is a set of techniques to monitor, control, and improve a process through statistical analysis. Control charts are SPC methods that are used to monitor processes to detect any change that may affect the quality of the output of the process. In production processes, observed output values of each quality characteristic almost always vary. The observed process variation can be considered to fall into two categories. One is called random (or common) causes, and the other is called assignable (or special) causes. Random causes are typically hard to determine. Random causes produce the variation that is inherent to the process. In contrast to random causes, assignable causes produce larger and significant variation in a quality characteristic and can be removed from the process. Assignable causes result in fundamental changes in the process. These causes alter the underlying distribution of the quality characteristics usually by changing the values of the parameters.

In control charts, relevant statistics, such as the sample mean or the sample variance,

are plotted on a chart versus the sample number or the sampling time. Often variability in some quality characteristic or variable of interest can be modeled by a probability distribution and chart statistics are used to detect changes in the underlying distribution corresponding to changes in the product quality. Because assignable causes of variation may occur in any process, it is desirable to quickly identify and remove any source of variation that lowers the quality of a production process. One can often reduce the variability of the quality characteristic by eliminating assignable causes of the deterioration in quality.

The purpose of control charts is to determine the presence of assignable causes by detecting changes in the parameters of the in-control distribution. Sometimes in practice it is hard to distinguish clearly between random and assignable causes, however, once assignable causes of variation are suspected then this possibility should be investigated carefully and any assignable causes that are found should be eliminated from the process. A process is in-control if the process contains only random causes of variation. A process is out-of-control if assignable causes are present, ideally indicated by non-random patterns on the chart.

If a computed statistic falls within the control limits, then one assumes that the variability of the plotted statistics is due to only random causes and concludes that the process is in-control. Control limits are usually chosen to give a specified false alarm rate, where a false alarm is a signal indicating the process is in out-of-control when the process actually is in-control. For example, Shewhart control charts, which will be defined in Section 2.3, frequently use 3-sigma limits for all statistics, in which case the false alarm rate does not vary from one type of statistic to another. Although quick detection of a process change is important, a method should not give a high rate of false alarms since this can cause a huge loss in cost and time. An effective control chart should signal quickly for changes in the process, but should signal rarely when the process is in-control.

The situation where the process is in-control can also be viewed as that the distribution of the quality characteristic of interest is stable over time. In this case, one should not intervene in the process and can continue sampling. If a computed statistic falls outside the

control limits, then a signal is given. One concludes that assignable causes are present in the process. One needs to take immediate action to remove these causes from the process. For this situation the form of the distribution of the observations changes over time, typically because the parameters of the underlying distribution change. The actual role of the control chart is not in just determining whether the process is in-control or out-of-control. Once a signal is given, more effort should be made in identifying possible assignable causes in order to eliminate them. This effort would require not only the information acquired from the control chart, but also basic understanding of the process.

A control chart is based on consecutive samples of $n \geq 1$ observations taken from a production process over time, usually at regular, equally spaced time intervals. One plots the values of chart statistics of interest. As an alternative approach to the standard control chart with fixed sampling rate (FSR), the variable sampling rate (VSR) control chart has been proposed to increase the sampling rate when a process change is suspected. The advantage of a VSR control chart compared to the FSR control chart is that when there is a change in a production process, the control chart has more power to detect the change and can give a signal more quickly. Two types of such control charts have been widely used. One is a variable sample size (VSS) control chart, where the sample size varies as a function of process data. With VSS plans, as usually defined, the sample size used at the current sampling point depends on past data, but not on any data obtained at the current sampling point. The other is a variable sampling interval (VSI) control chart, where the sampling interval between samples varies as a function of process data and is decreased under some conditions to give a quicker detection rate when a process is out-of-control. A VSSVSI control chart in which the VSS and VSI features are combined allows both the sample size and the sampling interval to vary. A number of papers have been published on VSR schemes based on several approaches to varying the sampling rate. Tagaras (1998) gave a general survey of different types of VSR charts and provided additional references.

In applying control charts, it is usually assumed that the observations sampled at different times are independent. In-control values of the parameters of the process distribution

and control limits are also necessary in the construction of the chart. The in-control values are often estimated using historical data.

The three types of control charts commonly employed in industry are Shewhart control charts (with and without runs rules), cumulative sum (CUSUM) control charts, and exponentially weighted moving average (EWMA) control charts. These control charts have been extended to multivariate control charts to monitor several quality characteristics simultaneously. In Chapter 2, these control charts are reviewed and compared in both the univariate and multivariate cases.

1.2 Multivariate Monitoring with Varying Sample Sizes

In many applications it is assumed that the quality of the process can be characterized by a single continuous random variable. In these applications it is usually assumed that this variable has a normal distribution, and the effect of the assignable cause is to change the mean and/or variance of this distribution. However, it is becoming increasingly common for the quality of processes to be characterized by more than one variable. Recent developments in modern industry, such as fast acquisition of data, online process monitoring, and advanced computing systems, have accelerated the need to monitor more than one quality characteristic. As a process gets more complicated, there is an increasing need to monitor several, usually correlated, quality characteristics simultaneously in manufacturing processes. For this reason, multivariate SPC approaches have received more attention recently by technicians and researchers in the field of quality control.

If p continuous random variables are used to characterize a process, then it is usually assumed in the design of multivariate control charts that the joint distribution of the vector of p variables is multivariate normal, and the effect of a special cause is to change the parameters of this multivariate distribution. If $n > 1$ observations are obtained on p variables, then this gives a sample consisting of n observation vectors, each of dimension p. It is usually assumed

that the n vectors of observations are independent, but there can be correlation between the p variables within a vector. For example, if the physical dimensions of items produced by a process are important quality characteristics, then p dimensions may be measured on each item in a sample of n items from the process. The items may be independent, but there may be correlation between the different dimensions of the same item.

Most work on multivariate control charts has considered the problem of monitoring the multivariate mean vector as an extended form of the univariate control charts. Among them, the multivariate exponentially weighted moving average (MEWMA) control chart proposed by Lowry, Woodall, Champ, and Rigdon (1992) has been favored by many technicians due to its ease of use and its ability to detect small sustained shifts in a process mean vector of the multivariate quality characteristics of interest.

In many applications of a manufacturing process, the costs associated with measurement or testing are substantial, and any reduction in these costs that can be achieved will be very beneficial. A reduction in these costs can be achieved by simply reducing the rate of sampling from the process by, for example, reducing the value of n. However, reducing the sampling rate will reduce the ability to detect changes in the process unless more efficient sampling methods are used.

This dissertation investigates a more efficient method of sampling that does not always require a fixed number of observation vectors at each sampling point, in particular, sequential sampling (SS) MEWMA control charts with two possible stages, where the total sample size taken at a sampling point depends on current and past sample data. For example, if the current practice is to take samples of $n = 5$ observation vectors at each sampling point, then a sequential sampling plan might specify that an initial group of two observation vectors be obtained. If this initial group of two does not show any indication of a problem with the process, then no more sampling would be done at this sampling point. But if the group of two does show some indication of a problem at the first stage, then an additional group of, say, 8 observations might be taken at the second stage. If the indication of a process problem

is strong enough after any group, then a signal could be given. The basic idea here is to take a small initial group of observation vectors at each sampling point and then to take additional group of observation vectors at a sampling point only in cases in which there is some indication of a problem with the process. With sequential sampling with two possible stages, the actual final sample size used at a sampling point is a random variable depending on the process data.

The motivation for using sequential sampling could be to reduce the expected sample size below the value of $n = 5$. For example, the expected sample size may be only 3.8. If the reduction in expected sample size is to be justified then it must be shown that there is no compromise in the ability to detect process changes. Although the motivation given above for sequential sampling is that the increased efficiency allows a reduction in the expected sample size while maintaining the ability to detect process shifts, there is another approach to expressing the increased efficiency of sequential sampling. If the increased efficiency of sequential sampling allows the same detection ability to be maintained with a smaller expected sample size, then it follows that maintaining the same expected sample size should result in an increased ability to detect process shifts. It will be convenient to investigate the efficiency of sequential sampling using this second approach. In particular, in comparing various sampling strategies the expected sample size of each is set to be a constant, and then compare the ability of different sampling plans to detect process shifts. A general discussion of these two approaches to using the increased efficiency of VSR control charts can be found in Baxley (1995) and Reynolds (1996a, 1996b).

In most applications of the standard MEWMA control charts, an equal sample size of n is assumed to be observed for each quality characteristic. However, in many cases there will be differences between the p variables in terms of the cost of measuring or testing the variable, or in terms of the importance of the variable. For example, if p dimensions are being measured on an item, then some dimensions may be more difficult and costly to measure, and some dimensions may be more critical in terms of the overall quality of the product. In this type of situation it may make sense to change the restriction that requires that each

variable always be measured on n items. The idea here is that, for a given sampling cost, it may be reasonable to measure expensive variables less frequently and measure critical variables more frequently.

This dissertation investigates MEWMA control charts with unequal sample sizes, which is denoted by unequal group size MEWMA (UG MEWMA) control charts to improve the performance of process monitoring. No previous research has been done to determine the performance of MEWMA control charts that are based on unequal sample sizes. Under this approach, variables with high measurement costs or those considered as less important are sampled less frequently, and variables with lower costs or those considered as more important are sampled more frequently. The sample sizes can be chosen to give good detection capabilities that can be optimized subject to a constraint on the total sampling cost. Also, SS MEWMA control charts with unequal group sizes, denoted by unequal group size sequential sampling MEWMA (UGSS MEWMA) control charts, are investigated. The basic idea is that if a variable is expensive to measure then it may be initially measured only a few times, with additional observations obtained on this variable only if there is an indication from the data that additional observations are necessary. If a variable is inexpensive to measure, then it would be reasonable to initially measure it a relatively large number of times. The number of times that a variable is initially measured could also depend on the importance of the variable.

The goal of the first part of this dissertation is to develop three proposed control charts for monitoring the process mean. The first control chart is the SS MEWMA control chart with equal group sizes developed in Chapter 3. The second is the UG MEWMA control chart developed in Chapter 4. Finally the third is the UGSS MEWMA control chart developed in Chapter 5. Decision rules for each proposed control chart will be developed and the choice of the smoothing parameter will be investigated for the SS MEWMA control chart and the UGSS MEWMA control chart. Different schemes will be compared by setting the average sampling costs to be equal for each scheme (neglecting administrative costs). Also the ability of each proposed control chart to detect various types of process changes will

be compared to two basic standard control charts, the Shewhart chart based on Hotelling's statistic and the standard MEWMA control chart. Recommendations about choosing group sizes will be given. The primary objective of these proposed applications is to improve the performance of the standard MEWMA control chart which is commonly used in practice.

1.3 Monitoring Linear Profiles

In statistical process control, most control charts are for monitoring single or multiple quality characteristics. However, in many practical situations, the quality of a process or product is characterized by a relationship (or profile) between two variables. In a profile problem, the relationship between two variables could be expressed by a linear or nonlinear function. The approach to a profile problem using control charts is different from that of standard statistical control charts, since we monitor the form of a functional relationship at each sampling point through a range of input variables instead of a sample statistic based on single or multiple quality characteristics. As a result, a different approach is required to check whether a process is in-control or out-of-control, as well as setting up the control limits for the sample profiles.

In this dissertation, a linear profile problem is considered, where a process is characterized by a linear relationship between two variables. Such linear functions occur frequently in practical situations, such as in calibration problems. Statistical process control charts are proposed for monitoring in Phase II a process or product that is characterized by a linear profile. The term Phase II is defined in Section 2.2. Kang and Albin (2000) proposed two control chart strategies to monitor such a process. One approach involves a multivariate T^2 chart. The other uses statistics based on the successive samples of deviations from the in-control line in a combination of an EWMA chart to monitor the average deviation and a range (R-) chart to monitor the variation of the deviations from the line. Both approaches are described in Section 6.1. In the proposed method, the independent variable is coded so

that the average value is zero and the estimated regression coefficients from each sample, i.e., the estimates of the Y-intercept and slope, are used to construct two univariate EWMA charts. Also, we study two different one-sided EWMA charts for monitoring a process standard deviation as replacements for their R-chart. One of these charts was developed by Crowder and Hamilton (1992). In practice a two-sided chart might be more appropriate in many applications to detect decreases in variability about the regression line as well as increases.

The statistical performance of the combined use of the three EWMA charts is compared to that of the methods of Kang and Albin (2000) in Section 6.4. Simulation was used to show that the proposed method has better overall performance than the competing methods. In Section 6.5, recommendations are made for the Phase I analysis. The objective of this proposed application is to develop a method for monitoring a linear profile and improve the method proposed by Kang and Albin (2000).

Chapter 2

Review of Control Charts and Performance Measures

2.1 Notation

First consider the case in which only one sample is taken at each sampling point, where all variables have equal sample sizes of n. Three proposed sampling procedures will be considered in detail later in Chapters 3-5, respectively. Let X_{kij} be the j^{th} observation for variable i at sampling point k, where $k = 1, 2, \cdots$, $i = 1, 2, \cdots, p$, and $j = 1, 2, \cdots, n$. It is assumed that $X_{ki1}, X_{ki2}, \cdots, X_{kin}$ are independent for $i = 1, 2, \cdots, p$, and X_{kij}'s are normally distributed with mean μ_i and variance σ_i^2. Let $\sigma_{ii'}$ be the covariance between variable i and i'. Define $\boldsymbol{\mu}_k = \boldsymbol{\mu}$, for $k = 1, 2, \cdots$, to be a $p \times 1$ mean vector, where μ_i is the i^{th} component of $\boldsymbol{\mu}$, and $\boldsymbol{\Sigma}$ to be a $p \times p$ covariance matrix, where σ_i^2 and $\sigma_{ii'}$ are the i^{th} diagonal component and the (i, i') component, for $i \neq i'$, of $\boldsymbol{\Sigma}$, respectively.

Let $\bar{\boldsymbol{X}}_k$ represent a $p \times 1$ sample mean vector observed at sampling point k. It is assumed that $\bar{\boldsymbol{X}}_k, k = 1, 2, \cdots$, are independent multivariate normal random vectors with the mean vector $\boldsymbol{\mu}$ and with the covariance matrix $\boldsymbol{\Sigma}/n$. Let $\boldsymbol{\mu}_0$ and $\boldsymbol{\Sigma}_0$ represent the in-

control values for $\boldsymbol{\mu}$ and $\boldsymbol{\Sigma}$, respectively. Also let μ_{0i} and σ_{0i} be the i^{th} component of $\boldsymbol{\mu}_0$ and the square root of the i^{th} diagonal component of $\boldsymbol{\Sigma}_0$, respectively, and let $\sigma_{0ii'}$ be the (i, i') component of $\boldsymbol{\Sigma}_0$ for $i \neq i'$. A sequence of sample mean vectors $\bar{\boldsymbol{X}}_k$ are given by

$$\bar{\boldsymbol{X}}_k = (\bar{X}_{k1}, \bar{X}_{k2}, \cdots, \bar{X}_{kp})^T, \quad k = 1, 2, \cdots, \tag{2.1}$$

where $\bar{X}_{ki} = \sum_{j=1}^{n} X_{kij}/n$, i.e., the average of the n observations for variable i obtained at sampling point k. Define the standardized sample mean to be

$$Z_{ki} = \frac{\sqrt{n}(\bar{X}_{ki} - \mu_{0i})}{\sigma_{0i}}, \quad i = 1, 2, \cdots, p,$$

and define a sequence of standardized sample mean vectors to be

$$\boldsymbol{Z}_k = (Z_{k1}, Z_{k2}, \cdots, Z_{kp})^T, \quad k = 1, 2, \cdots. \tag{2.2}$$

The univariate case (when $p = 1$) is a special case for notation given above.

2.2 Performance Measures

Control chart use can be divided into two stages. In Phase I, a set of historical data is checked for whether the process was in-control during the time period in which the samples were taken. Parameters are estimated in Phase I and then used to construct the control limits for future monitoring in Phase II. For example, for the $\bar{X}$-chart traditionally one needs at least 20-25 samples of size of 4 or 5 for Phase I, but more data is needed if the chart should have properties similar to the case in which μ_{01} and σ_{01} are known. In some applications, the in-control value could be specified either by design engineers or the consumer or by using the past experience with the product. In Phase II, control charts are used for the process monitoring based on the result from Phase I. Most comparisons of control charts are based on Phase II performance. Throughout the rest of this dissertation, Phase II performance is emphasized with the assumption that the in-control parameter values are known.

The objective of control charts is to detect a process change in the parameter of the distribution quickly to decrease the time that the process stays out-of-control. Two types of a process change can be defined. One is called a shift where the special cause occurs and changes the parameter of the distribution to a fixed sustained value. The other type is called a drift where the parameter of the distribution can be expressed as a function of time and changes slowly over time. A drift reflects a gradual deterioration in process quality.

Two metrics are commonly used to measure the performance of control charts. One is the average run length (ARL) and the other is the average time to signal (ATS). Both terms are measures of the effectiveness of a control chart in detecting a sustained shift in a process parameter. The ARL is the expected value of the run length, the random number of samples required for a procedure to signal. The average number of samples to signal (ANSS), which is defined to be the expected value of the number of samples to signal, has the same meaning as the ARL. Let the time to signal be the time interval between the starting time of the chart and the first time a signal is given. Then the ATS is defined as the expected length of time from the start of process monitoring until a signal is generated. The ATS for a particular process parameter shift provides a measure of the time required to detect this shift when it is present at the time that monitoring starts. If a sampling interval of fixed length d is used, then the ATS and the ARL have the relationship of ATS=dARL. Both the ARL and the ATS should be large when the process is in-control and small when the process is out-of-control.

The ATS defined above is computed by assuming that the parameter of the underlying distribution of the chart statistic is at some constant out-of-control value when the control chart starts at time zero and remains at this same value until a signal is given. However, a shift may occur at some random time in the future, after process monitoring has started. In this case, the appropriate measure of detection time is the expected length of time from the random point in time that the shift occurs until the time that the control chart signals.

For EWMA and CUSUM charts that accumulate information over time, the expected

length of time from the shift to the signal will depend on the value of the control statistic at the time that the shift occurs. When the shift occurs a relatively long time after monitoring has started, the effect of the value of the control statistic at the time of the shift can be modeled by using the steady-state ATS (SSATS). The steady state distribution of the chart statistic can be defined as the distribution of the chart statistic over its region of possible values during the period with no signals. The SSATS is computed assuming that the control statistic has reached its steady-state or stationary distribution by the random time point that the shift occurs. The SSATS also allows for the possibility that the shift can occur in a time interval between samples. In particular, it is assumed that when a process shift occurs within a particular interval d, the position of the process change within this interval is uniformly distributed over the interval. This means that the expected position of the shift within the interval between samples is the midpoint of the interval. Additional discussion of the SSATS in this context can be found in Reynolds and Stoumbos (2001,2003).

In addition to providing a measure of detection time, when the process is in-control the ATS also provides a measure of the average false alarm rate per unit time. In particular, for control charts that can be modeled as a renewal process, the in-control value of 1/ATS, which is the ratio of the expected number of alarm per renewal to the expected length of an interval, is the long run average false alarm rate per unit time.

A sampling pattern that involves n observations taken during every interval of d time units corresponds to a sampling rate of n/d observations per unit time. When sequential sampling is used the number of observations taken at each sampling point is a random variable, so we must look at the expected number of observations. It may be difficult to directly calculate the expected number of observations at a sampling point, but it is usually easier to evaluate this expectation using the expected total number of observations before a signal. Define the average number of observations to signal (ANOS) to be the total expected number of observations taken from the start of process monitoring until a signal is generated. The ratio ANOS/ATS is a measure of the average sampling rate per unit time. These ratios measuring the sampling rate will usually be of most interest in the case in which the process

is in control, because usually it will be reasonable that the process is in control most of the time.

False alarms adversely affect a user's confidence in a control chart, so the rate of false alarms must also be considered when evaluating a control chart. Fair comparisons of different control charts and sampling patterns can be done when the charts all have the same in-control ATS and ANOS. Requiring different control charts to have the same in-control ATS and ANOS then implies that they have the same in-control average sampling rates and false alarm rates.

2.3 Shewhart Control Charts

2.3.1 Univariate Shewhart Control Charts

The principles of control charts were originally developed by Shewhart (1931). Shewhart (1931) proposed the $\bar{X}$-chart, one of the most widely used and simplest control charts, to detect assignable causes that produce a shift in the mean of the observed samples. Various control charts of this type have been created to monitor parameters other than just the mean of a production process. The R-chart and s-chart were proposed to monitor the variation of a process; the p-chart and np-chart were created to monitor the proportion of non-conforming items; and the c-chart and u-chart were proposed for monitoring the average number of defects. In addition to these control charts, other control charts with the same structure also have been proposed to monitor the parameter (or parameters) of the process distribution. In general, these control charts are referred to as Shewhart control charts. The distinguishing feature of Shewhart control charts is that the statistic plotted at each point depends only on the current sample and not on previous data. Two widely used control charts that use previous data are CUSUM and EWMA control charts. These control charts are discussed in Sections 2.4 and 2.5.

Assume X follows a certain distribution with parameter θ, where θ could be a vector. Suppose θ_0 is the known in-control value of arbitrary parameter θ. Let $g_k = g_k(X_{k11}, X_{k12}, \cdots, X_{k1n})$ be a chart statistic of interest based on the k^{th} random sample collected over time. For example, if the Shewhart $\bar{X}$-chart is applied to monitor a process mean, then a sample mean $\bar{X}_{k1}$ is used as a chart statistic and $g_k = \bar{X}_{k1}$. A Shewhart control chart is used to detect assignable causes that change θ and one makes decisions based on the value of g_k. In order to monitor a parameter θ, the Shewhart chart signals whenever g_k falls the outside of the continuation region,

$$C = (\tau(\theta_0) - \xi\sqrt{\mathrm{VAR}(g_k)}, \tau(\theta_0) + \xi\sqrt{\mathrm{VAR}(g_k)}),$$

where $\tau(\theta_0)$ is defined as $E(g_k \mid \theta_0)$. The control limits are at ξ standard deviations from $\tau(\theta_0)$. The continuation regions have boundaries known as the upper control limit (UCL) and the lower control limit (LCL). In many applications, the value 3 is used for ξ resulting in 3-sigma limits since the control limits are set at ± 3 standard errors from the in-control value. Instead of using control limits given above, probability limits can be also used to give a specified false alarm rate when the process is in-control. If g_k has a known distribution and α is chosen as the specified false alarm rate, then the continuation region C is usually chosen to satisfy

$$\Pr(g_k < \mathrm{LCL} \mid \theta = \theta_0) = \Pr(g_k > \mathrm{UCL} \mid \theta = \theta_0) = \frac{\alpha}{2}.$$

If g_k falls within the continuation region, then one can observe the next sample and obtain the next chart statistic g_{k+1}.

If the form of the underlying distribution of the chart statistic is known along with values of the in-control parameters, then the two-sided Shewhart control chart can be viewed as a sequence of independent hypothesis tests of the form $H_0 : \theta = \theta_0$ vs. $H_1 : \theta \neq \theta_0$ (see Woodall (2000), for details). If H_0 is rejected, then there is evidence that the process is out-of-control. Otherwise, it can be interpreted that there is no evidence to think that special causes were present. Let the probability of rejecting the null hypothesis, which is equivalent

to a signal at time k, be defined by

$$p(\theta) = \Pr(g_k \notin C \mid \theta).$$

Then the distribution of the number of samples to signal follows a geometric distribution with parameter $p(\theta)$, and the ARL is $1/p(\theta)$.

Shewhart control charts have been the most commonly used control charts in industry because they are easy to construct and simple to interpret. There are many papers on Shewhart control charts and these charts are discussed in standard texts (see, for example, Ryan (2000) or Montgomery (2001)). However, since the Shewhart control charts use only the information contained in the current sample without considering the past sequence of samples, these charts show relatively poor performance in detecting small sustained shifts in the parameter of interest. Various types of modified Shewhart charts have been proposed to improve the performance of the standard Shewhart charts by adding past sample information. The basic idea of one of these modifications is to add supplementary rules, which are usually called runs rules, to the standard Shewhart charts in order to detect other unusual patterns on the chart. Among many runs rules that have been suggested to be used, commonly applied runs rules are for a signal to be given if (1) a specified number of the chart statistics out of a specified number of consecutive values falls in a subset region of C or (2) a number of consecutive chart statistics are either all steadily increasing or decreasing. Champ and Woodall (1987) developed a Markov chain model to evaluate the run length distribution for the use of several runs rules simultaneously. Shewhart charts with runs rules show better performance in detecting sustained small-to-moderate shifts than the standard Shewhart charts, however, adding runs rules also has the disadvantage of inflating the false alarm rate (see Woodall (2000), for details).

VSI Shewhart control charts were introduced by Reynolds, Amin, Arnold, and Nachlas (1988) and Runger and Pignatiello (1991). More references on VSI Shewhart control charts include Reynolds (1996a, 1996b). Costa (1994) proposed VSS Shewhart control charts and showed that the performance of VSS Shewhart charts are better than FSR Shewhart

charts. References on VSS Shewhart control charts include Prabhu, Runger, and Keats (1993), Park and Reynolds (1999), and Zimmer, Montgomery, and Runger (1998). Prabhu, Montgomery, and Runger (1994) and Costa (1997) also investigated VSSVSI Shewhart control charts, which combine VSS and VSI Shewhart control charts.

2.3.2 Multivariate Shewhart Control Charts

The most widely known multivariate control chart is a type of Shewhart chart proposed by Hotelling (1947). The multivariate Shewhart type control chart is a multivariate extension of the univariate Shewhart control chart. Hotelling's multivariate control chart, using Hotelling's T^2 statistic, was originally developed to monitor the mean vector of a continuous multivariate process variable consisting of p quality characteristics. With Hotelling's T^2 statistic, one assumes that the covariance matrix of the correlated p quality characteristics is unknown. However, if the covariance matrix is assumed to be known, then this control chart is equivalent to a multivariate control chart using a χ^2 statistic.

Suppose that p quality characteristics are monitored and a sequence of $p \times 1$ random vectors $\bar{\boldsymbol{X}}_1, \bar{\boldsymbol{X}}_2, \cdots$, which are defined in Equation (2.1), are observed over time. For $p > 1$ and $n(\geq 1)$ for all i, these vectors may represent individual observations with $n = 1$ or sample mean vectors with the sample size $n(> 1)$ for each quality characteristic. If the in-control process mean vector $\boldsymbol{\mu}_0$ and covariance matrix $\boldsymbol{\Sigma}_0$ are assumed to be known, then the multivariate Shewhart control chart signals at sampling point k as soon as

$$\chi_k^2 = n(\bar{\boldsymbol{X}}_k - \boldsymbol{\mu}_0)^T \boldsymbol{\Sigma}_0^{-1} (\bar{\boldsymbol{X}}_k - \boldsymbol{\mu}_0) > h_{\mathrm{MS}}, \quad k = 1, 2, \cdots, \tag{2.3}$$

where a control limit, $h_{\mathrm{MS}}(> 0)$, is chosen to give a specified ARL value. When the process is in-control, the χ_k^2 statistics follow a central chi-square distribution with p degrees of freedom and the upper control limit h_{MS} can be obtained as $h_{\mathrm{MS}} = \chi_{p,\alpha}^2$, where $\chi_{p,\alpha}^2$ is the $100(1-\alpha)$ percentile of the chi-square distribution with p degrees of freedom.

As in the univariate Shewhart control chart, the multivariate Shewhart control chart

only uses the information obtained from the most recent sample to determine whether to give a signal. This causes the multivariate Shewhart control chart to be insensitive to small and moderate-sized sustained shifts in the mean vector. There are few publications dealing with multivariate VSR control charts. Aparisi (1996) considered VSS control charts, and Aparisi and Haro (2001) considered VSI control charts. Both of these papers are concerned with multivariate Shewhart charts based on Hotelling's statistic.

2.4 CUSUM Control Charts

2.4.1 Univariate CUSUM Control Charts

As an alternative approach to the Shewhart control chart, the CUSUM control chart was originally proposed by Page (1954). In contrast to the Shewhart chart, the idea of the CUSUM chart is to use past information in the sequence of chart statistics in order to detect small shifts more efficiently. The past information included in CUSUM control chart has the form of a moving sum where a random number of samples is used to calculate the moving sum. The moving sum used in the CUSUM control chart includes only the recent sequence of samples that show a change in the mean of the observed samples.

For controlling a parameter θ in the process, it is assumed that θ_0 is the known in-control value and θ_1 is the desired value to be detected. Then the one-sided cumulative sum statistic designed to detect a shift to θ_1 can be defined as

$$Z_k = max\{0, Z_{k-1}\} + z_k, \quad k = 1, 2, \cdots, \tag{2.4}$$

where $z_k = ln\frac{f(\bar{X}_{k1}|\theta_1)}{f(\bar{X}_{k1}|\theta_0)}$ is the log likelihood ratio function of the sample mean $\bar{X}_{k1}$. The initial value Z_0 is usually set to be zero and for $k \geq 1$ the chart signals at sample k if

$$Z_k \geq h_{\mathrm{C}}, \tag{2.5}$$

where $h_C(\geq 0)$ is a constant called the decision interval and is chosen to give a specified in-control ARL. The CUSUM chart ignores any sequence of past sample information that indicates the process is in-control by resetting the CUSUM statistic to 0 and uses only the recent sample indicating a possible change in the parameter.

The one-sided CUSUM chart for detecting the shift from θ_0 to θ_1 can be considered to be equivalent to a sequence of independent sequential probability ratio tests (SPRT), which was proposed by Wald (1947). In the SPRT, each test has the form of $H_0 : \theta = \theta_0$ vs. $H_1 : \theta = \theta_1$ and has a lower boundary of 0 and an upper boundary of h_C. If a test statistic crosses the lower boundary (i.e., fail to reject H_0) then a new test is started with the same boundaries and if the upper boundary is crossed (i.e., reject H_0) then the procedure signals.

As a simple application of CUSUM control charts, consider the problem of monitoring the process mean in the positive direction. As assumed in Section 2.1, the quality characteristic X follows the normal distribution with mean μ and variance σ_{01}^2. Let μ_{01} be the known in-control value and μ_{11} be the desired value to be detected. In this special case the CUSUM chart determined by Z_k is equivalent to a CUSUM chart that plots the statistic

$$S_k = max\{0, S_{k-1}\} + s_k, \quad k = 1, 2, \cdots, \tag{2.6}$$

where $s_k = \bar{X}_{k1} - \mu_{01} - \Delta/2$ and $\Delta = (\mu_{11} - \mu_{01})$ represents the change in the mean considered to be detected quickly. The value $\Delta/2$ can be used as a tuning parameter of the chart to make the CUSUM control chart sensitive to small or large shifts because the choice of $\Delta/2$ can affect the size of the shifts that can be detected. For example, small values of $\Delta/2$ are effective for detecting small shifts, and larger values of $\Delta/2$ are effective for detecting large shifts. The relationship between Z_k in Equation (2.4) and S_k in Equation (2.6) is

$$Z_k = \frac{n(\mu_{11} - \mu_{01})}{\sigma_{01}^2} S_k.$$

The CUSUM chart signals as soon as

$$S_k \geq \frac{\sigma_{01}^2}{n(\mu_{11} - \mu_{01})} h_C,$$

where h_C is the decision interval given in Equation (2.5). S_k is usually plotted instead of Z_k when the CUSUM chart is used in applications.

For the two-sided CUSUM chart designed to monitor the mean, one needs to use two one-sided cumulative sum statistics: one to detect a shift in the positive direction and another to detect a shift in the negative direction. The one-sided cumulative sum statistics designed to detect a negative shift can be defined as

$$T_k = min\{0, T_{k-1}\} + t_k, \quad k = 1, 2, \cdots, \tag{2.7}$$

where $t_k = \bar{X}_{k1} - \mu_{01} + \Delta/2$. By combining two cumulative sum statistics defined in Equations (2.6) and (2.7), the two-sided CUSUM chart signals as soon as

$$S_k \geq \frac{\sigma_{01}^2}{n(\mu_{11} - \mu_{01})} h_C \quad \text{or} \quad T_k \leq -\frac{\sigma_{01}^2}{n(\mu_{11} - \mu_{01})} h_C,$$

where again h_C is the decision interval given in Equation (2.5).

In contrast to the Shewhart control chart, the run length distribution of the CUSUM chart is more difficult to determine exactly. van Dobben de Bruyn (1968) considered integral equations to evaluate the run length distribution of CUSUM control charts. Brook and Evans (1972) proposed a Markov chain method to obtain the run length distribution for a discrete one-sided CUSUM chart. Woodall (1984) extended the Markov chain method for a one-sided chart to a two-sided CUSUM chart. Hawkins (1992) improved the accuracy of the Markov chain method by proposing an algorithm that accelerates convergence. Reynolds (1995) proposed a unified Markov chain-integral equation method, which adds the accuracy of the integral equation to the Markov chain method. Hawkins and Olwell (1998) gave up-to-date references for CUSUM control charts.

VSI CUSUM control charts for monitoring the mean shift in the process were proposed by Reynolds, Amin, and Arnold (1990), where they showed that VSI CUSUM charts perform better than CUSUM charts with a fixed sampling rate in detecting sustained mean changes in a process. More references on VSI CUSUM charts include Reynolds (1995, 1996b). Annadi,

Keats, Runger, and Montgomery (1995) proposed VSS CUSUM control charts and VSSVSI CUSUM control charts were proposed by Arnold and Reynolds (2001).

2.4.2 Multivariate CUSUM Control Charts

As in the univariate CUSUM control chart, the multivariate versions of the CUSUM control chart were developed as an alternative to the multivariate Shewhart control chart to improve the detection efficiency in small to moderate sustained shifts by using past sample information. Woodall and Ncube (1985) proposed the multivariate CUSUM procedures by extending the individual CUSUM control chart. Healy (1987) showed that a univariate CUSUM control statistic formed as a linear combination of the variables is the appropriate CUSUM control chart for detecting a shift in the mean vector in a specific direction in the multivariate case. Crosier (1988) and Pignatiello and Runger (1990) developed multivariate CUSUM control charts, which form a univariate statistic from the multivariate data, with the ability to detect small to moderate shifts in the mean vector more quickly than Hotelling's T^2 chart.

Suppose that $\bar{\boldsymbol{X}}_1, \bar{\boldsymbol{X}}_2, \cdots$ are a sequence of sample mean vectors defined in Equation (2.1). Each random vector represents p quality characteristics of interest being monitored with $n(\geq 1)$ for all i. The multivariate CUSUM control chart proposed by Crosier (1988), denoted by MCUSUM, is based on the following statistics

$$C_k = \{n(\boldsymbol{S}_{k-1} + \bar{\boldsymbol{X}}_k)^T \boldsymbol{\Sigma}^{-1} (\boldsymbol{S}_{k-1} + \bar{\boldsymbol{X}}_k)\}^{\frac{1}{2}}$$

and

$$\boldsymbol{S}_k = \begin{cases} \boldsymbol{0} & \text{if } C_k \leq k_1, \\ (\boldsymbol{S}_{k-1} + \bar{\boldsymbol{X}}_k)(1 - \frac{k_1}{C_k}) & \text{if } C_k > k_1, \end{cases}$$

$k = 1, 2, \cdots$, where $\boldsymbol{S}_0 = \boldsymbol{0}$ and $k_1 > 0$. MCUSUM signals as soon as

$$Y_k = \{n \boldsymbol{S}_k^T \boldsymbol{\Sigma}^{-1} \boldsymbol{S}_k\}^{\frac{1}{2}} > h_{\mathrm{MC1}},$$

where $h_{\mathrm{MC1}} > 0$ is chosen to give a specified in-control ARL.

Pignatiello and Runger (1990) also proposed the multivariate CUSUM control chart, denoted by MC, based on the following statistics

$$\boldsymbol{D}_k = \sum_{j=k-l_k+1}^{k} \bar{\boldsymbol{X}}_j$$

and

$$\mathrm{MC}_k = \max\{0, (n\boldsymbol{D}_k^T \boldsymbol{\Sigma}^{-1} \boldsymbol{D}_k)^{\frac{1}{2}} - k_2 l_k\},$$

where $k_2 > 0$ and

$$l_k = \begin{cases} l_{k-1} + 1 & \text{if } \mathrm{MC}_{k-1} > 0, \\ 1 & \text{otherwise,} \end{cases}$$

$k = 1, 2, \cdots$. MC signals when $\mathrm{MC}_k > h_{\mathrm{MC2}}$, where $h_{\mathrm{MC2}} > 0$ is chosen to give a specified in-control ARL..

2.5 EWMA Control Charts

2.5.1 Univariate EWMA Control Charts

Roberts (1959) first investigated the properties of EWMA control charts. This control chart is sometimes referred to as the geometric moving average control chart. The EWMA control chart, like the CUSUM control chart, uses the past information in the sequence of chart statistics. The EWMA control chart, however, differs from the CUSUM control chart, which gives equal weight to a randomly varying number of values in calculating a moving sum, since the EWMA control chart uses a weighted average of observations where more recent observed samples have higher weight and the weight decreases in exponential progression as samples are more distant from the most recent sample. As noted by Lucas and Saccucci

(1990), the EWMA and CUSUM control charts have approximately equal performance, but the EWMA chart is easier to understand and interpret.

Suppose θ_0 is the known in-control value of arbitrary parameter θ. Let $g_k = g_k(X_{k11}, X_{k12}, \cdots, X_{k1n})$ be a chart statistic of interest observed at the k^{th} sampling point. The two-sided EWMA statistic for controlling changes in θ can be defined as

$$Y_k = rg_k + (1-r)Y_{k-1}, \quad k = 1, 2, \cdots, \tag{2.8}$$

where $r(0 < r \leq 1)$ is a smoothing parameter. The starting value Y_0 is chosen at $\tau(\theta_0)$, where $\tau(\theta)$ is defined as $E(g_k \mid \theta)$. An out-of-control signal is given as soon as Y_k is less than the LCL or Y_k is greater than the UCL, where

$$\begin{aligned} LCL &= \tau(\theta_0) - L\sqrt{\mathrm{Var}(Y_k)} \\ &= \tau(\theta_0) - L\sqrt{\frac{r}{2-r}\{1-(1-r)^{2k}\}\mathrm{Var}(g_k)} \end{aligned}$$

and

$$\begin{aligned} UCL &= \tau(\theta_0) + L\sqrt{\mathrm{Var}(Y_k)} \\ &= \tau(\theta_0) + L\sqrt{\frac{r}{2-r}\{1-(1-r)^{2k}\}\mathrm{Var}(g_k)}. \end{aligned}$$

$L(> 0)$ is a constant that is chosen to give a specified in-control ARL. In most applications, since the term $(1-r)^{2k}$ converges very quickly, one can use the asymptotic variance of Y_k in computing the control limits, i.e.,

$$\mathrm{Var}(Y_k) = \frac{r}{2-r}\mathrm{Var}(g_k).$$

The EWMA control chart is a good alternative to the Shewhart control chart in effectively detecting small shifts. The larger the smoothing parameter r is the more weight is given to the present sample. If the EWMA chart monitors an arbitrary parameter θ of a process with $r = 1$, then the EWMA chart is equivalent to the Shewhart control chart for monitoring θ with the control statistic g_k. Montgomery (2001) recommended the smoothing

parameter r to be chosen in the range of $0.05 \leq r \leq 0.25$ to more effectively detect small sustained shifts in the mean.

Crowder (1987) proposed a system of integral equations to evaluate the ARL of EWMA control charts. Lucas and Saccucci (1990) considered a Markov chain approach to find the run length distribution of the EWMA control chart. Saccucci, Amin, and Lucas (1992) proposed VSI EWMA control charts and showed that VSI EWMA charts can detect mean changes more quickly than the standard EWMA control chart with a fixed sampling rate. Reynolds (1995, 1996a, 1996b) investigated VSI EWMA charts. Reynolds (1996b) showed some limited results for VSS EWMA and CUSUM control charts. VSSVSI EWMA control charts were proposed by Reynolds and Arnold (2001).

2.5.2 Multivariate EWMA Control Charts

The MEWMA control chart developed by Lowry et al. (1992) is an extension of the univariate EWMA control chart to the multivariate case. The MEWMA control chart, which accumulates information from past samples as in the univariate EWMA control chart, was originally developed to more quickly detect small mean shifts than the multivariate Shewhart control chart. In the MEWMA control chart, a sequence of standardized sample mean vectors $\boldsymbol{Z}_1, \boldsymbol{Z}_2, \cdots$ are observed over time as defined in Equation (2.2).

As defined in Equation (2.8), let the EWMA statistic for variable i at sampling point k be

$$Y_{ki} = r_i Z_{ki} + (1 - r_i) Y_{k-1,i}, \quad k = 1, 2, \cdots .$$

Then the EWMA vector $\boldsymbol{Y}_k$ formed from these statistics is

$$\begin{aligned} \boldsymbol{Y}_k &= (Y_{k1}, Y_{k2}, \cdots, Y_{kp})^T \\ &= \boldsymbol{R}\boldsymbol{Z}_k + (\boldsymbol{I} - \boldsymbol{R})\boldsymbol{Y}_{k-1}, \end{aligned}$$

where $\boldsymbol{Y}_0 = \boldsymbol{0}$ and $\boldsymbol{R} = diag(r_1, r_2, \cdots, r_p)$ is a $p \times p$ diagonal matrix consisting of smoothing parameters $r_i (0 < r_i \leq 1), i = 1, 2, \cdots, p$, for each of the i^{th} quality characteristic. The

EWMA vector can be defined using different values of r for each of the p components, but if there is no a priori reason to weight past observations differently, it is assumed that each smoothing parameter r_i in the diagonal matrix $\boldsymbol{R}$ is equal to r (see Lowry et al. (1992), for details). Then the MEWMA vector at each sampling point k can be obtained as

$$\boldsymbol{Y}_k = r\boldsymbol{Z}_k + (1-r)\boldsymbol{Y}_{k-1}. \tag{2.9}$$

The decision rule is based on the statistic

$$T_k^2 = \boldsymbol{Y}_k^T \boldsymbol{\Sigma}_k^{-1} \boldsymbol{Y}_k, \tag{2.10}$$

where $\boldsymbol{\Sigma}_k$ is the covariance matrix of $\boldsymbol{Y}_k$. The MEWMA chart gives an out-of-control signal whenever $T_k^2 > h_{\mathrm{ME}}$, where the UCL, $h_{\mathrm{ME}}(> 0)$, is a constant chosen to give a specified in-control ARL. When it is assumed that equal number of n observations are obtained for each variable at each sampling point, Lowry et al. (1992) derived the exact covariance matrix $\boldsymbol{\Sigma}_k$ as

$$\boldsymbol{\Sigma}_k = \{r[1-(1-r)^{2k}]/(2-r)\}\boldsymbol{\Sigma}_c, \tag{2.11}$$

where $\boldsymbol{\Sigma}_c$ is the correlation matrix corresponding to the known covariance matrix $\boldsymbol{\Sigma}_0$ since standardized sample means are used instead of sample means. With the assumption that the process is more likely to stay in-control for a while before going to out-of-control, the asymptotic covariance matrix can be derived from the exact covariance matrix in Equation (2.11) by letting $k \to \infty$, that is,

$$\boldsymbol{\Sigma}_k = \{r/(2-r)\}\boldsymbol{\Sigma}_c. \tag{2.12}$$

The asymptotic covariance matrix is sometimes used in place of the exact covariance matrix in defining the control statistic. Lowry et al. (1992) pointed out that using the exact covariance matrix leads to a natural fast initial response for the chart. Stoumbos and Sullivan (2002) showed that using the asymptotic covariance matrix is more robust to the non-normal data than using the exact covariance matrix.

Lowry et al. (1992) used simulation to evaluate the properties of the MEWMA chart but other approaches based on Markov chains or integral equations have been developed. Rigdon (1995a, b) and Bodden and Rigdon (1999) proposed an integral equation approach, which is an expansion of the results of Crowder (1987), to calculate the in-control ARL value. Runger and Prabhu (1996) and Molnau, Runger, Montgomery, Skinner, Loredo, and Prabhu (2001) proposed Markov chain approaches to ARL calculation for MEWMA charts.

2.6 Multivariate Monitoring with Varying Sample Sizes

In this dissertation, control charts based on sequential sampling in which the number of observation vectors at a sampling point depends on current and past data are considered. Sequential sampling is a particular type of VSR sampling scheme in which the sampling rate varies as a function of process data.

It may be helpful to clearly point out the difference between VSS control charts, as usually defined, and sequential sampling control charts, because both of these types of control charts allow the sample size to depend on the data from the process. With a VSS control chart it is assumed that the current sample size to be used at a sampling point depends only on the position of the previous chart statistic relative to the threshold control limits, and thus the sample size to be used will be known before sampling starts at that sampling point. A VSS control chart would, therefore, be appropriate for applications in which the sample size must be known in advance, before sampling starts. On the other hand, with sequential sampling, the sample size at a sample point can depend on the data at that sampling point (as well as past sampling points). Sequential sampling would, therefore, be appropriate for applications in which it is feasible to adjust the sample size at a sampling point as data are obtained at that sampling point.

Two general approaches to sequential sampling for control charts have been investigated in the quality control literature. One approach is based on applying a sequential

probability ratio test (SPRT) at each sampling point. The SPRT is applied to test the null hypothesis that the process parameter of interest is at its in-control value against the alternative hypothesis that this parameter is at some specified out-of-control value. SPRT charts have been developed by Stoumbos and Reynolds (1996, 1997, 2001) and Reynolds and Stoumbos (1998). SPRT charts are usually based on the assumption that observations become available individually and thus a decision to stop sampling can be made after each observation. These charts typically have excellent properties in terms of the ability to detect changes in the process. However, it does not appear to be useful to try to develop decision rules for the current multivariate problem using the SPRT chart. The standard SPRT chart is designed to detect a shift in a process parameter to a specific out-of-control value (or, more generally, in a specific direction). In most applications in the multivariate case it will not be possible to say that the mean vector $\boldsymbol{\mu}$ will shift in just one specific direction. Thus, instead of applying an SPRT chart, a scheme, called the SS MEWMA chart, based on an extension of the MEWMA chart is used instead.

The second approach to sequential sampling is the double sampling control chart, which is the counterpart to double sampling plans in acceptance sampling. The double sampling control chart has two possible stages at each sampling point. At the first stage an initial group of observations is obtained, and if this group shows some indication of a problem with the process, which is the case when the current chart statistic falls in predetermined threshold control limits, then an additional group of observations is obtained at the second stage. At the first stage, three possible actions could be taken based on a chart statistic: (1) conclude the process is in-control, (2) conclude the process is out-of-control, or (3) take a second group. At the second stage a decision about the process is made based on the combined information in the two groups of observations, where a chart statistic is calculated based on combined groups collected both at the first and second stages. Two possible actions can be taken at the second stage: (1) conclude the process is in-control or (2) conclude the process is out-of-control. It is possible that sampling plans can be extended to multiple (more than two) stages of sampling. The sample sizes of the double sampling control chart

are based on either the current chart statistic or both the current and the previous chart statistics, depending on the type of control chart. For example, the sample sizes of double sampling Shewhart type control charts only depend on the current sample results. The advantage of the double sampling control chart over the VSS chart is that two consecutive samples, which can be represented by the same probability distribution, can be taken without any intervening time. Thus, the decision can be made more quickly than when using the VSS control chart.

It has been shown that univariate double sampling control charts have better performance than the standard univariate control chart in detecting a shift in a process. The double sampling $\bar{X}$ control chart was first introduced by Croasdale (1974) and later studied by Daudin (1992). Although Croasdale (1974) used the double sampling scheme similar to that of Daudin (1992), Croasdale (1974) did not allow a signal at the first stage and made a decision at the second stage solely based on the second sample. Daudin (1992) proposed a double sampling $\bar{X}$ control chart depending on five parameters: two sample sizes for each stage, two set of control limits for the first stage, and one set of control limits for the second stage. Croasdale (1974) and Daudin (1992) emphasized minimizing the average sample size. Daudin (1992) compared the double sampling $\bar{X}$ control chart in terms of the ARL performance with other various control charts, such as standard Shewhart charts, VSI Shewhart charts, EWMA charts, and CUSUM charts, and showed that the proposed control chart has better performance than other control charts.

Irianto and Shinozaki (1998) compared the method proposed by Daudin (1992) and Croasdale (1974) and proposed a method based on maximizing the power of the control chart instead of minimizing the average sample sizes. They also showed that double sampling $\bar{X}$ control charts are better than VSI and VSS $\bar{X}$ control charts at detecting small and moderate mean shifts. Carot, Jabaloyes, and Carot (2002) proposed a $\bar{X}$ control chart that combined the double sampling scheme and VSI (DSVSI) $\bar{X}$ control chart and gave an example. They used average time to signal (ATS) and steady state ATS (SSATS) to compare the chart with the CUSUM and EWMA charts and showed that the DSVSI control

chart has better performance at detecting small and moderate mean shifts in the process. Also, He, Grigoryan, and Sigh (2002) used a genetic algorithm to construct double and triple sampling $\bar{X}$ control charts. Little research has been done, however, on the subject of multivariate double sampling control charts. He (2002) proposed a multivariate double sampling T^2 control chart.

All double sampling charts that have been considered in the SPC literature are based on Shewhart type control charts. In this dissertation, the double sampling scheme is applied to the MEWMA control chart, in which the sample sizes depend on the current and previous chart statistics. We call this procedure a sequential sampling scheme, which is more general than a double sampling scheme.

2.7 Monitoring Linear Profiles

Lawless, MacKay, and Robinson (1999) gave examples in automotive engineering when the quality of a process or product is characterized by a profile between two variables. Kang and Albin (2000) presented two examples of situations for which product profiles are of interest. The first example involves aspartame (an artificial sweetener), which is characterized by the amount of dissolved aspartame per liter of water at different levels of temperature. In this case, there is a desired functional relationship between the amount of dissolved aspartame and the temperature. The other example is a semiconductor manufacturing application involving calibration of a mass flow controller in which the performance of the process is characterized by a linear function. Mestek, Pavlik, and Suchanek (1994) and Stover and Brill (1998) gave similar calibration applications.

Kang and Albin (2000) proposed Phase I and Phase II control chart methods for monitoring a process for which the quality of a product is characterized by a linear relationship. Stover and Brill (1998) also considered the Phase I problem, while Brill (2001) considered possible extensions to more general relationships than a linear one.

The monitoring of linear profiles is very closely related to the control charting of regression-adjusted variables as proposed by Mandel (1969), Zhang (1992), Hawkins (1991, 1993), Wade and Woodall (1993), and Hauck, Runger, and Montgomery (1999). In these approaches, a regression model is often used to account for the effect of an input quality variable X on the output quality variable Y when monitoring a particular stage of a manufacturing process. One can adjust the output variable, however, based on any number of upstream process or quality variables in what Hawkins (1993) referred to as a "cascade process". In a cascade process, variables have a natural ordering and if any variable undergoes a parameter shift, it may affect some or all of the variables following it, but none preceding it. The use of regression adjustment of a single quality variable based on a simple linear regression model is very similar to the linear profile situation except that the Phase I data usually consist of a single set of bivariate data points. In Phase II, one observes a sequence of deviations from the predicted values of Y based on the fitted Phase I regression model. In the regression-adjusted applications, however, the X-variable is usually considered to be a random variable, not taking fixed values as typically assumed in the linear profile monitoring application.

The problem of modeling and monitoring process or product quality using a function has been approached with other methods. Walker and Wright (2002) used additive models to represent the curves of interest in the monitoring of density profiles of particleboard. Jin and Shi (2001) used wavelets to monitor "waveform signals" for diagnosis of process faults. The use of linear functions as responses in designed experiments has also been studied recently. See, for example, Miller (2002) and Nair, Taam, and Ye (2002).

Chapter 3

The Sequential Sampling MEWMA Control Chart

The sequential sampling plan to be considered here consists of a sequence of two sampling stages that can be used at a sampling point. Each stage corresponds to a specific group of observation vectors at each sampling point. Also associated with each stage is a set of decision rules for determining when to continue to the next stage, when to signal, and when to stop sampling at the current sampling point and go to the next sampling point.

The sequential sampling plan with two possible stages is applied to MEWMA control charts, in which the number of times that a variable is measured at a sampling point depends on current and past data. The sequential sampling scheme with two possible stages at each sampling point is based on an extension of the MEWMA chart and will be called the SS MEWMA control chart.

To define the proposed SS MEWMA control chart, we first define the group sizes for the stages. Let $n_j \geq 1$ be the group size at stage j. This means that at each sampling point, at stage 1 we initially obtain n_1 observations for all variables. If the data at the first stage indicate that sampling should proceed to the second stage, then one obtains an additional

group of n_2 observations for all variables at the second stage.

In this dissertation, the sequential sampling scheme is considered in which two different ways of defining the EWMA vectors are considered and evaluated. The two methods of the sequential sampling scheme based on these two EWMA vectors will be called the SS_1 MEWMA chart and SS_2 MEWMA chart, respectively. The only difference between these two SS MEWMA charts is the way the information is used in the EWMA vectors at the second stage. In the proposed SS_1 MEWMA chart, at the second stage the EWMA vector is defined based on the sample mean vector of combined observations collected both at the first and second stages. The total number of observations for the two stages is $n_1 + n_2$, so that the total number of observations used for computing the sample mean at the second stage is now $n_1 + n_2$.

In the proposed SS_2 MEWMA chart, however, only the n_2 observations in the second stage are used for computing the sample mean vector at the second stage. Contrary to the proposed SS_1 MEWMA chart, the information in the first stage is used for defining the EWMA vector at the second stage, but not through the sample mean for the second stage. Both EWMA vectors used for the SS_1 MEWMA chart and SS_2 MEWMA chart are explicitly discussed later in this section. In the second stage, regardless of which proposed SS MEWMA charts are used, there exist two possible decisions: (1) conclude that the process is in-control or (2) conclude that the process is out-of-control. The number of stages actually used at a sampling point is a random variable depending on the process data, but the maximum total sample size possible at a sampling point, say τ, is $\tau = n_1 + n_2$.

Illustrations of the ways in which the stages could be defined are given here using an example for the case in which there are $p = 2$ variables. At the first stage a sample of 2 items is selected, and both variables are measured for both items. If the data at the first stage shows some indication of a problem, then a second stage of sampling is used in which 6 additional items are selected and both variables are measured for the six items. In this example the initial group size is $n_1 = 2$ and the group size at the second stage is $n_2 = 6$.

The group sizes of 8 and 6 are used to compute the sample mean vectors at stage 2 for the SS_1 MEWMA chart and SS_2 MEWMA chart, respectively.

A constraint on the ANOS is applied to both SS_1 and SS_2 MEWMA control charts so that each stage corresponds to a specific ANOS at each sampling point. The basic idea of applying the sequential sampling plan to MEWMA control charts would be that one might want to take the larger sample if the MEWMA chart statistic computed at a sampling point is close to the upper control limit.

3.1 The Proposed SS MEWMA Control Chart

Throughout the rest of this dissertation, we consider the situation in which an assignable cause can change one or more of the components of mean vectors $\boldsymbol{\mu}$, but a known covariance matrix $\boldsymbol{\Sigma}_0$ does not change. In most applications $\boldsymbol{\mu}_0$ and $\boldsymbol{\Sigma}_0$ will have to be estimated during an initial phase in which data were obtained for the purpose of estimating process parameters (see, for example, Sullivan and Woodall (1996, 1998)). Here it is assumed that data set used in this initial phase is large enough that any error associated with estimating $\boldsymbol{\mu}_0$ and $\boldsymbol{\Sigma}_0$ can be neglected.

The decision rule used at each stage is a function of the data at this stage, along with the data from past stages and sampling points. Let $\bar{X}_{kij}$ be the average of the n_j observations obtained for variable i at stage j at sampling point k, for $i = 1, 2, \cdots, p$, $j = 1, 2$, and $k = 1, 2, \cdots$.

In the SS_1 MEWMA chart, since the EWMA vector at the second stage is computed based on the sample mean of combined observations collected both at the first and second stages $\bar{W}_{ki2}$ is defined as the average of the $n_1 + n_2$ observations obtained for variable i at the second stage at sampling point k, where

$$\bar{W}_{ki2} = \frac{n_1 \bar{X}_{ki1} + n_2 \bar{X}_{ki2}}{n_1 + n_2}.$$

Corresponding to $\bar{X}_{ki1}$ and $\bar{W}_{ki2}$, we define the standardized sample mean at the first stage to be

$$U_{ki1} = \frac{\sqrt{n_1}(\bar{X}_{ki1} - \mu_{0i})}{\sigma_{0i}}$$

and at the second stage to be

$$U_{ki2} = \frac{\sqrt{n_1 + n_2}(\bar{W}_{ki2} - \mu_{0i})}{\sigma_{0i}}.$$

In the SS_2 MEWMA chart, since no combined information is used at the second stage the standardized sample mean for variable i at stage j is defined as

$$V_{kij} = \frac{\sqrt{n_j}(\bar{X}_{kij} - \mu_{0i})}{\sigma_{0i}}, \quad j = 1, 2.$$

Let the standardized sample mean vector for the SS_1 MEWMA chart be

$$\boldsymbol{U}_{kj} = (U_{k1j}, U_{k2j}, \cdots, U_{kpj})^T, \quad j = 1, 2,$$

and for the SS_2 MEWMA chart be

$$\boldsymbol{V}_{kj} = (V_{k1j}, V_{k2j}, \cdots, V_{kpj})^T, \quad j = 1, 2. \tag{3.1}$$

The number of groups of observation vectors actually taken at sampling point k is a random variable, so let $S(k)$ be the number of groups actually taken (the number of stages actually used) at sampling point k.

In the SS_1 MEWMA chart, we define the EWMA vector $\boldsymbol{D}_{kj}$ after sampling stage j at sampling point $k \geq 1$ to be

$$\boldsymbol{D}_{kj} = r_j \boldsymbol{U}_{kj} + (1 - r_j)\boldsymbol{D}_{k-1,S(k-1)}, \quad j = 1, 2,$$

where $\boldsymbol{D}_0 = \boldsymbol{0}$ and r_j is a smoothing parameter at stage j satisfying $0 < r_j \leq 1$. Thus at stage j the current EWMA vector is based on the current standardized sample mean vector

and the EWMA vector at the previous sampling point. After stage j at sampling point k, the decision rule will be based on the statistic

$$T_{kj}^2 = \boldsymbol{D}_{kj}^T \boldsymbol{\Sigma}_{kj}^{-1} \boldsymbol{D}_{kj},$$

where $\boldsymbol{\Sigma}_{kj}$ is the covariance matrix of $\boldsymbol{D}_{kj}$. The covariance matrix $\boldsymbol{\Sigma}_{kj}$ can be obtained recursively using

$$\boldsymbol{\Sigma}_{kj} = (1 - r_j)^2 \boldsymbol{\Sigma}_{k-1,S(k-1)} + r_j^2 \boldsymbol{\Sigma}_c \quad j = 1, 2,$$

where $\boldsymbol{\Sigma}_c$ is the correlation matrix corresponding to the known covariance matrix $\boldsymbol{\Sigma}_0$. In the above equation $\boldsymbol{\Sigma}_c$ is used because standardized sample means $\boldsymbol{Z}_{kj}$ are being used in obtaining EWMA vectors $\boldsymbol{D}_{kj}$.

In the SS_2 MEWMA chart, let $\boldsymbol{E}_{kj}$ be the EWMA vector after stage j at sampling point k, corresponding to the standardized sample mean vector in Equation (3.1). Then, after the first stage at sampling point $k \geq 1$,

$$\boldsymbol{E}_{k1} = r_1 \boldsymbol{V}_{k1} + (1 - r_1) \boldsymbol{E}_{k-1,S(k-1)},$$

and, for the second stage at sampling point k,

$$\boldsymbol{E}_{k2} = r_2 \boldsymbol{V}_{k2} + (1 - r_2) \boldsymbol{E}_{k1},$$

where $\boldsymbol{E}_0 = \boldsymbol{0}$ and r_j is a smoothing parameter at stage j satisfying $0 < r_j \leq 1$. At stage 1 the current EWMA vector is based on the current standardized sample mean vector and the EWMA vector at the previous sampling point, however at stage 2 the EWMA vector is based on the current standardized sample mean vector and the EWMA vector for the previous group. The EWMA vector used in the SS_2 MEWMA chart at stage 2 is different from that of the SS_1 MEWMA chart, since in the SS_1 MEWMA chart the EWMA vector is based on the current standardized sample mean vector and the EWMA vector at the previous sampling point, not based on the previous group. The statistic used for the decision rule is

$$T_{kj}^2 = \boldsymbol{E}_{kj}^T \boldsymbol{\Sigma}_{kj}^{-1} \boldsymbol{E}_{kj},$$

where $\boldsymbol{\Sigma}_{kj}$ is the covariance matrix of $\boldsymbol{E}_{kj}$ and for $k \geq 1$, the covariance matrix $\boldsymbol{\Sigma}_{kj}$ is given by

$$\boldsymbol{\Sigma}_{kj} = \begin{cases} (1-r_1)^2\boldsymbol{\Sigma}_{k-1,S(k-1)} + r_1^2\boldsymbol{\Sigma}_c & j = 1, \\ (1-r_2)^2\boldsymbol{\Sigma}_{k1} + r_2^2\boldsymbol{\Sigma}_c & j = 2, \end{cases}$$

where $\boldsymbol{\Sigma}_c$ is the correlation matrix corresponding to the known covariance matrix $\boldsymbol{\Sigma}_0$. As in the SS_1 MEWMA chart, $\boldsymbol{\Sigma}_c$ is used because standardized sample means $\boldsymbol{V}_{kj}$ are used in obtaining EWMA vectors $\boldsymbol{E}_{kj}$.

The decision rule for both SS_1 and SS_2 MEWMA charts requires the specification of two limits, denoted by g and h, satisfying $0 < g < h$. Then the decision rule for the SS_1 MEWMA chart is defined as follows. The same decision rule applies to the SS_2 MEWMA chart except that corresponding EWMA vectors $\boldsymbol{E}_{kj}$ and standardized sample means $\boldsymbol{V}_{kj}$, $j = 1, 2$, are used. If the current sampling point is k,

1. Observe the first group of n_1 observations.
2. Compute $\boldsymbol{U}_{k1}$ based on the group size of n_1.
3. Compute $\boldsymbol{D}_{k1} = r_1\boldsymbol{U}_{k1} + (1-r_1)\boldsymbol{D}_{k-1,S(k-1)}$.
4. Compute $T_{k1}^2 = \boldsymbol{D}_{k1}^T\boldsymbol{\Sigma}_{k1}^{-1}\boldsymbol{D}_{k1}$.
   (a) If $T_{k1}^2 \leq g$, then stop sampling at sampling point k, define $S(k) = 1$, and wait until sampling point $k+1$ to sample again.
   (b) If $g < T_{k1}^2 \leq h$, then go to Step 5.
   (c) If $T_{k1}^2 > h$, then signal that there has been a change in the mean vector $\boldsymbol{\mu}$.
5. Take the second group of n_2 observations.
6. Compute $\boldsymbol{U}_{k2}$ based on the group size of $n_1 + n_2$.
7. Compute $\boldsymbol{D}_{k2} = r_2\boldsymbol{U}_{k2} + (1-r_2)\boldsymbol{D}_{k-1,S(k-1)}$.

8. Compute $T_{k2}^2 = \boldsymbol{D}_{k2}^T \boldsymbol{\Sigma}_{k2}^{-1} \boldsymbol{D}_{k2}$.

   (a) If $T_{k2}^2 \leq h$, then stop sampling at sampling point k, define $S(k) = 2$, and wait until sampling point $k+1$ to sample again.

   (b) If $T_{k2}^2 > h$, then signal that there has been a change in the mean vector $\boldsymbol{\mu}$.

At stage 1, an out-of-control signal is given whenever T_{k1}^2 is greater than the upper control limit h. Another design parameter, g, is used to decide whether additional observations are needed after the first stage. Both g and h are chosen to give a specified in-control ATS and ANOS for each of the SS_1 and SS_2 MEWMA charts. In both SS_1 and SS_2 MEWMA control charts, if the group size n_j is considered as one parameter then one needs a number of design parameters to be determined: 2 smoothing parameter values (r_1 and r_2), 2 group sizes (n_1 and n_2), and 2 control limits (g and h).

The in-control ATS and ANOS of each of the SS_1 and SS_2 MEWMA charts were evaluated using simulation with 1,000,000 runs. Adjusting the values of g and h to obtain specific values of the in-control ATS and ANOS was accomplished by simulating the ATS and ANOS for some initial guesses for g and h, then regressing the logarithms of the ATS and ANOS on g and h, and finally solving the regression equations to find the required values of g and h. The SSATS was obtained by simulating the operation of each of the SS_1 and SS_2 MEWMA charts for 100 in-control observation vectors, and then introducing a shift in $\boldsymbol{\mu}$.

3.2 Parameter Choices for the Comparisons

Two basic control charts that do not use sequential sampling will be used as reference charts for evaluating the efficiency of the SS_1 and SS_2 MEWMA charts. The first reference control chart is the Shewhart chart based on Hotelling's statistic, and the other is the standard MEWMA chart. For both of these charts, a sample size of $n = 5$, a sampling interval of $d = 1$ time unit, and an in-control ATS of 200 will be considered. This means that the

in-control ANOS is 1000. In discussing the results in this dissertation, the time unit will be frequently referred to as an hour.

Shifts in the process mean vector are measured in units of the non-centrality parameter

$$\delta = \sqrt{\boldsymbol{\nu}^T \boldsymbol{\Sigma}_c^{-1} \boldsymbol{\nu}},$$

where $\boldsymbol{\Sigma}_c$ is the correlation matrix corresponding to the known covariance matrix $\boldsymbol{\Sigma}_0$ and the i^{th} component of $\boldsymbol{\nu}$ is the standardized mean shift

$$\nu_i = \frac{\mu_i - \mu_{0i}}{\sigma_{0i}}, \quad i = 1, 2, \cdots, p.$$

The properties of MEWMA charts, if all variables have the same sample size, depend on $\boldsymbol{\mu}$ only through the value of δ, so this simplifies the evaluation of the properties of the MEWMA chart (see Lowry et al. (1992)). Numerical results indicate that the SSATS values of the SS MEWMA charts depend on $\boldsymbol{\mu}$ only through the value of δ. The value of the smoothing parameter (r) used in the reference MEWMA chart is $r = 0.1$, and the values of r used for the SS_1 and SS_2 MEWMA charts are adjusted to correspond to the group sizes, which will be discussed in the following section. According to Lowry et al. (1992), $r = 0.1$ should be optimal for detecting a shift of about $\delta = 1.0/\sqrt{n}$ in the standard MEWMA chart. The out-of-control values of δ considered in the tables in this dissertation cover a wide range from 0.1 up to 5.0. If the p variables are independent then a given value of δ is achieved when each of the p variables shifts by $\nu_i = \delta/\sqrt{p}$. A given value of δ is also achieved when only one of the p variables shifts by $\nu_i = \delta$. Thus the shifts considered in the tables range from very small to quite large. It is assumed here that it is desirable to detect small as well as large shifts, but a very small shift such as $\delta = 0.1$ may be too small to be of much practical concern in most applications.

3.3 The Choice of the Smoothing Parameter for Groups

In this dissertation, the SS_1 and SS_2 MEWMA charts with different group sizes will be compared, so the values of the smoothing parameter r used must be chosen carefully to ensure fair comparisons. It seems reasonable that a sample mean vector corresponding to a large group size should get more weight than a sample mean vector corresponding to a small group size. Let $r(n_j)$ represent the value of r used when the group size is n_j. Consider a group size $n_j \geq 1$, and any sample of total size τ where $\tau = n_j m_j$, with m_j a positive integer. A reasonable approach to making a fair comparison of control charts is to choose $r(n_j)$, for n_j, so that the sum of the group weights for the sample of τ observation vectors equals the weight that would be given for a sample of τ observations. This requires that

$$r(n_j) = 1 - (1 - r(\tau))^{n_j/\tau}, \tag{3.2}$$

so this equation provides a method for determining $r(n_j)$ from $r(\tau)$, for the SS_1 and SS_2 MEWMA charts considered here. For example, suppose that a sample of $\tau = 6$ observations is to be taken, and it can be taken in two groups of three observation vectors each. If the weight for the sample of $\tau = 6$ should be $r = 0.1$, then Equation (3.2) implies that the r that should be used for groups of size three is $r(3) = 1 - (1 - 0.1)^{3/6} = 0.05132$. See Reynolds and Stoumbos (2003) for additional discussion of this issue.

In the example concerning the choice of r in the previous paragraph, it was assumed that a sample consists of groups of equal size. But in some cases it may be desirable to have groups of unequal size. For example, a sample of $\tau = 6$ could be obtained using one group of 2 and a second group of 4. When different groups have different group sizes, there are several options for choosing the value of r for each stage. One option is for each stage to use the value of r appropriate for the group size at that stage, and another option is to use the value of r appropriate for the average group size. Both of these options are investigated next.

Tables 3.1-3.2 give SSATS values of the SS_1 and SS_2 MEWMA charts for the case

of $p = 2$ and $p = 4$ when the group sizes are $(n_1, n_2) = \{(3, 7), (3, 15)\}$ and Tables 3.3-3.4 give SSATS values for the case of $p = 2$ and $p = 4$ when the group sizes are $(n_1, n_2) = \{(4, 6), (4, 14)\}$. In two of these cases the maximum total sample size at a sampling point is $\tau = 10$, and in the other two cases it is $\tau = 18$. For each of these cases there are two columns. In the first column different values of r are used for different group sizes, and in the second column the same value of r is used for all groups (the value appropriate for the average group size). Tables 3.3-3.4 have the same structure as Tables 3.1-3.2 except that the results are for the case of initial group sizes of $n_1 = 4$.

We see from Tables 3.1-3.4 that using the same value of r for all groups gives better performance for small shifts and slightly better performance for some large shifts, but performance is slightly worse for some intermediate shifts. It is assumed that it is desirable to have good performance for a range of shifts from small to large. Thus, in terms of good overall performance, it seems to be reasonable to use the same value of r for all group sizes. Thus the remaining results in this dissertation are presented for the case in which the r appropriate for the average group size is used for all groups.

3.4 The Effects of the Choice of the Group Sizes

Now we consider the effects of different choices for the group sizes and the related issue of the maximum possible sample size τ that is allowed at each sampling point. In some applications, there may be constraints on the total number of observations τ, that must be considered. Thus for the SS_1 and SS_2 MEWMA charts one needs to determine whether τ needs to be large for good performance.

The tables presenting results on the choice of group sizes in the SS_1 and SS_2 MEWMA charts are organized so that the tables for an initial group size of $n_1 = 2$ are given first, and these tables are followed by the tables for initial group sizes of $n_1 = 3$ and $n_1 = 4$. If the average sample size is 5, then the largest value for the initial group sizes of n_1 that will give

Table 3.1: SSATS Values of the SS_1 and SS_2 MEWMA Chart with Different Choices of r and an Initial Group Size of $n_1 = 3$ when $p = 2$

		MEWMA	SS_1 MEWMA				SS_2 MEWMA			
n_1		5	3	3	3	3	3	3	3	3
n_2		—	7	7	15	15	7	7	15	15
τ		5	10	10	18	18	10	10	18	18
r_1		0.1	0.06126	0.07868	0.06126	0.08877	0.06126	0.07868	0.06126	0.08877
r_2		—	0.13714	0.07868	0.27100	0.08877	0.13714	0.07868	0.27100	0.08877
δ	0.0	200.0	200.0	200.0	200.0	200.0	200.0	200.0	200.0	200.0
	0.1	87.5	76.0	73.4	78.5	74.1	84.6	78.9	86.8	74.5
	0.15	50.6	40.7	39.6	41.0	39.4	45.6	42.8	46.0	39.9
	0.2	32.3	25.1	24.8	24.3	24.2	27.3	26.1	26.7	24.4
	0.25	22.5	17.4	17.5	16.4	16.7	18.2	17.8	17.5	16.8
	0.3	16.9	13.1	13.4	12.2	12.6	13.3	13.2	12.6	12.6
	0.4	10.9	8.7	9.0	8.1	8.3	8.5	8.6	8.0	8.3
	0.5	8.0	6.4	6.7	6.0	6.1	6.2	6.3	5.9	6.2
	0.75	4.7	3.8	4.1	3.7	3.7	3.6	3.8	3.6	3.6
	1.0	3.3	2.7	2.9	2.7	2.5	2.5	2.6	2.6	2.5
	1.5	2.1	1.5	1.8	1.8	1.5	1.4	1.5	1.7	1.5
	2.0	1.5	1.1	1.2	1.4	1.0	1.0	1.0	1.3	1.1
	3.0	1.0	0.7	0.7	0.9	0.7	0.7	0.6	0.9	0.7
	4.0	0.6	0.6	0.5	0.7	0.5	0.6	0.5	0.7	0.6
	5.0	0.5	0.5	0.5	0.6	0.5	0.5	0.5	0.6	0.5
h		8.786	8.712	7.826	8.144	7.249	8.571	8.977	7.437	8.882
g		—	1.458	1.600	1.868	2.616	1.216	1.767	1.643	3.020

Table 3.2: SSATS Values of the SS_1 and SS_2 MEWMA Chart with Different Choices of r and an Initial Group Size of $n_1 = 3$ when $p = 4$

		MEWMA	SS_1 MEWMA				SS_2 MEWMA			
n_1		5	3	3	3	3	3	3	3	3
n_2		—	7	7	15	15	7	7	15	15
τ		5	10	10	18	18	10	10	18	18
r_1		0.1	0.06126	0.07868	0.06126	0.08877	0.06126	0.07868	0.06126	0.08877
r_2		—	0.13714	0.07868	0.27100	0.08877	0.13714	0.07868	0.27100	0.08877
δ	0.0	200.0	200.0	200.0	200.0	200.0	200.0	200.0	200.0	200.0
	0.1	105.0	93.1	89.0	96.7	90.7	102.4	96.7	105.1	92.0
	0.15	63.3	51.5	49.1	52.9	49.7	58.1	54.3	58.9	50.8
	0.2	40.4	31.4	30.5	31.2	30.2	34.8	33.0	34.4	30.7
	0.25	27.8	21.4	21.2	20.6	20.6	22.9	22.1	22.2	20.7
	0.3	20.6	15.9	16.0	15.0	15.3	16.5	16.2	15.8	15.3
	0.4	13.0	10.3	10.6	9.7	10.0	10.3	10.3	9.8	9.9
	0.5	9.4	7.6	7.9	7.3	7.3	7.4	7.5	7.2	7.3
	0.75	5.4	4.6	4.8	4.5	4.4	4.3	4.4	4.4	4.3
	1.0	3.8	3.2	3.4	3.3	3.0	3.0	3.1	3.2	3.0
	1.5	2.3	1.9	2.2	2.2	1.8	1.8	1.9	2.1	1.8
	2.0	1.7	1.3	1.5	1.7	1.3	1.2	1.2	1.6	1.3
	3.0	1.1	0.9	0.8	1.1	0.8	0.8	0.7	1.1	0.9
	4.0	0.7	0.7	0.6	0.9	0.6	0.6	0.6	0.8	0.7
	5.0	0.5	0.6	0.5	0.7	0.5	0.6	0.5	0.7	0.5
h		12.913	12.831	11.838	12.082	11.153	12.656	13.148	11.286	13.033
g		—	3.468	3.688	4.083	5.194	3.051	3.944	3.715	5.739

Table 3.3: SSATS Values of the SS_1 and SS_2 MEWMA Chart with Different Choices of r and an Initial Group Size of $n_1 = 4$ when $p = 2$

		MEWMA	SS_1 MEWMA				SS_2 MEWMA			
n_1		5	4	4	4	4	4	4	4	4
n_2		—	6	6	14	14	6	6	14	14
τ		5	10	10	18	18	10	10	18	18
r_1		0.1	0.08083	0.08635	0.08083	0.09366	0.08083	0.08635	0.08083	0.09366
r_2		—	0.11877	0.08635	0.25548	0.09366	0.11877	0.08635	0.25548	0.09366
δ	0.0	200.0	200.0	200.0	200.0	200.0	200.0	200.0	200.0	200.0
	0.1	87.5	76.6	76.7	79.2	77.6	84.1	80.6	88.0	75.8
	0.15	50.6	41.5	41.6	42.4	41.8	46.0	44.0	47.7	41.0
	0.2	32.3	25.6	25.8	25.5	25.5	27.7	26.7	28.2	25.0
	0.25	22.5	17.7	17.9	17.1	17.4	18.5	18.1	18.4	17.1
	0.3	16.9	13.2	13.4	12.5	12.9	13.5	13.3	13.1	12.7
	0.4	10.9	8.7	8.9	8.0	8.4	8.5	8.5	8.0	8.2
	0.5	8.0	6.4	6.6	5.8	6.1	6.1	6.2	5.7	6.0
	0.75	4.7	3.8	3.9	3.5	3.6	3.5	3.6	3.3	3.5
	1.0	3.3	2.6	2.8	2.5	2.4	2.4	2.5	2.3	2.4
	1.5	2.1	1.5	1.7	1.6	1.5	1.3	1.4	1.5	1.5
	2.0	1.5	1.0	1.1	1.2	1.1	0.9	0.9	1.1	1.1
	3.0	1.0	0.7	0.6	0.8	0.7	0.6	0.6	0.8	0.7
	4.0	0.6	0.5	0.5	0.6	0.5	0.5	0.5	0.6	0.5
	5.0	0.5	0.5	0.5	0.5	0.5	0.5	0.5	0.5	0.5
h		8.786	8.691	8.001	8.230	7.587	8.692	8.904	7.144	8.840
g		—	2.629	2.579	3.375	3.772	2.346	2.645	2.998	4.079

Table 3.4: SSATS Values of the SS_1 and SS_2 MEWMA Chart with Different Choices of r and an Initial Group Size of $n_1 = 4$ when $p = 4$

		MEWMA	SS_1 MEWMA				SS_2 MEWMA			
n_1		5	4	4	4	4	4	4	4	4
n_2		—	6	6	14	14	6	6	14	14
τ		5	10	10	18	18	10	10	18	18
r_1		0.1	0.08083	0.08635	0.08083	0.09366	0.08083	0.08635	0.08083	0.09366
r_2		—	0.11877	0.08635	0.25548	0.09366	0.11877	0.08635	0.25548	0.09366
δ	0.0	200.0	200.0	200.0	200.0	200.0	200.0	200.0	200.0	200.0
	0.1	105.0	93.7	93.3	97.6	95.0	102.3	98.5	106.9	93.5
	0.15	63.3	52.5	52.3	54.6	53.0	58.8	56.0	61.4	52.3
	0.2	40.4	32.1	32.1	32.7	32.2	35.5	34.1	36.6	31.7
	0.25	27.8	21.8	22.0	21.6	21.7	23.4	22.7	23.6	21.3
	0.3	20.6	16.1	16.3	15.6	15.9	16.8	16.5	16.6	15.6
	0.4	13.0	10.3	10.6	9.7	10.1	10.3	10.3	9.9	9.9
	0.5	9.4	7.5	7.8	7.0	7.3	7.3	7.4	6.9	7.2
	0.75	5.4	4.4	4.6	4.1	4.2	4.2	4.3	4.0	4.1
	1.0	3.8	3.1	3.3	2.9	2.9	2.9	3.0	2.8	2.9
	1.5	2.3	1.8	2.0	1.9	1.7	1.6	1.7	1.8	1.8
	2.0	1.7	1.2	1.4	1.4	1.3	1.1	1.1	1.4	1.3
	3.0	1.1	0.8	0.8	0.9	0.8	0.7	0.7	0.9	0.8
	4.0	0.7	0.6	0.6	0.7	0.6	0.6	0.6	0.7	0.6
	5.0	0.5	0.5	0.5	0.6	0.5	0.5	0.5	0.6	0.5
h		12.913	12.817	12.032	12.165	11.550	12.805	13.060	10.917	12.980
g		—	5.201	5.136	6.213	6.763	4.798	5.221	5.709	7.145

the non-trivial SS_1 and SS_2 MEWMA charts is $n_1 = 4$.

Table 3.5 gives SSATS values for the case of $p = 2$ for the SS_1 and SS_2 MEWMA charts that have an initial group size of $n_1 = 2$. For purposes of comparison, columns 2 and 3 contain SSATS values for the standard Shewhart and standard MEWMA charts with the sample size of $n = 5$, respectively. Columns 4-6 correspond to SS_1 MEWMA charts, where the values considered for n_2 are 8, 10, and 16, corresponding to a maximum sample size of $\tau = 10$, 12, and 18, respectively. Columns 7-9 contain SSATS values for SS_2 MEWMA charts that have the same structure as SS_1 MEWMA charts in columns 4-6. Table 3.6 has the same structure as Table 3.5, except that $p = 4$.

Tables 3.7 and 3.8 give SSATS values for the case of $p = 2$ and $p = 4$, respectively, for the SS_1 and SS_2 MEWMA charts that have an initial group size of $n_1 = 3$. The structure is similar to Tables 3.5 and 3.6. In columns 4-6 the SSATS values of SS_1 MEWMA charts considered for n_2 are 7, 9, and 15, to correspond to a maximum sample size of $\tau = 10$, 12, and 18, respectively. Columns 7-9 correspond to SS_2 MEWMA charts with $n_2 = 7$, 9, and 15, respectively.

Tables 3.9 and 3.10 with $n_1 = 4$ use the same structure as previous tables. In columns 4-6 the values of n_2 considered for SS_1 MEWMA charts are now 6, 8, and 14. Columns 7-9 correspond to SS_2 MEWMA charts with $n_2 = 6$, 8, and 14, respectively.

Tables 3.11 and 3.12 give ANOS values for the case of $p = 2$ and $p = 4$, respectively, for SS_1 MEWMA charts that have the initial group sizes of $n_1 = 2$, 3, and 4, corresponding to a maximum sample size of $\tau = 10$, 12, and 18, respectively.

From Tables 3.5 and 3.6 where $n_1 = 2$, we see that the SS_1 and SS_2 MEWMA charts perform much better than the Shewhart chart in detecting small-to-moderate shifts and are moderately better than the standard MEWMA chart. When the SS_1 MEWMA chart and the SS_2 MEWMA chart are compared, the SS_1 MEWMA chart performs better than the SS_2 MEWMA chart in detecting small shifts and the SS_2 MEWMA chart performs better than the SS_1 MEWMA chart in detecting moderate shifts. Both charts give almost equal

performance in detecting large shifts. In terms of good overall performance, it is hard to say that one method of defining the EWMA vector is better than the other method because no method is uniformly better than the other method for all range of shifts.

Comparing Tables 3.7 and 3.8 with Tables 3.5 and 3.6 shows that, when the SS_1 MEWMA chart is used, using $n_1 = 3$ gives better performance than using $n_1 = 2$ except for detecting very small shifts. However when the SS_2 MEWMA chart is used, using $n_1 = 3$ gives uniformly better performance than using $n_1 = 2$. Comparing the SS_1 MEWMA chart and the SS_2 MEWMA chart also shows that for small shifts the SS_1 MEWMA chart is slightly better than the SS_2 MEWMA chart and for moderate shifts the SS_2 MEWMA chart is slightly better than the SS_1 MEWMA chart. Examining Tables 3.5-3.10 shows that $n_1 = 3$ or 4 seem to be the best choices for the first sample size for both the SS_1 and the SS_2 MEWMA charts. For small shifts $n_1 = 3$ is slightly better than $n_1 = 4$, and for intermediate shifts $n_1 = 4$ is slightly better than $n_1 = 3$. This seems to be intuitively reasonable. If there is one additional group after the first group, the first group size needs to large enough to get a reasonable amount of information to decide whether to take the second group. It appears that it is best to choose n_2 as large as is feasible, but n_2 does not need to be extremely large to give significant reductions in the SSATS compared to the standard MEWMA chart. For example, when $p = 2$ the standard MEWMA takes an average of 8.0 hours to detect a shift of size 0.5. Using the SS_2 MEWMA chart with $n_1 = 4$ and $n_2 = 6$ will require 6.2 hours on average. If n_2 is increased to 14 then the expected time required for detection drops a little to 6.0.

From Tables 3.11 and 3.12, we see that the SS_1 MEWMA chart gives smaller ANOS values than the standard Shewhart and standard MEWMA charts with the fixed sample size for detecting small shifts. In terms of good overall ANOS performance, using $n_1 = 4$ seems to be the best choice. However, the ANOS values between using $n_1 = 3$ and $n_1 = 4$ are not significantly different.

Table 3.5: SSATS Values of the SS_1 and SS_2 MEWMA Chart with an Initial Group Size of $n_1 = 2$ when $p = 2$

		Shewhart	MEWMA	SS_1 MEWMA			SS_2 MEWMA		
n_1		5	5	2	2	2	2	2	2
n_2		—	—	8	10	16	8	10	16
τ		5	5	10	12	18	10	12	18
r_j		—	0.1	0.07376	0.07785	0.08490	0.07376	0.07785	0.08490
	0.0	200.0	200.0	200.0	200.0	200.0	200.0	200.0	200.0
	0.1	175.7	87.5	72.6	72.6	73.7	80.5	79.1	76.7
	0.15	151.9	50.6	39.5	39.1	39.4	43.9	42.9	41.3
	0.2	126.6	32.3	25.0	24.6	24.5	27.0	26.3	25.5
	0.25	102.8	22.5	17.8	17.4	17.1	18.6	18.1	17.7
	0.3	82.3	16.9	13.7	13.3	13.0	13.9	13.6	13.4
	0.4	51.7	10.9	9.3	9.0	8.7	9.1	9.0	9.0
δ	0.5	32.4	8.0	7.0	6.8	6.5	6.8	6.7	6.7
	0.75	11.0	4.7	4.3	4.1	3.9	4.1	4.0	4.1
	1.0	4.4	3.3	3.1	3.0	2.8	2.9	2.8	2.8
	1.5	1.2	2.1	2.0	1.8	1.6	1.7	1.6	1.7
	2.0	0.6	1.5	1.3	1.2	1.1	1.1	1.1	1.2
	3.0	0.5	1.0	0.7	0.7	0.8	0.7	0.7	0.8
	4.0	0.5	0.6	0.5	0.6	0.6	0.6	0.6	0.6
	5.0	0.5	0.5	0.5	0.5	0.5	0.5	0.5	0.5
h		10.597	8.786	7.704	7.482	7.034	9.025	8.984	8.917
g		—	—	1.109	1.371	1.971	1.348	1.690	2.449

Table 3.6: SSATS Values of the SS_1 and SS_2 MEWMA Chart with an Initial Group Size of $n_1 = 2$ when $p = 4$

		Shewhart	MEWMA	SS_1 MEWMA			SS_2 MEWMA		
n_1		5	5	2	2	2	2	2	2
n_2		—	—	8	10	16	8	10	16
τ		5	5	10	12	18	10	12	18
r_j		—	0.1	0.07376	0.07785	0.08490	0.07376	0.07785	0.08490
	0.0	200.0	200.0	200.0	200.0	200.0	200.0	200.0	200.0
	0.1	184.1	105.0	87.5	87.8	89.8	98.2	96.7	94.2
	0.15	167.3	63.3	48.3	48.2	49.1	55.6	54.4	52.4
	0.2	147.4	40.4	30.4	30.0	30.2	33.9	33.0	31.9
	0.25	126.7	27.8	21.4	21.0	20.9	22.9	22.3	21.7
	0.3	106.9	20.6	16.4	16.0	15.7	16.8	16.4	16.1
	0.4	73.1	13.0	11.1	10.7	10.4	10.8	10.6	10.6
δ	0.5	48.7	9.4	8.3	8.0	7.8	7.9	7.8	7.9
	0.75	17.6	5.4	5.1	4.9	4.7	4.7	4.7	4.8
	1.0	7.0	3.8	3.6	3.5	3.3	3.4	3.3	3.3
	1.5	1.6	2.3	2.3	2.2	2.0	2.1	2.0	2.0
	2.0	0.7	1.7	1.7	1.5	1.4	1.4	1.3	1.5
	3.0	0.5	1.1	0.9	0.8	0.9	0.8	0.9	1.0
	4.0	0.5	0.7	0.6	0.6	0.7	0.6	0.7	0.7
	5.0	0.5	0.5	0.5	0.5	0.6	0.6	0.6	0.6
h		14.860	12.913	11.709	11.445	10.906	13.207	13.158	13.076
g		—	—	2.879	3.317	4.255	3.284	3.826	4.945

Table 3.7: SSATS Values of the SS_1 and SS_2 MEWMA Chart with an Initial Group Size of $n_1 = 3$ when $p = 2$

		Shewhart	MEWMA	SS_1 MEWMA			SS_2 MEWMA		
n_1		5	5	3	3	3	3	3	3
n_2		—	—	7	9	15	7	9	15
τ		5	5	10	12	18	10	12	18
r_j		—	0.1	0.07868	0.08259	0.08877	0.07868	0.08259	0.08877
	0.0	200.0	200.0	200.0	200.0	200.0	200.0	200.0	200.0
	0.1	175.7	87.5	73.4	73.4	74.1	78.9	77.3	74.5
	0.15	151.9	50.6	39.6	39.3	39.4	42.8	41.6	39.9
	0.2	126.6	32.3	24.8	24.4	24.2	26.1	25.3	24.4
	0.25	102.8	22.5	17.5	17.1	16.7	17.8	17.3	16.8
	0.3	82.3	16.9	13.4	12.9	12.6	13.2	12.9	12.6
	0.4	51.7	10.9	9.0	8.6	8.3	8.6	8.4	8.3
δ	0.5	32.4	8.0	6.7	6.4	6.1	6.3	6.2	6.2
	0.75	11.0	4.7	4.1	3.9	3.7	3.8	3.7	3.6
	1.0	4.4	3.3	2.9	2.8	2.5	2.6	2.6	2.5
	1.5	1.2	2.1	1.8	1.6	1.5	1.5	1.4	1.5
	2.0	0.6	1.5	1.2	1.1	1.0	1.0	1.0	1.1
	3.0	0.5	1.0	0.7	0.6	0.7	0.6	0.7	0.7
	4.0	0.5	0.6	0.5	0.5	0.5	0.5	0.5	0.6
	5.0	0.5	0.5	0.5	0.5	0.5	0.5	0.5	0.5
h		10.597	8.786	7.826	7.629	7.249	8.977	8.939	8.882
g		—	—	1.600	1.921	2.616	1.767	2.170	3.020

Table 3.8: SSATS Values of the SS_1 and SS_2 MEWMA Chart with an Initial Group Size of $n_1 = 3$ when $p = 4$

		Shewhart	MEWMA	SS_1 MEWMA			SS_2 MEWMA		
n_1		5	5	3	3	3	3	3	3
n_2		—	—	7	9	15	7	9	15
τ		5	5	10	12	18	10	12	18
r_j		—	0.1	0.07868	0.08259	0.08877	0.07868	0.08259	0.08877
δ	0.0	200.0	200.0	200.0	200.0	200.0	200.0	200.0	200.0
	0.1	184.1	105.0	89.0	89.2	90.7	96.7	95.0	92.0
	0.15	167.3	63.3	49.1	49.1	49.7	54.3	53.0	50.8
	0.2	147.4	40.4	30.5	30.1	30.2	33.0	32.0	30.7
	0.25	126.7	27.8	21.2	20.8	20.6	22.1	21.4	20.7
	0.3	106.9	20.6	16.0	15.6	15.3	16.2	15.7	15.3
	0.4	73.1	13.0	10.6	10.3	10.0	10.3	10.1	9.9
	0.5	48.7	9.4	7.9	7.6	7.3	7.5	7.3	7.3
	0.75	17.6	5.4	4.8	4.6	4.4	4.4	4.4	4.3
	1.0	7.0	3.8	3.4	3.3	3.0	3.1	3.0	3.0
	1.5	1.6	2.3	2.2	2.0	1.8	1.9	1.8	1.8
	2.0	0.7	1.7	1.5	1.3	1.3	1.2	1.2	1.3
	3.0	0.5	1.1	0.8	0.8	0.8	0.7	0.8	0.9
	4.0	0.5	0.7	0.6	0.6	0.6	0.6	0.6	0.7
	5.0	0.5	0.5	0.5	0.5	0.5	0.5	0.5	0.5
h		14.860	12.913	11.838	11.605	11.153	13.148	13.103	13.033
g		—	—	3.688	4.181	5.194	3.944	4.543	5.739

Table 3.9: SSATS Values of the SS_1 and SS_2 MEWMA Chart with an Initial Group Size of $n_1 = 4$ when $p = 2$

		Shewhart	MEWMA	SS_1 MEWMA			SS_2 MEWMA		
n_1		5	5	4	4	4	4	4	4
n_2		—	—	6	8	14	6	8	14
τ		5	5	10	12	18	10	12	18
r_j		—	0.1	0.08635	0.08940	0.09366	0.08635	0.08940	0.09366
δ	0.0	200.0	200.0	200.0	200.0	200.0	200.0	200.0	200.0
	0.1	175.7	87.5	76.7	76.9	77.6	80.6	78.8	75.8
	0.15	151.9	50.6	41.6	41.5	41.8	44.0	42.7	41.0
	0.2	126.6	32.3	25.8	25.5	25.5	26.7	26.0	25.0
	0.25	102.8	22.5	17.9	17.6	17.4	18.1	17.6	17.1
	0.3	82.3	16.9	13.4	13.2	12.9	13.3	13.0	12.7
	0.4	51.7	10.9	8.9	8.6	8.4	8.5	8.4	8.2
	0.5	32.4	8.0	6.6	6.3	6.1	6.2	6.1	6.0
	0.75	11.0	4.7	3.9	3.8	3.6	3.6	3.6	3.5
	1.0	4.4	3.3	2.8	2.6	2.4	2.5	2.4	2.4
	1.5	1.2	2.1	1.7	1.5	1.5	1.4	1.4	1.5
	2.0	0.6	1.5	1.1	1.0	1.1	0.9	1.0	1.1
	3.0	0.5	1.0	0.6	0.6	0.7	0.6	0.7	0.7
	4.0	0.5	0.6	0.5	0.5	0.5	0.5	0.5	0.5
	5.0	0.5	0.5	0.5	0.5	0.5	0.5	0.5	0.5
h		10.597	8.786	8.001	7.834	7.587	8.904	8.877	8.840
g		—	—	2.579	2.973	3.772	2.645	3.129	4.079

Table 3.10: SSATS Values of the SS_1 and SS_2 MEWMA Chart with an Initial Group Size of $n_1 = 4$ when $p = 4$

		Shewhart	MEWMA	SS_1 MEWMA			SS_2 MEWMA		
n_1		5	5	4	4	4	4	4	4
n_2		—	—	6	8	14	6	8	14
τ		5	5	10	12	18	10	12	18
r_j		—	0.1	0.08635	0.08940	0.09366	0.08635	0.08940	0.09366
δ	0.0	200.0	200.0	200.0	200.0	200.0	200.0	200.0	200.0
	0.1	184.1	105.0	93.3	93.7	95.0	98.5	96.6	93.5
	0.15	167.3	63.3	52.3	52.3	53.0	56.0	54.5	52.3
	0.2	147.4	40.4	32.1	32.0	32.2	34.1	33.0	31.7
	0.25	126.7	27.8	22.0	21.7	21.7	22.7	22.0	21.3
	0.3	106.9	20.6	16.3	16.0	15.9	16.5	16.0	15.6
	0.4	73.1	13.0	10.6	10.3	10.1	10.3	10.0	9.9
	0.5	48.7	9.4	7.8	7.5	7.3	7.4	7.2	7.2
	0.75	17.6	5.4	4.6	4.5	4.2	4.3	4.2	4.1
	1.0	7.0	3.8	3.3	3.1	2.9	3.0	2.9	2.9
	1.5	1.6	2.3	2.0	1.9	1.7	1.7	1.7	1.8
	2.0	0.7	1.7	1.4	1.3	1.3	1.1	1.2	1.3
	3.0	0.5	1.1	0.8	0.8	0.8	0.7	0.8	0.8
	4.0	0.5	0.7	0.6	0.6	0.6	0.6	0.6	0.6
	5.0	0.5	0.5	0.5	0.5	0.5	0.5	0.5	0.5
h		14.860	12.913	12.032	11.836	11.550	13.060	13.026	12.980
g		—	—	5.136	5.687	6.763	5.221	5.887	7.145

Table 3.11: ANOS Values of the SS_1 MEWMA Chart when $p = 2$

		Shewhart	MEWMA	SS_1 MEWMA								
n_1		5	5	2	2	2	3	3	3	4	4	4
n_2		—	—	8	10	16	7	9	15	6	8	14
τ		5	5	10	12	18	10	12	18	10	12	18
δ	0.0	1000.0	1000.0	1000.0	1000.0	1000.0	1000.0	1000.0	1000.0	1000.0	1000.0	1000.0
	0.1	878.4	437.3	402.1	405.7	417.4	404.1	407.5	417.1	412.5	416.2	424.2
	0.15	759.7	253.2	234.3	236.8	245.5	233.8	236.4	243.9	237.6	240.1	246.9
	0.2	632.9	161.5	155.5	157.5	164.0	153.9	155.7	161.4	154.3	156.0	161.2
	0.25	514.1	112.6	113.8	115.4	120.5	111.7	113.0	117.5	110.6	111.8	115.9
	0.3	411.3	84.3	88.9	90.2	94.4	86.7	87.8	91.5	84.9	85.9	89.4
	0.4	258.3	54.7	61.2	62.2	65.5	59.2	60.0	62.9	57.1	57.8	60.5
	0.5	162.2	39.9	46.3	47.2	50.0	44.6	45.2	47.7	42.7	43.3	45.5
	0.75	55.2	23.4	28.5	29.1	31.4	27.1	27.7	29.6	25.8	26.2	28.0
	1.0	22.1	16.4	20.3	20.9	22.6	19.3	19.7	21.3	18.2	18.6	20.2
	1.5	5.8	10.3	12.6	12.8	15.2	11.9	12.1	14.3	11.2	11.4	13.1
	2.0	3.0	7.4	8.8	9.2	12.4	8.4	8.7	10.9	7.7	7.8	9.3
	3.0	2.5	4.8	5.5	6.4	8.6	4.8	5.3	6.7	4.3	4.6	5.5
	4.0	2.5	3.2	4.2	4.7	5.9	3.2	3.5	4.2	2.8	3.0	3.3
	5.0	2.5	2.6	3.0	3.2	3.7	2.2	2.2	2.4	2.2	2.2	2.2

Table 3.12: ANOS Values of the SS_1 MEWMA Chart when $p = 4$

		Shewhart	MEWMA	SS_1 MEWMA								
n_1		5	5	2	2	2	3	3	3	4	4	4
n_2		—	—	8	10	16	7	9	15	6	8	14
τ		5	5	10	12	18	10	12	18	10	12	18
δ	0.0	1000.0	1000.0	1000.0	1000.0	1000.0	1000.0	1000.0	1000.0	1000.0	1000.0	1000.0
	0.1	920.5	524.9	480.0	485.1	499.7	483.8	488.2	500.7	495.6	499.8	510.3
	0.15	836.5	316.7	284.3	288.3	300.0	285.8	289.5	299.4	293.2	296.4	305.0
	0.2	737.2	201.9	187.4	190.1	198.6	186.6	189.0	196.2	188.8	191.1	197.6
	0.25	633.7	139.2	135.7	137.8	144.2	133.9	135.6	141.1	133.6	135.1	140.2
	0.3	534.3	102.9	105.3	106.9	112.0	103.0	104.3	108.7	101.5	102.7	106.7
	0.4	365.5	65.2	71.8	73.0	76.8	69.6	70.5	73.7	67.4	68.1	71.1
	0.5	243.5	46.9	54.2	55.1	58.3	52.1	52.9	55.6	49.9	50.6	53.0
	0.75	87.9	27.1	33.2	33.9	36.3	31.6	32.2	34.3	30.0	30.4	32.3
	1.0	34.8	18.9	23.7	24.3	26.2	22.4	22.9	24.6	21.2	21.5	23.2
	1.5	8.2	11.7	14.8	15.2	17.1	13.9	14.2	16.3	13.1	13.3	15.0
	2.0	3.5	8.5	10.4	10.8	13.9	9.9	10.2	12.6	9.1	9.3	10.9
	3.0	2.5	5.5	6.5	7.4	10.1	5.9	6.3	8.0	5.2	5.5	6.6
	4.0	2.5	3.7	4.9	5.6	7.2	4.0	4.4	5.4	3.4	3.7	4.3
	5.0	2.5	2.7	3.8	4.2	5.2	2.8	3.0	3.4	2.5	2.5	2.7

3.5 Conclusions and Recommendations for Applications

We have shown that the SS_1 and SS_2 MEWMA control charts have substantially better performance than the standard MEWMA chart that does not use sequential sampling. In terms of good overall performance, it seems to be reasonable to use the same value of the smoothing parameter r for all group sizes, which is the value appropriate for the average group size. The best overall performance of the SS_1 and SS_2 MEWMA charts seems to be achieved when the first group size is $n_1 = 3$ or 4 relative to the average sample size of 5. It is hard to determine whether the SS_1 or SS_2 MEWMA chart has better performance, but both are still better than the standard MEWMA chart. The SS MEWMA chart can effectively replace the standard MEWMA chart if no extra administrative costs are needed for the sequential sampling. Since the SSATS performance of the SS_1 and SS_2 MEWMA charts depends on the choice of group sizes and the number of variables monitored, in practical applications sampling constraints of choosing the group sizes need to be considered in designing the SS_1 and SS_2 MEWMA charts.

Chapter 4

The MEWMA Control Chart with Unequal Sample Sizes

There are many different situations that could call for multivariate monitoring with unequal sample sizes. Some variables are very expensive to measure, but others are inexpensive. Also, some variables may be much more important for the quality of a product than others. Another reason for considering control charts with unequal sample sizes is the situation where date are missing when running standard control charts. This section investigates the UG MEWMA chart that improves the performance of the standard MEWMA chart for the situation in which some variables are inexpensive to measure so that more observations are measured for the inexpensive variables.

To define the proposed UG MEWMA control chart, first define the vector of sample sizes. At each sampling point, n_i observations are obtained on variable i for $i = 1, 2, \cdots, p$. The vector representing the sample sizes from the process is defined as $\boldsymbol{n}$, where $\boldsymbol{n} = (n_1, n_2, \cdots, n_p)^T$ and n_i represents the sample size for the i^{th} variable. Throughout the rest of this chapter, it is assumed, without loss of generality, that the quality characteristic X_i, where $i = 1, 2, \cdots, p$, has the sample size of n_i such that $n_1 \leq n_2 \leq \cdots \leq n_p$. If $n_1 = n_2 = \cdots = n_p$, then the sample size vector is defined as $\boldsymbol{n} = (n, n, \cdots, n)^T$ and one has

the standard MEWMA chart as given in Section 2.5.2.

Table 4.1 gives an illustration of the ways in which the sample sizes of p quality characteristics could be defined for the proposed method of the UG MEWMA control chart. Suppose that there are $p = 5$ quality characteristics to be monitored and that a total of 6 items are available at each sampling point of the process. The symbol M in each cell of Table 4.1 indicates that a variable is measured for the corresponding item at each sampling point. After sorting each quality characteristic from lowest to highest by the measurement cost, the quality characteristic X_1 is now the most expensive variable to measure and the quality characteristic X_2 is the second most expensive variable to measure, and so on. For example, the variable X_5 is measured for a total of 6 items, but the variable X_1 is measured for only 2 items. The second most expensive variable X_2 is measured for 3 items and the third and fourth most expensive variables, which are assumed to have the equal measurement cost, are measured for 4 items. In this example the sample size vector is $\boldsymbol{n} = (2, 3, 4, 4, 6)^T$.

Table 4.1: Data Structure of an Example of the UG MEWMA Chart

	Variable				
Item	X_1	X_2	X_3	X_4	X_5
1	M	M	M	M	M
2	M	M	M	M	M
3		M	M	M	M
4			M	M	M
5					M
6					M
Sample Size	2	3	4	4	6

4.1 The Proposed UG MEWMA Control Chart

For the proposed UG MEWMA chart, since now a different sample size is used for each quality characteristic some modifications are made in the assumptions, given in Section 2.5.2, for the standard MEWMA control chart with equal sample sizes. The modified assumptions are mainly caused by the fact that the covariance structure between the sample means for variables changes when each variable has a different sample size. A more detailed discussion of this issue is given later in this section.

Let X_{kij} be the j^{th} observed value of the quality characteristic i at the k^{th} sampling point for $j = 1, 2, \cdots, n_i$ and let $\bar{X}_{ki}$ be the average of the n_i observations obtained for variable i at sampling point k, for $i = 1, 2, \cdots, p$ and $k = 1, 2, \cdots$. A sequence of $p \times 1$ sample mean vectors at the k^{th} sampling point is defined as

$$\bar{\boldsymbol{X}}_k = (\bar{X}_{k1}, \bar{X}_{k2}, \cdots, \bar{X}_{kp})^T, \tag{4.1}$$

where $\bar{X}_{ki} = \sum_{j=1}^{n_i} X_{kij}/n_i$. Corresponding to $\bar{X}_{ki}$ and $\bar{\boldsymbol{X}}_k$, define the standardized sample mean to be

$$Z_{ki} = \frac{\sqrt{n_i}(\bar{X}_{ki} - \mu_{0i})}{\sigma_{0i}}, \quad i = 1, 2, \cdots, p,$$

and the standardized sample mean vector to be

$$\boldsymbol{Z}_k = (Z_{k1}, Z_{k2}, \cdots, Z_{kp})^T. \tag{4.2}$$

We define the EWMA vector $\boldsymbol{Y}_k$ at sampling point $k \geq 1$ to be

$$\boldsymbol{Y}_k = r\boldsymbol{Z}_k + (1 - r)\boldsymbol{Y}_{k-1}, \quad k = 1, 2, \cdots,$$

where $\boldsymbol{Y}_0 = \boldsymbol{0}$ and r is a smoothing parameter satisfying $0 < r \leq 1$. At sampling point k, the decision rule will be based on the statistic

$$T_k^2 = \boldsymbol{Y}_k^T \boldsymbol{\Sigma}_k^{-1} \boldsymbol{Y}_k, \tag{4.3}$$

where $\boldsymbol{\Sigma}_k$ is the covariance matrix of $\boldsymbol{Y}_k$. The covariance matrix $\boldsymbol{\Sigma}_k$ at sampling point k can be obtained using

$$\begin{aligned}\boldsymbol{\Sigma}_k &= (1-r)^2\boldsymbol{\Sigma}_{k-1} + r^2\boldsymbol{\Sigma}_Z \\ &= \{r[1-(1-r)^{2k}]/(2-r)\}\boldsymbol{\Sigma}_Z,\end{aligned}$$

where $\boldsymbol{\Sigma}_Z$ is the covariance matrix of $\boldsymbol{Z}_k$, the standardized sample mean vector defined in Equation (4.2).

A major difference in assumptions between the standard MEWMA control chart with equal sample sizes and the UG MEWMA control chart is that covariance matrices ($\boldsymbol{\Sigma}_k$) used for calculating the MEWMA statistic in Equations (2.10) and (4.3) are different. This difference originates from the data structure, which is illustrated in detail as follows.

Let $\boldsymbol{\Sigma}_{\bar{\boldsymbol{X}}}$ be a covariance matrix of $\bar{\boldsymbol{X}}_k$ in Equation (4.1). A $p \times p$ covariance matrix $\boldsymbol{\Sigma}_{\bar{\boldsymbol{X}}}$ can be obtained for each of the p quality characteristics as

$$\boldsymbol{\Sigma}_{\bar{\boldsymbol{X}}} = \begin{pmatrix} \frac{\sigma_{01}^2}{n_1} & \frac{\sigma_{012}}{n_2} & \frac{\sigma_{013}}{n_3} & \cdots & \frac{\sigma_{01p}}{n_p} \\ & \frac{\sigma_{02}^2}{n_2} & \frac{\sigma_{023}}{n_3} & \cdots & \frac{\sigma_{02p}}{n_p} \\ & & \frac{\sigma_{03}^2}{n_3} & \cdots & \frac{\sigma_{03p}}{n_p} \\ & symmetric & & \ddots & \vdots \\ & & & & \frac{\sigma_{0p}^2}{n_p} \end{pmatrix}, \tag{4.4}$$

where, as defined in Section 2.1, σ_{0i}^2 is the i^{th} diagonal component of $\boldsymbol{\Sigma}_0$ and $\sigma_{0ii'}$, for $i \neq i'$, is the (i, i') component of $\boldsymbol{\Sigma}_0$. Derivation of the covariance between two quality characteristics i and i' is given below with the assumption that $n_i < n_{i'}$. We have

$$\begin{aligned}\mathrm{Cov}(\bar{X}_{ki}, \bar{X}_{ki'}) &= E(\bar{X}_{ki}\bar{X}_{ki'}) - E(\bar{X}_{ki})E(\bar{X}_{ki'}) \\ &= \frac{1}{n_i n_{i'}} E\left\{\left(\sum_{t=1}^{n_i} X_{kit}\right)\left(\sum_{s=1}^{n_{i'}} X_{ki's}\right)\right\} - E(\bar{X}_{ki})E(\bar{X}_{ki'}) \\ &= \frac{1}{n_i n_{i'}} \sum_{t=1}^{n_i}\sum_{s=1}^{n_{i'}} \mathrm{Cov}(X_{kit}, X_{ki's})\end{aligned}$$

$$\begin{cases} \text{if} \quad t = s \quad \text{then} \quad \text{Cov}(X_{kit}, X_{ki's}) = \sigma_{0ii'} \\ \text{if} \quad t \neq s \quad \text{then} \quad \text{Cov}(X_{kit}, X_{ki's}) = 0 \end{cases}$$

$$= \frac{1}{n_i n_{i'}} n_i \text{Cov}(X_{kit}, X_{ki's})$$

$$= \frac{1}{n_{i'}} \sigma_{0ii'},$$

where if the j^{th} observation is obtained for both quality characteristic i and i', then the covariance between two quality characteristics is $\sigma_{0ii'}$, i.e.,

$$\text{Cov}(X_{kij}, X_{ki'j}) = \sigma_{0ii'} \quad \text{if } j \leq min(n_i, n_{i'}).$$

Since $\boldsymbol{Z}_k$ is the standardized sample mean vector, the covariance matrix of the standardized sample mean vector $\boldsymbol{Z}_k$ ($\boldsymbol{\Sigma}_Z$) can be obtained directly from the covariance matrix of the sample mean vector ($\boldsymbol{\Sigma}_{\bar{\boldsymbol{X}}}$) given in Equation (4.4) as

$$\boldsymbol{\Sigma}_Z = \begin{pmatrix} 1 & \sqrt{\frac{n_1}{n_2}}\rho_{12} & \sqrt{\frac{n_1}{n_3}}\rho_{13} & \cdots & \sqrt{\frac{n_1}{n_p}}\rho_{1p} \\ & 1 & \sqrt{\frac{n_2}{n_3}}\rho_{23} & \cdots & \sqrt{\frac{n_2}{n_p}}\rho_{2p} \\ & & 1 & \cdots & \sqrt{\frac{n_3}{n_p}}\rho_{3p} \\ & symmetric & & \ddots & \vdots \\ & & & & 1 \end{pmatrix}, \tag{4.5}$$

where $\rho_{ii'}$ is the correlation coefficient between variables i and i' satisfying

$$\rho_{ii'} = \frac{\sigma_{0ii'}}{\sigma_{0i}\sigma_{0i'}}.$$

Specifically, the following decision rule is proposed for the UG MEWMA chart. The decision rule is same as that of the standard MEWMA chart described in Section 2.5.2 except the way that the covariance matrix is determined. If the current sampling point is k,

1. Observe a set of observations.

2. Compute $\boldsymbol{Z}_k$ based on $\boldsymbol{n} = (n_1, n_2, \cdots, n_p)^T$, where $n_1 \leq n_2 \leq \cdots \leq n_p$.

3. Compute $\boldsymbol{Y}_k = r\boldsymbol{Z}_k + (1-r)\boldsymbol{Y}_{k-1}$.

4. Compute $T_k^2 = \boldsymbol{Y}_k^T \boldsymbol{\Sigma}_k^{-1} \boldsymbol{Y}_k$.

   (a) If $T_k^2 \leq h$, then stop sampling at sampling point k and wait until sampling point $k+1$ to sample again.

   (b) If $T_k^2 > h$, then signal that there has been a change in the mean vector $\boldsymbol{\mu}$.

As in the standard MEWMA chart defined in Section 2.5.2, one gives an out-of-control signal whenever T_k^2 is greater than the upper control limit h, where h (> 0) is chosen to give a specified in-control ATS.

4.2 Parameter Choices for the Comparisons

Two basic control charts, the Shewhart chart based on Hotelling's statistic and the standard MEWMA chart with equal sample sizes with the smoothing parameter of $r = 0.1$, are used as reference charts for evaluating the efficiency of the proposed UG MEWMA chart. For both of these reference charts, a sample size of $n = 5$ and an in-control ATS of 200 are considered.

The in-control ANOS can only be defined as a vector since each quality characteristic has an unequal sample size so that the ANOS can be defined for each quality characteristic. The proposed UG MEWMA control chart is designed to match the total expected measurement cost instead of the ANOS with those of the reference charts for the fair comparison of the ATS performance when the process is in-control. In the proposed method, it is assumed that each quality characteristic has a fixed measurement cost. Let f_i be the fixed measurement cost for the quality characteristic i, where $i = 1, 2, \cdots, p$. The vector representing the fixed measurement cost is defined as $\boldsymbol{f}$, where $\boldsymbol{f} = (f_1, f_2, \cdots, f_p)^T$. Then the measurement cost at each sampling point is computed as

$$\boldsymbol{f}^T \boldsymbol{n} = f_1 n_1 + f_2 n_2 + \cdots + f_p n_p. \tag{4.6}$$

The total expected measurement cost, which is used instead of the ANOS to measure sampling costs in this given situation, now can be obtained by multiplying the ANSS by the measurement cost given in Equation (4.6).

In this section, for the case of $p = 2$ the cost ratio is defined as f_1/f_2, the ratio of the fixed measurement cost of each quality characteristic, with the assumption that $f_1 \geq f_2$. We now consider the cost ratio of 10 in these simulation studies, which is the case in which one variable is more expensive to measure than the other. In this case, if the less expensive quality characteristic (X_2) has a unit measurement cost, then the measurement cost of the more expensive quality characteristic (X_1) is 10 unit times larger than that of X_2. Since the standard Shewhart and MEWMA control charts with the equal sample size of 5 are compared to the proposed UG MEWMA control charts, the out-of-control ATS performance comparisons are made while maintaining the in-control measurement cost of 55 per sampling point for the proposed UG MEWMA control charts. This means that all control charts, including reference charts, studied are designed to give the same total in-control measurement cost of 11,000.

As described in the Section 3.2, shifts in the process mean vector are measured in units of the non-centrality parameter

$$\delta = \sqrt{\boldsymbol{\nu}^T \boldsymbol{\Sigma}_c^{-1} \boldsymbol{\nu}},$$

where $\boldsymbol{\Sigma}_c$ is the correlation matrix corresponding to the known covariance matrix $\boldsymbol{\Sigma}_0$. The i^{th} component of $\boldsymbol{\nu}$, the sustained standardized mean shift vector from the in-control mean vector $\boldsymbol{\mu}_0$ is

$$\nu_i = \frac{\mu_i - \mu_{0i}}{\sigma_{0i}}, \quad i = 1, 2, \cdots, p.$$

If the standard MEWMA chart has the sample size vector of $\boldsymbol{n} = (n, n, \cdots, n)^T$ (with the equal sample size n for all p variables), then the i^{th} component of the standardized sample

mean shift vector $\boldsymbol{\nu}'$, for $i = 1, 2, \cdots, p$, is now

$$\begin{aligned}\nu_i' &= \mathrm{E}(Z_{ki}) \\ &= \sqrt{n}\frac{\mu_i - \mu_{0i}}{\sigma_{0i}} \\ &= \sqrt{n}\nu_i,\end{aligned}$$

where the sizes of the standardized sample mean shifts (ν_i') are proportional to the square root of the sample size n. The properties of the standard MEWMA chart with the equal sample size n depend on $\boldsymbol{\mu}$ only through the value of $\sqrt{n}\delta$. Thus, the performance of the standard MEWMA chart is said to be directionally invariant.

In the proposed UG MEWMA chart, however, if a different sample size is used for each quality characteristic, then now the i^{th} component of the standardized sample mean shift vector is

$$\begin{aligned}\nu_i' &= \mathrm{E}(Z_{ki}) \\ &= \sqrt{n_i}\frac{\mu_i - \mu_{0i}}{\sigma_{0i}} \\ &= \sqrt{n_i}\nu_i.\end{aligned}$$

For a given value of δ the sizes of the standardized sample mean shifts depend on the unequal sample size n_i, which means more weight is given to the axis having the larger sample size with the weight proportional to the square root of the sample size n_i. So that the performance of the proposed UG MEWMA chart is no longer directionally invariant. Even though the SSATS performance depends on the direction of shifts in addition to a given value of δ, future comparisons in the unequal sample size case will be indexed by δ. For example, assume the case that only one of the p variables shifts when the p variables are independent. If the variable having the largest sample size of n_p shifts in the direction of its own axis then the shift size of the standardized sample mean for this variable is $\sqrt{n_p}\delta$, and if the variable having the smallest sample size of n_1 shifts in the direction of its own axis then the shift size of the standardized sample mean for this variable is $\sqrt{n_1}\delta$. If the p variables are correlated with each other, for a given value of δ a shift direction close to the

axis of the largest sample size has a larger shift size than a shift direction close to the axis of the smallest sample size.

A total of 4 different values of the correlation coefficient ρ, given in Equation (4.5), are considered from the independent case ($\rho = 0$) to the more strongly dependent case ($\rho = 0.9$) with two mild values of correlation corresponding to $\rho = 0.3$ and $\rho = 0.6$. The values for the size of a sustained shift (δ) considered in the tables are 0.1, 0.15, 0.2, 0.25, 0.3, 0.4, 0.5, 0.75, 1.0, 1.5, 2.0, 3.0, 4.0, and 5.0.

4.3 The Effects of the Choice of the Sample Sizes

The in-control ATS of the proposed UG MEWMA charts were evaluated using simulation with 1,000,000 runs. As given in Section 3.4 for SS_1 and SS_2 MEWMA charts, the value of h is adjusted to obtain a specific value of the in-control ATS. The in-control total expected measurement cost is set to be a constant for all proposed UG MEWMA charts considered. Based on some initial guesses for h, the required value of h is obtained by iterating steps of regressing the logarithms of the ATS on h and then solving the regression equation. The SSATS was obtained by simulating the operation of the proposed UG MEWMA charts for 100 in-control observation vectors, and then introducing a shift in $\boldsymbol{\mu}$.

Sample size vectors of $\boldsymbol{n} = \{(1,45), (2,35), (3,25), (4,15)\}$ are chosen for the proposed UG MEWMA control charts and SSATS values are compared to those of the reference charts. In Section 3.3 for the SS_1 and SS_2 MEWMA charts, the average sample size was used to determine the smoothing parameter (r), which gives fair comparisons for control charts with different sample sizes. The value of the smoothing parameter ($r = 0.1$) is used for the proposed UG MEWMA charts, where the value of 0.1 is chosen to match with the smoothing parameter of the standard MEWMA chart.

Since the ATS performance of the proposed UG MEWMA charts depends on shift directions in addition to the value of δ as discussed previously, the effect of the shift direction

was investigated first. For the sample size vectors of $\boldsymbol{n} = \{(1,45), (4,15)\}$ and correlation coefficients $\rho = \{0.0, 0.3, 0.6, 0.9\}$, the SSATS is evaluated for varying shift directions.

The shift direction angle θ is defined to be an angle made by the shift direction with the axis for the first variable. The shift direction could be expressed using a line having the slope $\tan(\theta)$ and the zero intercept. The values of θ used to generate the figures were chosen in a range from 0° to 180° by increasing 10°, and SSATS values were evaluated using simulation with 1,000,000 runs for each shift direction. Later in this section, instead of specifying some directions of interest, the case of randomly generated shift directions will be considered.

The figures presenting results as a function of the shift direction in the proposed UG MEWMA charts are organized so that the figures for the size of shift $\delta = 0.25$ are given in Figures 4.1-4.2 and the figures for the size of shift $\delta = 1.0$ are given in Figures 4.3-4.4. For purposes of comparison, a reference line is added to the figure for the standard MEWMA chart with the fixed sample size of $n = 5$. Since the performance of the standard MEWMA chart is directionally invariant, a reference line is a horizontal line. Figures 4.1-4.2 show SSATS values of shift directions for the proposed UG MEWMA charts for the case of $\rho = \{0, 0.3\}$ and $\rho = \{0.6, 0.9\}$, respectively.

From Figure 4.1, we see that for the independent case ($\rho = 0$) and a relatively small value of correlation ($\rho = 0.3$), the minimum SSATS value can be achieved in the shift direction of $\theta = 90^\circ$, which is the axis having the larger sample size. The SSATS values get larger as the shift direction approaches $\theta = 0^\circ$ or 180°, which is the axis of the variable having the smaller sample size. We can also see that when $\rho = 0$ the SSATS values are symmetric around the shift direction of $\theta = 90^\circ$. From Figure 4.2, we notice that as the value of correlation between two variables increases ($\rho = \{0.6, 0.9\}$) the SSATS values are not symmetric and the minimum SSATS value is in the shift direction of about $\theta = 45^\circ$. The maximum value of the SSATS is in the shift direction of $\theta = 0^\circ$ or 180° for all choices of ρ. As ρ increases the difference between the minimum and maximum values of the SSATS is

getting larger, which causes the poor ATS performance as ρ increases when averaged SSATS values are considered later in this section. Also the range of shift directions for which the UG MEWMA chart has a smaller SSATS than the standard MEWMA chart is getting smaller as ρ increases. For example, for $\rho = 0$ the shift directions having better SSATS performance for the UG MEWMA chart range from 17.55° to 162.45° regardless of which sample size vectors and shift sizes are used. When $\rho > 0$ the range of shift directions for which the UG MEWMA chart has better SSATS performance is a function of the sample size vector and ρ. For example, the shift directions giving smaller SSATS values for the UG MEWMA chart range from 18.30° to 151.27° for $\rho = 0.6$ and from 24.87° to 109.67° for $\rho = 0.9$ with the sample size vector (1,45), and from 23.34° to 138.19° for $\rho = 0.6$ and from 32.22° to 77.95° for $\rho = 0.9$ with the sample size vector (4,15). Figures 4.3-4.4 show the same pattern of SSATS performance as Figures 4.1-4.2, except that the size of shift considered is $\delta = 1.0$.

Examining Figures 4.1-4.4 shows that it would be advantageous to apply the proposed UG MEWMA chart in situations where one is more interested in a shift which is likely to be in directions where performance is good rather than overall chart performance. For example, if one needs to quickly detect a shift in the less expensive variable (i.e., one variable is less expensive than the other, so that the specific direction has more observations), then it would be advantageous to use the proposed UG MEWMA chart instead of the standard MEWMA chart with the equal sample size regardless of the correlation structure between the two variables.

In this section SSATS values averaged over randomly generated shift directions are evaluated. The shift directions are randomly generated for each simulation run using the algorithm proposed by Johnson (1987), where the algorithm assumes all directions are equally likely (assuming a uniform distribution), and then the averaged SSATS value is calculated over the SSATS values evaluated for each simulation run. This means that a total of 1,000,000 shift directions are used to calculate the averaged SSATS.

Tables 4.2-4.5 give SSATS values for the case of $p = 2$ for the proposed UG MEWMA

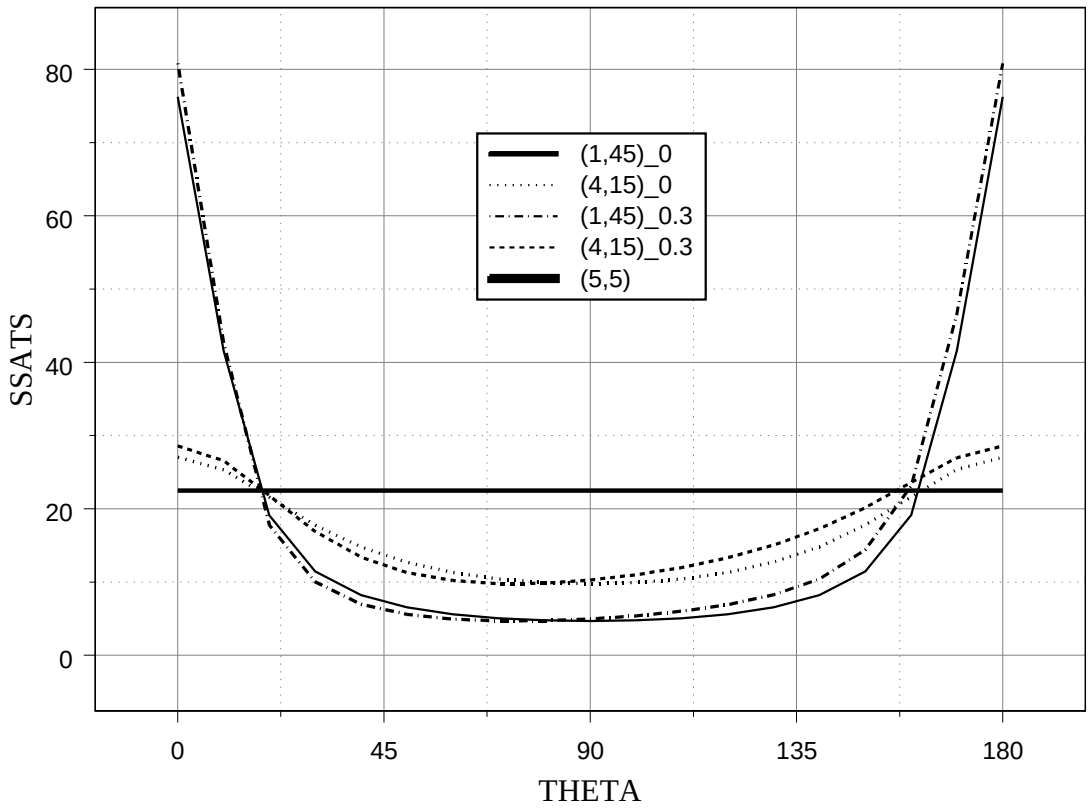

Figure 4.1: SSATS Values of the UG MEWMA Chart by Varying Shift Directions when ρ = {0, 0.3} for $\delta = 0.25$

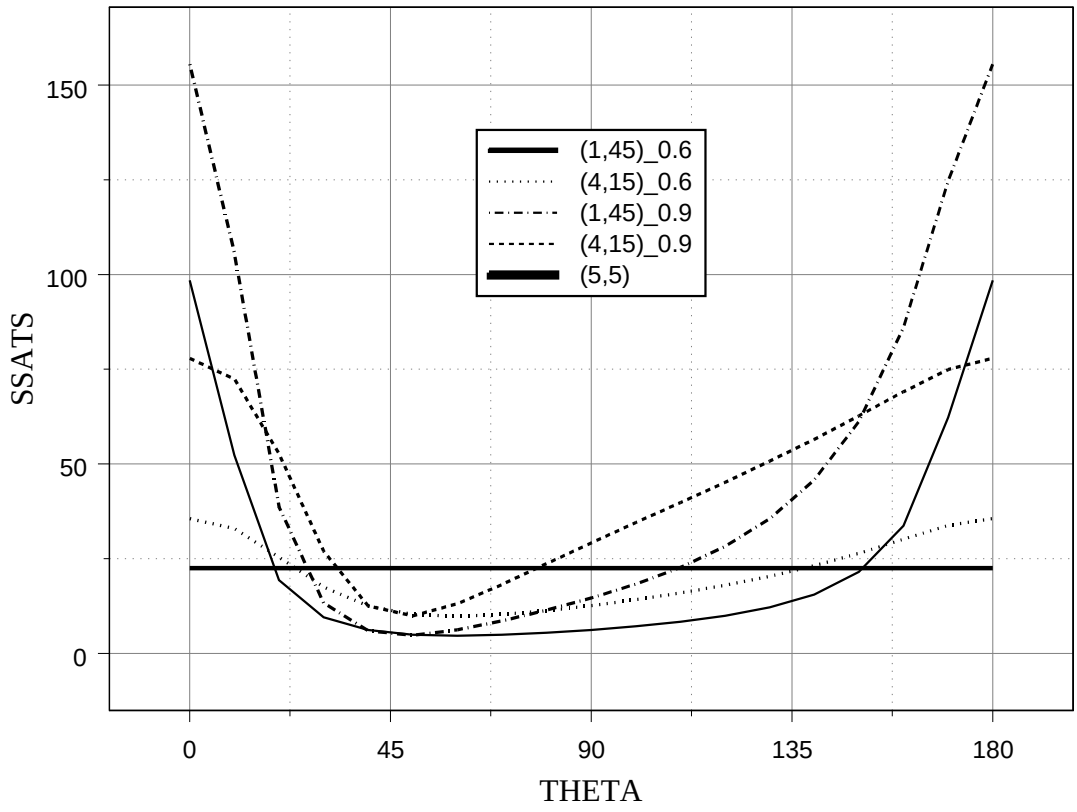

Figure 4.2: SSATS Values of the UG MEWMA Chart by Varying Shift Directions when ρ = {0.6, 0.9} for $\delta = 0.25$

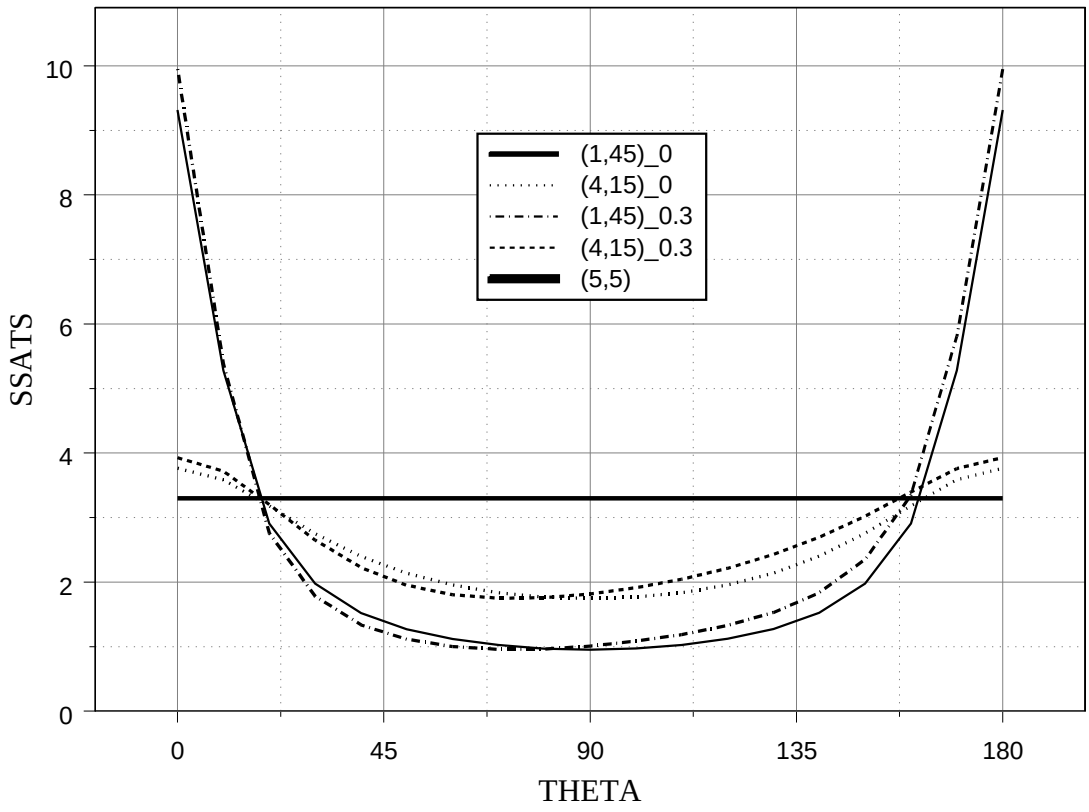

Figure 4.3: SSATS Values of the UG MEWMA Chart by Varying Shift Directions when ρ = {0, 0.3} for $\delta = 1.0$

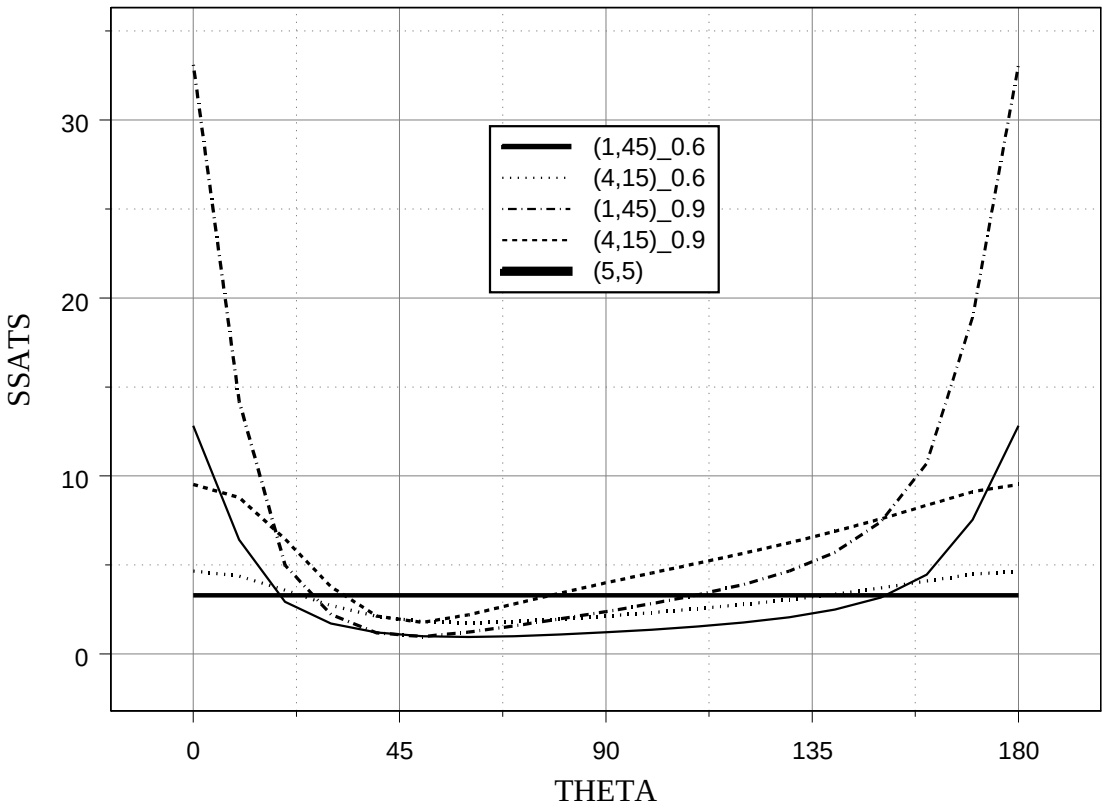

Figure 4.4: SSATS Values of the UG MEWMA Chart by Varying Shift Directions when ρ = {0.6, 0.9} for $\delta = 1.0$

control charts that have different values of correlation coefficient ρ=0.0, 0.3, 0.6, and 0.9, respectively. For purposes of comparison, columns 2 and 3 contain SSATS values for the standard Shewhart and standard MEWMA charts with the fixed sample size of $n = 5$, respectively. Columns 4-6 correspond to UG MEWMA charts, where the sample size vectors considered for $\boldsymbol{n}$ are (1,45), (2,35), (3,25), and (4,15), respectively, corresponding to the measurement cost 55 at each sampling point.

Tables 4.6-4.9 have the same structure as Tables 4.2-4.5, except that Tables 4.6-4.9 give total expected measurement costs for the proposed UG MEWMA charts.

From Tables 4.2-4.5, we see that unless the two variables are highly correlated, the proposed UG MEWMA charts perform much better than both reference charts in detecting small-to-moderate sustained shifts. In terms of good overall performance, the sample size vectors of (2,35) or (3,25) seem to be the best choices. The SSATS performance of the four chosen sample size vectors is the same for large shift sizes but the sample size vectors of (2,35) or (3,25) are better for small-to-moderate shifts (except for the very small shift of 0.1) than the sample size vectors of (1,45) or (4,15). If two variables are highly correlated ($\rho = 0.9$), the proposed UG MEWMA charts are still better than the standard Shewhart chart in detecting small shifts but worse than the standard MEWMA chart over the entire range of shifts.

From Tables 4.6-4.9, we see that when each sample size vectors are compared in terms of the total expected measurement cost, the sample size vectors of (2,35) or (3,25) have the smaller total expected measurement cost for small-to-moderate shifts (except for very small shifts of 0.1 and 0.15) than the other two sample size vector, so using the sample size vectors of (2,35) or (3,25) would be the best choices in terms of good overall performance both in the ATS and measurement cost. When two variables are not highly correlated, the reduction in measurement costs is large when the proposed UG MEWMA charts are used instead of the reference charts.

Table 4.2: SSATS Values of the UG MEWMA Chart when $\rho = 0$

		Shewhart	MEWMA	UG MEWMA			
$\boldsymbol{n}$		(5,5)	(5,5)	(1,45)	(2,35)	(3,25)	(4,15)
r		—	0.1	0.1	0.1	0.1	0.1
δ	0.0	200.0	200.0	200.0	200.0	200.0	200.0
	0.1	175.7	87.5	50.8	51.6	55.0	63.2
	0.15	151.9	50.6	31.6	30.2	31.0	35.1
	0.2	126.6	32.3	21.7	19.9	20.0	22.4
	0.25	102.8	22.5	15.8	14.2	14.2	15.8
	0.3	82.3	16.9	12.2	10.8	10.8	12.0
	0.4	51.7	10.9	8.0	7.1	7.2	7.9
	0.5	32.4	8.0	5.8	5.2	5.3	5.8
	0.75	11.0	4.7	3.4	3.1	3.2	3.5
	1.0	4.4	3.3	2.3	2.2	2.3	2.5
	1.5	1.2	2.1	1.4	1.4	1.4	1.6
	2.0	0.6	1.5	1.0	1.0	1.0	1.1
	3.0	0.5	1.0	0.7	0.7	0.7	0.7
	4.0	0.5	0.6	0.6	0.6	0.6	0.6
	5.0	0.5	0.5	0.6	0.5	0.5	0.5
h		10.597	8.786	8.786	8.786	8.786	8.786

Table 4.3: SSATS Values of the UG MEWMA Chart when $\rho = 0.3$

		Shewhart	MEWMA	UG MEWMA			
$\boldsymbol{n}$		(5,5)	(5,5)	(1,45)	(2,35)	(3,25)	(4,15)
r		—	0.1	0.1	0.1	0.1	0.1
δ	0.0	200.0	200.0	200.0	200.0	200.0	200.0
	0.1	175.7	87.5	53.1	54.0	57.5	65.7
	0.15	151.9	50.6	33.3	32.0	32.9	36.8
	0.2	126.6	32.3	23.0	21.1	21.2	23.5
	0.25	102.8	22.5	16.9	15.1	15.0	16.5
	0.3	82.3	16.9	13.0	11.5	11.4	12.5
	0.4	51.7	10.9	8.5	7.6	7.5	8.2
	0.5	32.4	8.0	6.2	5.5	5.6	6.1
	0.75	11.0	4.7	3.6	3.3	3.3	3.6
	1.0	4.4	3.3	2.5	2.3	2.3	2.6
	1.5	1.2	2.1	1.5	1.4	1.5	1.6
	2.0	0.6	1.5	1.1	1.0	1.0	1.2
	3.0	0.5	1.0	0.8	0.7	0.7	0.7
	4.0	0.5	0.6	0.6	0.6	0.6	0.6
	5.0	0.5	0.5	0.6	0.5	0.5	0.5
h		10.597	8.786	8.786	8.786	8.786	8.786

Table 4.4: SSATS Values of the UG MEWMA Chart when $\rho = 0.6$

		Shewhart	MEWMA	UG MEWMA			
$\boldsymbol{n}$		(5,5)	(5,5)	(1,45)	(2,35)	(3,25)	(4,15)
r		—	0.1	0.1	0.1	0.1	0.1
δ	0.0	200.0	200.0	200.0	200.0	200.0	200.0
	0.1	175.7	87.5	62.4	64.0	67.9	75.7
	0.15	151.9	50.6	40.5	39.4	40.3	44.0
	0.2	126.6	32.3	28.5	26.6	26.5	28.3
	0.25	102.8	22.5	21.2	19.2	18.9	20.0
	0.3	82.3	16.9	16.5	14.6	14.2	15.0
	0.4	51.7	10.9	10.8	9.5	9.3	9.8
	0.5	32.4	8.0	7.8	6.9	6.8	7.1
	0.75	11.0	4.7	4.4	4.0	4.0	4.2
	1.0	4.4	3.3	3.0	2.8	2.8	3.0
	1.5	1.2	2.1	1.8	1.7	1.7	1.8
	2.0	0.6	1.5	1.3	1.2	1.2	1.3
	3.0	0.5	1.0	0.9	0.8	0.8	0.8
	4.0	0.5	0.6	0.7	0.7	0.6	0.6
	5.0	0.5	0.5	0.6	0.6	0.6	0.5
h		10.597	8.786	8.786	8.786	8.786	8.786

Table 4.5: SSATS Values of the UG MEWMA Chart when $\rho = 0.9$

		Shewhart	MEWMA	UG MEWMA			
$\boldsymbol{n}$		(5,5)	(5,5)	(1,45)	(2,35)	(3,25)	(4,15)
r		—	0.1	0.1	0.1	0.1	0.1
δ	0.0	200.0	200.0	200.0	200.0	200.0	200.0
	0.1	175.7	87.5	98.7	103.2	109.2	117.0
	0.15	151.9	50.6	71.9	73.8	77.0	81.3
	0.2	126.6	32.3	55.1	55.0	56.1	58.0
	0.25	102.8	22.5	43.7	42.3	42.2	42.8
	0.3	82.3	16.9	35.6	33.5	32.8	32.6
	0.4	51.7	10.9	24.9	22.4	21.4	20.9
	0.5	32.4	8.0	18.3	16.0	15.2	14.8
	0.75	11.0	4.7	10.2	8.7	8.3	8.1
	1.0	4.4	3.3	6.7	5.8	5.5	5.5
	1.5	1.2	2.1	3.8	3.4	3.3	3.3
	2.0	0.6	1.5	2.6	2.4	2.3	2.3
	3.0	0.5	1.0	1.6	1.5	1.4	1.4
	4.0	0.5	0.6	1.2	1.1	1.1	1.1
	5.0	0.5	0.5	1.0	0.9	0.9	0.8
h		10.597	8.786	8.786	8.786	8.786	8.786

Table 4.6: Total Expected Measurement Costs of the UG MEWMA Chart when $\rho = 0$

		Shewhart	MEWMA	UG MEWMA			
$\boldsymbol{n}$		(5,5)	(5,5)	(1,45)	(2,35)	(3,25)	(4,15)
δ	0.0	11000	11000	11000	11000	11000	11000
	0.1	9662	4810	2794	2836	3026	3478
	0.15	8357	2785	1737	1661	1704	1931
	0.2	6962	1776	1193	1092	1099	1229
	0.25	5655	1239	870	782	782	868
	0.3	4524	928	669	596	596	658
	0.4	2841	601	441	393	394	435
	0.5	1784	439	320	289	291	322
	0.75	607	257	185	171	174	192
	1.0	243	181	129	121	124	137
	1.5	64	113	78	75	78	86
	2.0	33	82	57	54	55	62
	3.0	28	52	41	38	37	39
	4.0	28	35	35	33	31	30
	5.0	28	28	32	30	29	28

Table 4.7: Total Expected Measurement Costs of the UG MEWMA Chart when $\rho = 0.3$

		Shewhart	MEWMA	UG MEWMA			
$\boldsymbol{n}$		(5,5)	(5,5)	(1,45)	(2,35)	(3,25)	(4,15)
δ	0.0	11000	11000	11000	11000	11000	11000
	0.1	9662	4810	2919	2967	3162	3611
	0.15	8357	2785	1832	1761	1808	2022
	0.2	6962	1776	1264	1163	1165	1290
	0.25	5655	1239	928	833	828	909
	0.3	4524	928	714	633	629	689
	0.4	2841	601	469	416	415	454
	0.5	1784	439	341	305	306	334
	0.75	607	257	196	180	182	199
	1.0	243	181	136	127	129	141
	1.5	64	113	82	78	81	89
	2.0	33	82	60	56	57	64
	3.0	28	52	42	39	39	40
	4.0	28	35	36	33	32	31
	5.0	28	28	32	30	29	28

Table 4.8: Total Expected Measurement Costs of the UG MEWMA Chart when $\rho = 0.6$

		Shewhart	MEWMA	UG MEWMA			
$\boldsymbol{n}$		(5,5)	(5,5)	(1,45)	(2,35)	(3,25)	(4,15)
	0.0	11000	11000	11000	11000	11000	11000
	0.1	9662	4810	3430	3522	3736	4162
	0.15	8357	2785	2229	2166	2219	2420
	0.2	6962	1776	1569	1462	1457	1557
	0.25	5655	1239	1166	1057	1037	1098
	0.3	4524	928	905	803	783	827
	0.4	2841	601	596	522	510	538
δ	0.5	1784	439	431	379	372	393
	0.75	607	257	244	219	217	231
	1.0	243	181	167	153	153	162
	1.5	64	113	100	94	95	102
	2.0	33	82	72	67	68	73
	3.0	28	52	49	45	44	46
	4.0	28	35	39	37	35	35
	5.0	28	28	35	32	31	30

Table 4.9: Total Expected Measurement Costs of the UG MEWMA Chart when $\rho = 0.9$

		Shewhart	MEWMA	UG MEWMA			
$\boldsymbol{n}$		(5,5)	(5,5)	(1,45)	(2,35)	(3,25)	(4,15)
	0.0	11000	11000	11000	11000	11000	11000
	0.1	9662	4810	5428	5674	6005	6432
	0.15	8357	2785	3957	4058	4236	4471
	0.2	6962	1776	3030	3025	3088	3192
	0.25	5655	1239	2405	2329	2323	2354
	0.3	4524	928	1956	1840	1805	1794
	0.4	2841	601	1368	1230	1175	1149
δ	0.5	1784	439	1008	881	833	813
	0.75	607	257	562	480	455	445
	1.0	243	181	368	318	304	300
	1.5	64	113	209	185	180	179
	2.0	33	82	144	129	126	127
	3.0	28	52	89	81	79	80
	4.0	28	35	65	60	59	58
	5.0	28	28	53	49	47	46

4.4 Conclusions and Recommendations for Applications

We have shown that when variables are not highly correlated the proposed UG MEWMA control chart has substantially better performance averaged over all directions of the shift compared to the standard MEWMA chart. The best overall performance of the proposed UG MEWMA charts seems to be achieved when the sample size vectors of (2,35) or (3,25) are used. If a specific direction close to the axis of the less expensive variable is considered to be more important, then the SSATS comparisons show that the proposed UG MEWMA charts are more effective for detecting shifts in that direction than the standard MEWMA chart with the equal sample size. In practical applications, the choice of sample size vector may be affected by sampling constraints, so these constraints need to be considered in designing the proposed UG MEWMA charts.

Chapter 5

The Sequential Sampling MEWMA Control Chart with Unequal Group Sizes

The sequential sampling plan is now investigated for the case in which different variables can have different group sizes. Two different ways of defining the EWMA vectors in the sequential sampling plan were investigated in Chapter 3, and here the SS_2 MEWMA chart is investigated. Since the SSATS performance of both the SS_1 and the SS_2 MEWMA charts is better than the standard MEWMA chart, for simplicity, only the SS_2 MEWMA chart is considered in this chapter instead of investigating both the SS MEWMA charts. Also it would be advantageous to consider the SS_2 MEWMA chart since the EWMA vectors form a Markov precess.

The idea of applying the sequential sampling plan to the UG MEWMA control chart would be that one might want to take more observations on some variables if the MEWMA statistic computed at a sampling point is close to the upper control limit. For example, one might initially take many observations on the inexpensive variables, but only a few observations on the expensive variables, and then take additional observations on the expensive

variables only if there is some indication of a problem. Additional discussion of the sequential sampling plan is given in Section 3.1.

First we define the group sizes for the stages for the proposed UGSS MEWMA chart. Let $n_{ij} \geq 0$ be the group size for variable i at stage j, and let $\boldsymbol{n}_j = (n_{1j}, n_{2j}, \cdots, n_{pj})^T$ be the vector of group sizes for stage j, for $j = 1, 2$. This means that at each sampling point, at stage 1 we initially obtain n_{i1} observations ($n_{i1} \geq 0$) for variable i, where $i = 1, 2, \cdots, p$. It is assumed without loss of generality that the quality characteristic X_i has the group size of n_{i1} such that $n_{11} \leq n_{21} \leq \cdots \leq n_{p1}$. There exist three possible decision rules at the first stage: (1) conclude that the process is in-control or (2) conclude that the process is out-of-control or (3) move to the second stage and take additional observations.

If the data indicate that sampling should proceed to the second stage, then one obtains an additional group of n_{i2} observations ($n_{i2} \geq 0$) for variable i at the second stage. In the proposed UGSS MEWMA chart, if a positive number of observations are collected for the i^{th} variable at the second stage, then the sample mean for defining the EWMA vector is computed based on only n_{i2} observations. If n_{i2} equals zero then there is no change in the EWMA vector for that variable from the value at the first stage. In the second stage, regardless of which group size vectors are used for the proposed UGSS MEWMA chart, there exist two possible decisions: (1) conclude that the process is in-control or (2) conclude that the process is out-of-control. The number of stages actually used at a sampling point is a random variable depending on the process data, but the maximum total sample size possible for variable i at a sampling point, say τ_i, is $\tau_i = n_{i1} + n_{i2}$. It is assumed that $\tau_i > 0$ for all variables.

Illustrations of the ways in which the stages could be defined will be given using an example for the case in which there are $p = 4$ variables. In this example, suppose that the first two variables are much more expensive to measure than the second two variables. At the first stage a sample of 5 items is selected, but the first two expensive variables are measured on only 2 items, while the second two inexpensive variables are measured on all 5 items. If

the data available at the first stage show some indication of a problem, then a second stage of sampling is used in which the first two variables are measured on the remaining three items. Thus the expensive variables will be measured only twice unless there is some indication of a problem. In this example the group size vector for the first stage is $\boldsymbol{n}_1 = (2, 2, 5, 5)^T$ and the group size vector for the second stage is $\boldsymbol{n}_2 = (3, 3, 0, 0)^T$. Here the maximum total sample size (τ_i) possible at a sampling point is 5 for each variable. As in the UG MEWMA chart in Chapter 4, a constraint on the total expected measurement cost is applied to the UGSS MEWMA chart so that each stage corresponds to a specific measurement cost at each sampling point.

5.1 The Proposed UGSS MEWMA Control Chart

For the proposed UGSS MEWMA chart, since a different group size may be used for each quality characteristic at each sampling stage, some modifications are made to the assumptions given in Chapter 4. Let X_{kijl} be the l^{th} observed value of the quality characteristic i at the j^{th} stage at the k^{th} sampling point for $l = 1, 2, \cdots, n_{ij}$ and let $\bar{X}_{kij}$ be the average of the n_{ij} observations obtained for variable i at stage j at sampling point k, for $i = 1, 2, \cdots, p$, $j = 1, 2$, and $k = 1, 2, \cdots$. A sequence of $p \times 1$ sample mean vectors at the j^{th} stage and the k^{th} sampling point is defined to be

$$\bar{\boldsymbol{X}}_{kj} = (\bar{X}_{k1j}, \bar{X}_{k2j}, \cdots, \bar{X}_{kpj})^T,$$

where $\bar{X}_{kij} = \sum_{l=1}^{n_{ij}} X_{kijl}/n_{ij}$. Corresponding to $\bar{X}_{kij}$ and $\bar{\boldsymbol{X}}_{kj}$, we define the standardized sample means at sampling point k to be

$$V_{kij} = \frac{\sqrt{n_{ij}}(\bar{X}_{kij} - \mu_{0i})}{\sigma_{0i}},$$

and the standardized sample mean vector to be

$$\boldsymbol{V}_{kj} = (V_{k1j}, V_{k2j}, \cdots, V_{kpj})^T.$$

The number of groups of observation vectors actually taken at sampling point k is a random variable, so let $S(k)$ be the number of stages actually used at sampling point k.

Let $\boldsymbol{E}_{kj}$ be the EWMA vector corresponding to the standardized sample mean vector $\boldsymbol{V}_{kj}$, where

$$\boldsymbol{E}_{kj} = (E_{k1j}, E_{k2j}, \cdots, E_{kpj})^T.$$

For stage 1 at sampling point $k \geq 1$, the EWMA vector $\boldsymbol{E}_{k1}$ is defined to be

$$\boldsymbol{E}_{k1} = \boldsymbol{R}_1 \boldsymbol{V}_{k1} + (\boldsymbol{I} - \boldsymbol{R}_1)\boldsymbol{E}_{k-1,S(k-1)}, \tag{5.1}$$

where $\boldsymbol{E}_0 = \boldsymbol{0}$, $\boldsymbol{R}_1 = \text{diag}(r_{11}, r_{21}, \cdots, r_{p1})$, and r_{i1} is a smoothing parameter for variable i at stage 1 satisfying $0 < r_{i1} \leq 1$. If no observation is collected for variable i at stage j, i.e., $n_{ij} = 0$, then no update is needed for the i^{th} variable at the j^{th} stage and the value of the smoothing parameter for the i^{th} variable at the j^{th} stage is now $r_{ij} = 0$. The EWMA vector $\boldsymbol{E}_{k2}$ for stage 2 at sampling point $k \geq 1$ is

$$\boldsymbol{E}_{k2} = \boldsymbol{R}_2 \boldsymbol{V}_{k2} + (\boldsymbol{I} - \boldsymbol{R}_2)\boldsymbol{E}_{k1}, \tag{5.2}$$

where $\boldsymbol{R}_2 = \text{diag}(r_{12}, r_{22}, \cdots, r_{p2})$ and r_{i2} is a smoothing parameter for variable i at stage 2. At stage j and sampling point k, the decision rule will be based on the statistic

$$T^2_{kj} = \boldsymbol{E}^T_{kj} \boldsymbol{\Sigma}^{-1}_{kj} \boldsymbol{E}_{kj},$$

where $\boldsymbol{\Sigma}_{kj}$ is the covariance matrix of $\boldsymbol{E}_{kj}$.

For $k \geq 1$, the value of $\boldsymbol{\Sigma}_{kj}$ is not constant, but can be determined by using the current group sizes to update from the value at the previous sampling point for $j = 1$ and from the value at the previous group for $j = 2$. The (i, i) component of $\boldsymbol{\Sigma}_{k1}$ at the first stage and $\boldsymbol{\Sigma}_{k2}$ at the second stage, respectively, are now

$$\text{Var}(E_{ki1}) = r^2_{i1}\text{Var}(V_{ki1}) + (1 - r_{i1})^2 \text{Var}(E_{k-1,i,S(k-1)}),$$

and

$$\mathrm{Var}(E_{ki2}) = r_{i2}^2\mathrm{Var}(V_{ki2}) + (1-r_{i2})^2\mathrm{Var}(E_{ki1}).$$

The (i, i') component of $\mathbf{\Sigma}_{k1}$ at the first stage, where it is assumed that $n_{i1} \leq n_{i'1}$ for $i < i'$, and $\mathbf{\Sigma}_{k2}$ at the second stage, respectively, are (assuming that if $n_{ij} = 0$ then no observation is collected for variable i but a positive number of observations are collected for variable i')

$$\begin{aligned}\mathrm{Cov}(E_{ki1}, E_{ki'1}) =&(1-r_{i1})(1-r_{i'1})\mathrm{Cov}(E_{k-1,i,S(k-1)}, E_{k-1,i',S(k-1)}) \\ &+ r_{i1}r_{i'1}\mathrm{Cov}(V_{ki1}, V_{ki'1}),\end{aligned}$$

and

$$\begin{aligned}\mathrm{Cov}(E_{ki2}, E_{ki'2}) =&(1-r_{i2})(1-r_{i'2})\mathrm{Cov}(E_{ki1}, E_{ki'1}) \\ &+ r_{i2}r_{i'2}\mathrm{Cov}(V_{ki2}, V_{ki'2}) \\ &+ r_{i2}(1-r_{i'2})\mathrm{Cov}(V_{ki2}, E_{ki'1}).\end{aligned} \tag{5.3}$$

Notice that at stage 2, $\mathrm{Cov}(E_{ki2}, E_{ki'2})$ in Equation (5.3) has an extra term of $r_{i2}(1 - r_{i'2})\mathrm{Cov}(V_{ki2}, E_{ki'1})$. We are assuming here that at the second stage one may measure the expensive variable on some items for which the cheap variable has been measured. This causes V_{ki2} in $E_{ki2} = r_{i2}V_{ki2} + (1-r_{i2})E_{ki1}$ and $E_{ki'1}$ in $E_{ki'2} = r_{i'2}V_{ki'2} + (1-r_{i'2})E_{ki'1}$ to be correlated, i.e.,

$$\begin{aligned}\mathrm{Cov}(V_{ki2}, E_{ki'1}) &= \mathrm{Cov}(V_{ki2}, r_{i'1}V_{ki'1} + (1-r_{i'1})E_{k-1,i',S(k-1)}) \\ &= r_{i'1}\mathrm{Cov}(V_{ki2}, V_{ki'1}) + (1-r_{i'1})\mathrm{Cov}(V_{ki2}, E_{k-1,i',S(k-1)}) \\ &= r_{i'1}\mathrm{Cov}(V_{ki2}, V_{ki'1}),\end{aligned}$$

where $\mathrm{Cov}(V_{ki2}, E_{k-1,i',S(k-1)}) = 0$ since V_{ki2} and $E_{k-1,i',S(k-1)}$ are independent. In Equation (5.3), another possible term of covariance structure between E_{ki1} and $V_{ki'2}$ (i.e., $(1 - r_{i2})r_{i'2}\mathrm{Cov}(E_{ki1}, V_{ki'2})$) has a value of 0, since

$$\begin{aligned}\mathrm{Cov}(E_{ki1}, V_{ki'2}) &= \mathrm{Cov}(r_{i1}V_{ki1} + (1-r_{i1})E_{k-1,i,S(k-1)}, V_{ki'2}) \\ &= r_{i1}\mathrm{Cov}(V_{ki1}, V_{ki'2}) + (1-r_{i1})\mathrm{Cov}(E_{k-1,i,S(k-1)}, V_{ki'2}) \\ &= r_{i1}\mathrm{Cov}(V_{ki1}, V_{ki'2})\end{aligned}$$

and V_{ki1} and $V_{ki'2}$ are independent by the assumption that $n_{i1} \leq n_{i'1}$ for $i < i'$, which means no item is measured both for variable i at the first stage and for variable i' at the second stage. At stage 1, the similar term $\mathrm{Cov}(V_{ki1}, E_{k-1,i',S(k-1)})$ has a value of 0 since V_{ki1} and $E_{k-1,i',S(k-1)}$ are independent. $\mathrm{Cov}(E_{ki2}, E_{ki'2})$ in Equation (5.3) now can be simplified as

$$\begin{aligned}\mathrm{Cov}(E_{ki2}, E_{ki'2}) = (1-r_{i2})(1-r_{i'2})\mathrm{Cov}(E_{ki1}, E_{ki'1}) \\ + r_{i2}r_{i'2}\mathrm{Cov}(V_{ki2}, V_{ki'2}) \\ + r_{i2}r_{i'1}(1-r_{i'2})\mathrm{Cov}(V_{ki2}, V_{ki'1}).\end{aligned}$$

The covariance matrix of the standardized sample mean vector $\boldsymbol{V}_{kj}$, $\boldsymbol{\Sigma}_{V_j}$, can be obtained using the derivations in Section 4.1 as

$$\boldsymbol{\Sigma}_{V_j} = \begin{pmatrix} 1 & \sqrt{\frac{n_{1j}}{n_{2j}}}\rho_{12} & \sqrt{\frac{n_{1j}}{n_{3j}}}\rho_{13} & \cdots & \sqrt{\frac{n_{1j}}{n_{pj}}}\rho_{1p} \\ & 1 & \sqrt{\frac{n_{2j}}{n_{3j}}}\rho_{23} & \cdots & \sqrt{\frac{n_{2j}}{n_{pj}}}\rho_{2p} \\ & & 1 & \cdots & \sqrt{\frac{n_{3j}}{n_{pj}}}\rho_{3p} \\ & symmetric & & \ddots & \vdots \\ & & & & 1 \end{pmatrix},$$

where $\rho_{ii'}$ is the correlation coefficient between variables i and i' and the (i, i') element of $\boldsymbol{\Sigma}_{V_j}$ can be simplified as

$$\mathrm{Cov}(V_{kij}, V_{ki'j}) = \frac{\rho_{ii'}\min\{n_{ij}, n_{i'j}\}}{\sqrt{n_{ij}n_{i'j}}}.$$

The decision rule for the UGSS MEWMA chart requires the specification of two limits g and h, satisfying $0 < g < h$. Then the decision rule is defined as follows. If the current sampling point is k,

1. Observe the first group of n_{i1} observations.
2. Compute $\boldsymbol{V}_{k1}$ based on $\boldsymbol{n}_1 = (n_{11}, n_{21}, \cdots, n_{p1})^T$, where $n_{11} \leq n_{21} \leq \cdots \leq n_{p1}$.
3. Compute $\boldsymbol{E}_{k1} = \boldsymbol{R}_1\boldsymbol{V}_{k1} + (\boldsymbol{I} - \boldsymbol{R}_1)\boldsymbol{E}_{k-1,S(k-1)}$.

4. Compute $T_{k1}^2 = \boldsymbol{E}_{k1}^T \boldsymbol{\Sigma}_{k1}^{-1} \boldsymbol{E}_{k1}$.

   (a) If $T_{k1}^2 \leq g$, then stop sampling at sampling point k, define $S(k) = 1$, and wait until sampling point $k+1$ to sample again.

   (b) If $g < T_{k1}^2 \leq h$, then go to Step 5.

   (c) If $T_{k1}^2 > h$, then signal that there has been a change in the mean vector $\boldsymbol{\mu}$.

5. Take the second group of n_{i2} observations.

6. Compute $\boldsymbol{V}_{k2}$ based on $\boldsymbol{n}_2 = (n_{12}, n_{22}, \cdots, n_{p2})^T$.

7. Compute $\boldsymbol{E}_{k2} = \boldsymbol{R}_2 \boldsymbol{V}_{k2} + (\boldsymbol{I} - \boldsymbol{R}_2)\boldsymbol{E}_{k1}$.

8. Compute $T_{k2}^2 = \boldsymbol{E}_{k2}^T \boldsymbol{\Sigma}_{k2}^{-1} \boldsymbol{E}_{k2}$.

   (a) If $T_{k2}^2 \leq h$, then stop sampling at sampling point k, define $S(k) = 2$, and wait until sampling point $k+1$ to sample again.

   (b) If $T_{k2}^2 > h$, then signal that there has been a change in the mean vector $\boldsymbol{\mu}$.

An out-of-control signal is given at stage 1 whenever T_{k1}^2 is greater than the upper control limit h. The limit, g is used to decide whether additional observations are needed at the second stage. Both g and h are chosen to give a specified in-control ATS. In the proposed UGSS MEWMA control charts, one needs a number of design parameters to be determined: 2 smoothing parameter matrices ($\boldsymbol{R}_1$ and $\boldsymbol{R}_2$), 2 vectors of group sizes ($\boldsymbol{n}_1$ and $\boldsymbol{n}_2$), and 2 control limits (g and h).

5.2 Parameter Choices for the Comparisons

As in the comparisons of MEWMA charts in the previous chapters, two basic control charts, the multivariate Shewhart chart and the standard MEWMA chart with the smoothing parameter of $r = 0.1$, are used as reference charts for evaluating the efficiency of the proposed

UGSS MEWMA chart. For both of the reference charts, a sample size of $n = 5$ and an in-control ATS of 200 are considered.

The proposed UGSS MEWMA control chart is designed to match the total expected measurement cost with that of the reference charts when the process is in-control for the fair comparison of the ATS performance. As assumed in the UG MEWMA control chart in Section 4.2, each quality characteristic has the fixed measurement cost of f_i for $i = 1, 2, \cdots, p$. Since we have two sets of group size vectors for two stages, the expected measurement cost at each sampling point is calculated. The $p \times 1$ vector representing the fixed measurement cost is defined as $\boldsymbol{f}$, where $\boldsymbol{f} = (f_1, f_2, \cdots, f_p)^T$. Let $\boldsymbol{n}_{\text{SS}}$ be the $p \times 2$ matrix representing the group sizes at both stage. The matrix $\boldsymbol{n}_{\text{SS}}$ consists of two sub-vectors: (1) the $p \times 1$ observation vector $\boldsymbol{n}_1$ obtained at the first stage and (2) the $p \times 1$ observation vector $\boldsymbol{n}_2$ obtained at the second stage. That is, we have

$$\boldsymbol{n}_{\text{SS}} = [\boldsymbol{n}_1 \quad \boldsymbol{n}_2].$$

Let p_j be the long-run proportion of sampling points at which the j^{th} stage is reached, and $\boldsymbol{p}$ be the 2×1 vector representing these long-run proportions. The long-run proportion is computed as the ratio of the expected number of samples reaching the j^{th} stage to the ANSS. Since stage 1 is always reached at each sampling point, we obtain $p_1 = 1$ and $\boldsymbol{p} = (1, p_2)^T$. Then the expected measurement cost at each sampling point is computed as

$$\boldsymbol{f}^T \boldsymbol{n}_{\text{SS}} \boldsymbol{p} = \boldsymbol{f}^T \boldsymbol{n}_1 + \boldsymbol{f}^T \boldsymbol{n}_2 p_2.$$

Total expected measurement costs can be obtained by multiplying the ANSS by the expected measurement cost. For the standard MEWMA chart, having measurement costs of $\boldsymbol{f}^T \boldsymbol{n}$ with the sample size n, the value of p_2 for the UGSS MEWMA chart should satisfy the following equation to match measurement costs of the standard MEWMA chart, i.e.,

$$p_2 = \frac{\boldsymbol{f}^T \boldsymbol{n} - \boldsymbol{f}^T \boldsymbol{n}_1}{\boldsymbol{f}^T \boldsymbol{n}_2}, \tag{5.4}$$

where $\boldsymbol{n} = (n, n, \cdots, n)^T$ is the sample size vector of the standard MEWMA chart with the sample size n for all p variables.

As defined in Section 4.2, the cost ratio of variables is used in these simulation studies. The cost ratio of the i^{th} variable is defined as f_i/f_p, for $i = 1, 2, \cdots, p$, with the assumption that $f_1 \geq f_2 \geq \cdots \geq f_p$. For example, for the case of $p = 4$, if the measurement cost of the two expensive variables are 10 unit times larger than the other two inexpensive variables with an assumption that each of the two variables has an equal measurement cost, then the cost ratio of the first and second variables is 10. Since the reference charts (standard Shewhart and MEWMA control charts) with the equal sample size of 5 are compared to the UGSS MEWMA control chart, the out-of-control SSATS performance comparisons are made while maintaining the in-control measurement cost of the reference charts equal to the expected in-control measurement cost of the proposed UGSS MEWMA chart, where the in-control measurement cost at each sampling point for the reference charts is 110. So the control limits g and h are adjusted to give the in-control ATS of 200 and the expected in-control measurement cost of 110. This means that all control charts, including reference charts, studied are designed to give the same total expected in-control measurement cost depending on the given group size vectors $\boldsymbol{n}_j$ for $j = 1, 2$.

As described in Section 4.2, shifts in the process mean vector are measured in units of the non-centrality parameter

$$\delta = \sqrt{\boldsymbol{\nu}^T \boldsymbol{\Sigma}_c^{-1} \boldsymbol{\nu}},$$

where $\boldsymbol{\Sigma}_c$ is the correlation matrix corresponding to the known covariance matrix $\boldsymbol{\Sigma}_0$. The i^{th} component of $\boldsymbol{\nu}$, the sustained standardized mean shift vector from the in-control mean vector $\boldsymbol{\mu}_0$ is

$$\nu_i = \frac{\mu_i - \mu_{0i}}{\sigma_{0i}}, \quad i = 1, 2, \cdots, p.$$

In the proposed UGSS MEWMA chart, the i^{th} component of the standardized sample mean

shift vector $\boldsymbol{\nu}'_j$ at the j^{th} stage is defined to be

$$\begin{aligned}\nu'_{ij} &= \mathrm{E}(V_{kij}) \\ &= \sqrt{n_{ij}}\frac{\mu_i - \mu_{0i}}{\sigma_{0i}} \\ &= \sqrt{n_{ij}}\nu_i.\end{aligned}$$

As a result, for a given value of δ, the sizes of the standardized sample mean shifts depend on the group sizes at each sampling stage. Since different variables can have different group sizes at each sampling stage, the sizes of the standardized sample mean shifts vary by the variable and sampling stage, and is proportional to the square root of the group size n_{ij} considered. A more detailed discussion of this issue is given in Section 4.2.

Different values of the correlation coefficient ρ are considered for the case of $p = 2$ and $p = 4$ from the independent case to the more strongly dependent case. The values for the size of a sustained shift (δ) considered in the tables are 0.1, 0.15, 0.2, 0.25, 0.3, 0.4, 0.5, 0.75, 1.0, 1.5, 2.0, 3.0, 4.0, and 5.0. All SSATS values and total expected measurement costs are evaluated using simulation with 1,000,000 runs. The procedures used in Section 3.1 to obtain the values of h and g for specific values of the in-control ATS and total expected measurement cost are applied to the UGSS MEWMA chart.

5.3 The Choice of the Smoothing Parameter for Groups

In this section, different choices of the smoothing parameter for the UGSS MEWMA chart are considered to ensure fair comparisons with other proposed UGSS MEWMA charts having different group sizes and a reference chart of the standard MEWMA control chart. As discussed in Section 3.3, the smoothing parameter must be chosen carefully and given proper weight corresponding to a group size at each stage. Let $r(n)$ be the value of the smoothing parameter corresponding to a given sample size of n. The approach introduced in Section 3.3 is applied to the proposed UGSS MEWMA chart, where the idea is that a sample mean

corresponding to a large group size gets more weight than a sample mean corresponding to a small group size. The method for determining r_{ij} from $r(n)$ for the UGSS MEWMA chart requires that

$$r_{ij} = 1 - (1 - r(n))^{n_{ij}/n}. \tag{5.5}$$

More detailed discussion of this issue is given in Section 3.3.

A total of three options are examined for choosing the values of r_{ij} for the proposed UGSS MEWMA chart. The first option is for each stage to use the value of r_{ij} appropriate for the group size at that stage. For example, for $p = 2$, if group size vectors of $\boldsymbol{n}_1 = (2, 6)^T$ for the first stage and $\boldsymbol{n}_2 = (4, 0)^T$ for the second stage are used for the UGSS MEWMA chart and a reference chart of the standard MEWMA chart with the sample size of 5 ($n = 5$) having the weight of $r(n) = 0.1$ is considered, then by using Equation (5.5) the values of r_{ij} are given by

$$r_{11} = 1 - (1 - 0.1)^{2/5} = 0.04127 \qquad r_{21} = 1 - (1 - 0.1)^{6/5} = 0.11877$$
$$r_{12} = 1 - (1 - 0.1)^{4/5} = 0.08083 \qquad r_{22} = 0.$$

The second option considered is to use the value of the smoothing parameter appropriate for the average group size (AGS). First we define the average number of groups to signal (ANGS) to be the expected value of the number of groups to signal. The ANGS can be obtained by multiplying the ANSS by the sum of the two long-run proportions given in Equation (5.4). That is, ANGS = ANSS$(1 + p_2)$. The unit measurement cost is defined as the cost of measuring one observation for all variables. The AGS is defined to be the ratio of the expected measurement cost per group to the unit measurement cost, i.e.,

$$\begin{aligned} \text{AGS} &= \frac{\text{Total Expected Measurement Cost}}{(\text{ANSS})(1 + p_2)(\text{Unit Measurement Cost})} \\ &= \frac{\boldsymbol{f}^T \boldsymbol{n}_1 + \boldsymbol{f}^T \boldsymbol{n}_2 p_2}{\boldsymbol{f}^T \mathbf{1}(1 + p_2)}, \end{aligned}$$

where $\mathbf{1} = (1, 1, \cdots, 1)^T$. The value of r_{ij} can be obtained by replacing n_{ij} with AGS in Equation (5.5) as

$$r_{ij} = 1 - (1 - r(n))^{\text{AGS}/n}.$$

If no observation is collected for the i^{th} variable at the second stage, then the value of r_{i1} appropriate for the group size at the first stage and $r_{i2} = 0$ are used. It seems reasonable to use those values since the group size of n_{i1} is only used for computing an EWMA vector for variable i. The third option is to use the value of $r(n)$ for all r_{ij} except for the case of $n_{ij} = 0$, where $r(n)$ is the value of the smoothing parameter for a reference chart of the standard MEWMA chart with the sample size n. This third option is considered since the proposed UGSS MEWMA chart is designed to match both the in-control ATS and the total expected measurement cost with a reference chart of the standard MEWMA chart so that the value of the smoothing parameter is also chosen to match with each other.

Tables 5.1-5.2 give SSATS values of UGSS MEWMA charts for the case of $p = 2$. A selected set of the initial group size vectors $\boldsymbol{n}_1 = \{(4, 10), (4, 12)\}$ are considered, where the values of $n_{12} = 6$ and 8 are measured for variable 1 at stage 2, respectively, for two values of correlation coefficient ρ=0 and 0.6. For purposes of comparison, column 2 contains SSATS values for the standard MEWMA chart with the sample size of $n = 5$ having the smoothing parameter of $r(n) = 0.1$. For each group size vector, there are a series of three columns, where the columns correspond to the three options discussed previously.

From Tables 5.1-5.2 we see that the third option, which uses $r(n) = 0.1$ for all values of r_{ij} ($\neq 0$), gives better performance for small shifts and equal performance for large shifts. The third option performs slightly worse for some intermediate shifts. Since it is desirable to have good performance for a range of shifts from small to large, it seems reasonable to use the third option for choosing the value of the smoothing parameter. The remaining results in this chapter are presented using the third option.

5.4 The Effects of the Choice of the Group Sizes

As discussed in Section 5.3, since the proposed UGSS MEWMA chart depends on shift directions for the SSATS performance, a selected set of group size vectors are investigated

Table 5.1: SSATS Values of the UGSS MEWMA Chart with Different Choices of r_{ij} and an Initial Group Size of $\boldsymbol{n}_1 = \{(4, 10), (4, 12)\}$ when $\rho = 0$ and $p = 2$

		MEWMA	UGSS MEWMA					
$\boldsymbol{n}_1$		(5,5)	(4,10)	(4,10)	(4,10)	(4,12)	(4,12)	(4,12)
$\boldsymbol{n}_2$		—	(6,0)	(6,0)	(6,0)	(8,0)	(8,0)	(8,0)
(τ_1, τ_2)		5	(10,10)	(10,10)	(10,10)	(12,12)	(12,12)	(12,12)
(r_{11}, r_{12})		0.1	(0.08083,0.19)	(0.09268,0.19)	(0.1,0.1)	(0.08083,0.22343)	(0.09657,0.22343)	(0.1,0.1)
(r_{21}, r_{22})		—	(0.11877,0)	(0.09268,0)	(0.1,0)	(0.15513,0)	(0.09657,0)	(0.1,0)
δ	0.0	200.0	200.0	200.0	200.0	200.0	200.0	200.0
	0.1	87.5	78.6	77.9	69.6	78.2	76.5	65.4
	0.15	50.6	42.8	42.0	38.0	42.6	41.2	35.6
	0.2	32.3	25.7	25.4	23.5	25.6	24.7	22.2
	0.25	22.5	17.1	16.9	16.2	17.0	16.4	15.4
	0.3	16.9	12.4	12.3	12.1	12.1	11.8	11.5
	0.4	10.9	7.7	7.6	7.8	7.4	7.3	7.5
	0.5	8.0	5.4	5.4	5.7	5.2	5.1	5.5
	0.75	4.7	3.1	3.1	3.4	2.8	2.9	3.2
	1.0	3.3	2.1	2.1	2.3	1.9	1.9	2.3
	1.5	2.1	1.2	1.2	1.4	1.1	1.1	1.4
	2.0	1.5	0.8	0.8	1.0	0.8	0.8	1.0
	3.0	1.0	0.6	0.6	0.6	0.6	0.6	0.6
	4.0	0.6	0.5	0.5	0.5	0.5	0.5	0.5
	5.0	0.5	0.5	0.5	0.5	0.5	0.5	0.5
h		8.786	9.357	9.456	9.063	9.366	9.586	9.002
g		—	4.126	4.271	4.161	5.423	5.657	5.429

Table 5.2: SSATS Values of the UGSS MEWMA Chart with Different Choices of r_{ij} and an Initial Group Size of $\boldsymbol{n}_1 = \{(4, 10), (4, 12)\}$ when $\rho = 0.6$ and $p = 2$

		MEWMA	UGSS MEWMA					
$\boldsymbol{n}_1$		(5,5)	(4,10)	(4,10)	(4,10)	(4,12)	(4,12)	(4,12)
$\boldsymbol{n}_2$		—	(6,0)	(6,0)	(6,0)	(8,0)	(8,0)	(8,0)
(τ_1, τ_2)		5	(10,10)	(10,10)	(10,10)	(12,12)	(12,12)	(12,12)
(r_{11}, r_{12})		0.1	(0.08083,0.19)	(0.09268,0.19)	(0.1,0.1)	(0.08083,0.22343)	(0.09657,0.22343)	(0.1,0.1)
(r_{21}, r_{22})		—	(0.11877,0)	(0.09268,0)	(0.1,0)	(0.15513,0)	(0.09657,0)	(0.1,0)
δ	0.0	200.0	200.0	200.0	200.0	200.0	200.0	200.0
	0.1	87.5	92.7	89.7	80.0	94.8	90.1	77.3
	0.15	50.6	53.4	50.9	45.0	55.9	51.5	43.8
	0.2	32.3	32.6	30.9	28.0	34.5	31.5	27.4
	0.25	22.5	21.5	20.4	19.1	22.8	20.9	18.8
	0.3	16.9	15.2	14.6	14.1	16.1	14.8	13.9
	0.4	10.9	9.1	8.8	8.9	9.4	8.9	8.9
	0.5	8.0	6.3	6.2	6.5	6.3	6.1	6.4
	0.75	4.7	3.5	3.5	3.8	3.4	3.4	3.7
	1.0	3.3	2.4	2.4	2.6	2.3	2.3	2.6
	1.5	2.1	1.4	1.4	1.6	1.3	1.3	1.6
	2.0	1.5	0.9	0.9	1.1	0.9	0.9	1.1
	3.0	1.0	0.6	0.6	0.7	0.6	0.6	0.7
	4.0	0.6	0.5	0.5	0.5	0.6	0.5	0.6
	5.0	0.5	0.5	0.5	0.5	0.5	0.5	0.5
h		8.786	9.115	9.256	8.837	9.193	9.437	8.813
g		—	4.055	4.199	4.065	5.387	5.608	5.348

to check the SSATS performance for varying shift directions. For three selected values of correlation coefficient ρ= {0, 0.3, 0.6} and the group size vectors of $\boldsymbol{n}_1$ = {(4,10), (4,12)}, the SSATS is evaluated, where the values of $n_{12} = 6$ and 8, respectively, are measured for variable 1 at stage 2. SSATS values are plotted for shift directions ranged from $\theta = 0°$ to $\theta = 180°$ by increasing 10°. For each shift direction SSATS values are computed using simulation with 1,000,000 runs. Two shift sizes of $\delta = 0.25$ and 1.0 are considered and given in Figures 5.1 and 5.2, respectively. For purposes of comparison, a reference line, which is a bold horizontal line in both figures, is added to the figures for a reference chart of the standard MEWMA chart with the sample size of $n = 5$ having the smoothing parameter of $r(n) = 0.1$.

Figure 5.1 shows that for both selected group size vectors the minimum SSATS value moves from the shift direction of $\theta = 90°$ to the shift direction of $\theta = 45°$ as the correlation coefficient increases from the independent case ($\rho = 0$) to a relatively large value of $\rho = 0.6$. The SSATS values are symmetric around the shift direction of $\theta = 90°$ for $\rho = 0$ and skewed toward the peak at the shift direction of around $\theta = 60°$ for $\rho = 0.6$. The maximum SSATS is in the shift direction of $\theta = 0°$ or 180° for all selected group size vectors and values of ρ. However, as the value of ρ approaches 0, the UGSS MEWMA chart has better SSATS performance than the standard MEWMA chart for the wider range of shift directions. When the independent case ($\rho = 0$) is considered, the UGSS MEWMA chart has the uniformly better SSATS performance than the standard MEWMA chart. Figure 5.2 shows the same pattern of SSATS performance as Figure 5.1, except that the size of shift considered is $\delta = 1.0$.

Examining Figures 5.1-5.2 shows that the proposed UGSS MEWMA chart would give much better SSATS performance for a shift in the direction where performance is good as discussed in Section 4.3.

We now consider the effects of different choices for the group sizes and the issue of the maximum possible sample size (τ_i) based on the SSATS values averaged over randomly

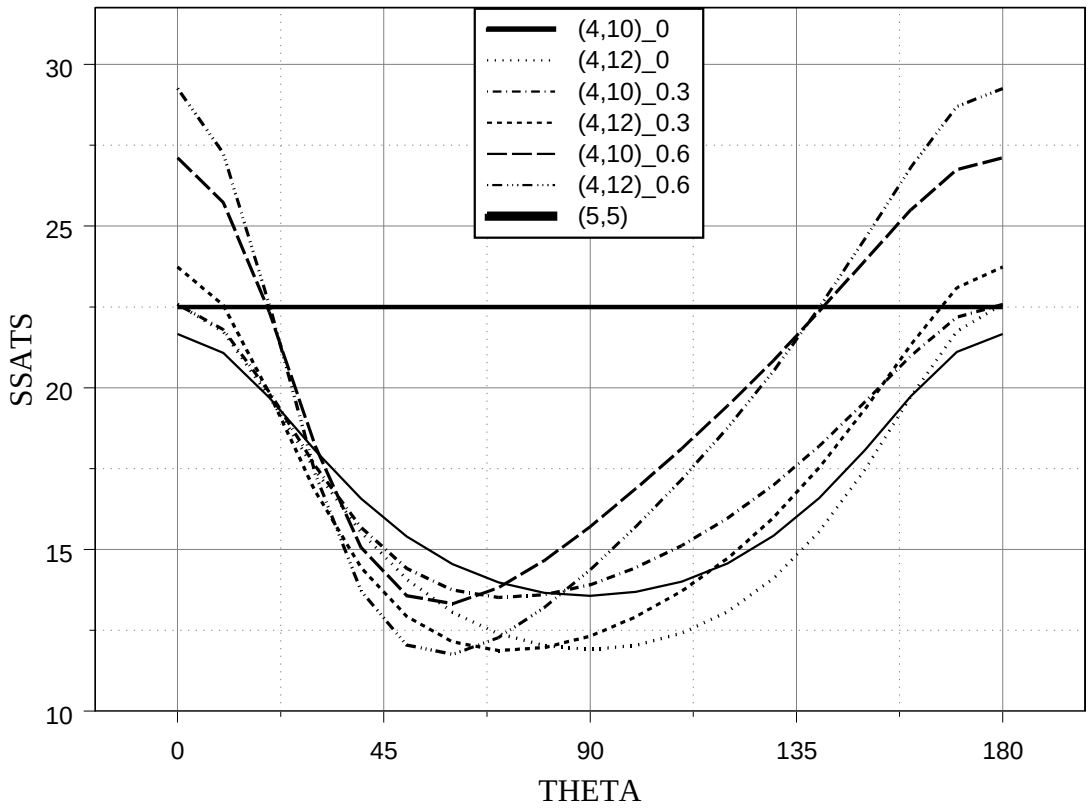

Figure 5.1: SSATS Values of the UGSS MEWMA Chart by Varying Shift Directions when $\rho = \{0, 0.3, 0.6\}$ for $\delta = 0.25$

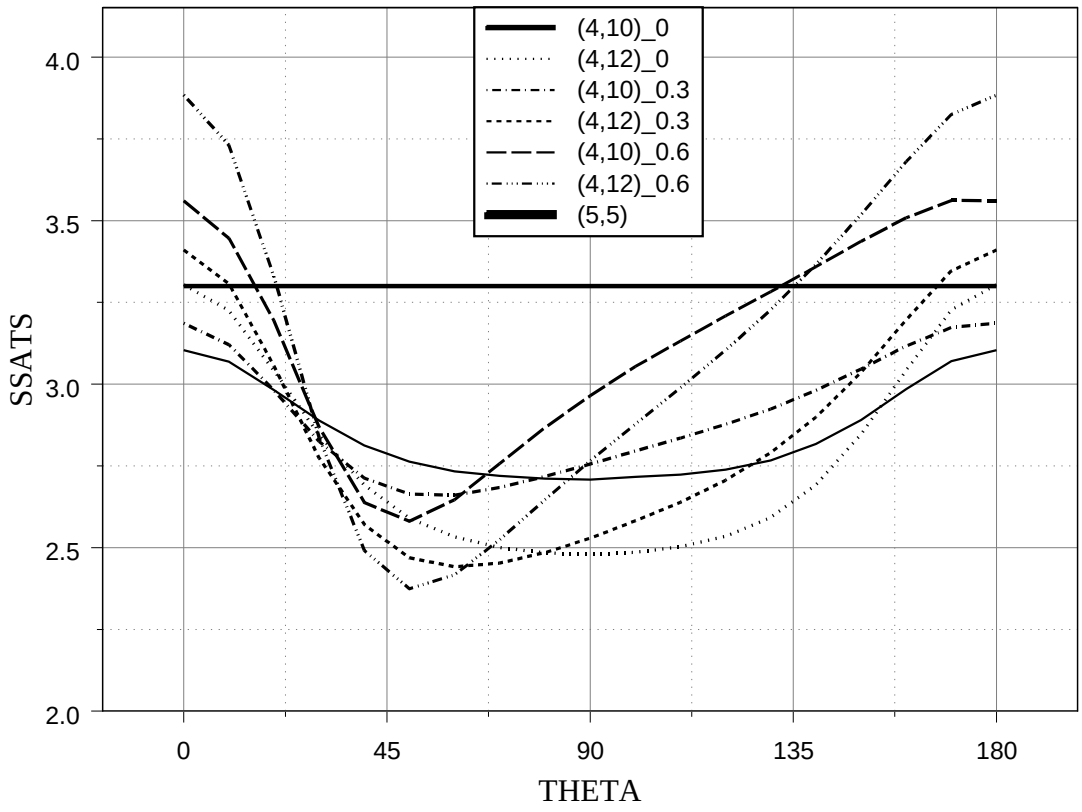

Figure 5.2: SSATS Values of the UGSS MEWMA Chart by Varying Shift Directions when $\rho = \{0, 0.3, 0.6\}$ for $\delta = 1.0$

generated shift directions. The algorithm proposed by Johnson (1987), as discussed in Section 4.3, is used to generate a total of 1,000,000 shift directions from which the averaged SSATS is calculated. In these simulation studies, the value of τ_i is selected to be the same for each i for the group size vectors considered. The tables presenting results on the choice of group of sizes are organized so that the tables for the case of $p = 2$ are given first and the tables for the case of $p = 4$ are given next. For $p = 4$ case, the case that the correlation matrix ($\mathbf{\Sigma}_c$) has all equal off-diagonal components of ρ is considered first and the case that the correlation matrix has unequal off-diagonal components is considered next.

Tables 5.3-5.7 show SSATS values for UGSS MEWMA control charts that have different values of correlation coefficients $\rho = \{0.0, 0.3, 0.6, 0.7, 0.8\}$, respectively. Columns 2 and 3 contain SSATS values for the reference charts of the standard Shewhart and standard MEWMA charts with the sample size of $n = 5$ having the smoothing parameter of $r(n) = 0.1$. Columns 4-6 correspond to UGSS MEWMA charts that have a maximum sample size of $\tau_i = 10$. The initial group size vectors considered here are $\boldsymbol{n}_1 = \{(2,10), (3,10), (4,10)\}$ and the additional groups of $n_{i2} = 8$, 7, and 6 can be measured, respectively, for the first variable at the second stage. Consequently, no additional observation is collected at the second stage. Columns 7-9 correspond to $\tau_i = 12$ and the initial group size vectors of $\boldsymbol{n}_1 = \{(2,12), (3,12), (4,12)\}$ are considered. Columns 10-11 correspond to $\tau_i = 18$ and the initial group size vectors of $\boldsymbol{n}_1 = \{(2,18), (3,18)\}$ are considered. In columns 4-11 an additional $\tau_1 - n_{11}$ items are measured for the first variable at the second stage and no additional observations on the second variable are collected at the second stage.

From Tables 5.3-5.7, we see that the proposed UGSS MEWMA chart performs much better than the Shewhart chart in detecting small-to-moderate shifts regardless of correlation coefficients considered. The proposed UGSS MEWMA chart performs moderately better than the standard MEWMA chart unless the two variables are highly correlated. The proposed UGSS MEWMA chart has uniformly better SSATS performance for the correlation coefficient below 0.7. Examining Tables 5.3-5.7 shows that using a group size vector of $\boldsymbol{n}_1 = (2, 18)$ and $\boldsymbol{n}_2 = (16, 0)$ has better SSATS performance than other group size vectors

considered for almost all ranges of the shift size δ. However, there is little difference in the SSATS values for the group size vectors for moderate-to-large shifts. When SSATS performances of different group sizes at the first stage are compared, using a group size of $n_{11} = 3$ for the first expensive variable seems to be better than $n_{11} = 2$ and 4 for $\tau_i = 10$ and 12. If two variables are highly correlated ($\rho = 0.8$), then the proposed UGSS MEWMA chart is still better than the standard Shewhart chart in detecting small-to-moderate shifts but worse than the standard MEWMA chart over the entire ranges of shifts.

Tables 5.8-5.12 have the same structure as Tables 5.3-5.7, except that Tables 5.8-5.12 give total expected measurement costs for the proposed UGSS MEWMA chart.

Examining Tables 5.8-5.12 shows that as a maximum total sample size (τ_i) increases, the total expected measurement cost tends to decrease. As in the case of comparisons of SSATS performance, unless two variables are highly correlated, the total expected measurement cost for the proposed UGSS MEWMA chart is much lower than the cost for the standard Shewhart chart for small-to-moderate shifts, and moderately lower than the cost for the standard MEWMA chart over almost all ranges of shifts. When different group size vectors are compared, $n_{11} = 4$ seems to give the lower total expected measurement cost than $n_{11} = 2$ and 3.

Tables 5.13-5.18 show SSATS values for UGSS MEWMA charts that have different values of correlation coefficients ρ= {0.0, 0.3, 0.6} for the case of $p = 4$. Tables 5.13-5.14 correspond to the correlation coefficient $\rho = 0.0$, Tables 5.15-5.16 correspond to the correlation coefficient $\rho = 0.3$, and Tables 5.17-5.18 correspond to the correlation coefficient $\rho = 0.6$. In Tables 5.13-5.18, columns 2 and 3 contain SSATS values for the standard Shewhart and the standard MEWMA charts with the sample size of $n = 5$ having the smoothing parameter of $r(n) = 0.1$. Columns 4-5 in Table 5.13 correspond to UGSS MEWMA charts that have a maximum sample size of $\tau_i = 10$. The initial group size vectors considered here are $\boldsymbol{n}_1$ = {(2,10,10,10), (3,10,10,10)}, and the groups of $n_{12} = 8$ and 7 can be additionally measured, respectively, for the first variable at the second stage. Columns 4-5 are based on the

assumption that only the first variable has expensive measurement costs with the cost ratio of 10. Consequently, no additional observations are collected on the other three variables at the second stage. Columns 6-8 of Table 5.13 consider the case when the first two variables have expensive measurement costs. Here the initial group size vectors considered are $\boldsymbol{n}_1 = \{(2,2,10,10), (3,3,10,10), (4,4,10,10)\}$ with a maximum sample size of $\tau_i = 10$ and the additional groups of $n_{i2} = 8$, 7, and 6, respectively, can be measured for the first two variables at the second stage. Columns 4-6 in Table 5.14 correspond to UGSS MEWMA charts that have a maximum sample size of $\tau_i = 12$. The initial group size vectors considered here are $\boldsymbol{n}_1 = \{(2,2,12,12), (3,3,12,12), (4,4,12,12)\}$, and the groups of $n_{i2} = 10$, 9, and 8 can be taken, respectively, for the first two variables at the second stage. Columns 7-8 of Table 5.14 consider the initial group size vectors of $\boldsymbol{n}_1 = \{(2,2,18,18), (3,3,18,18)\}$ with a maximum sample size of $\tau_i = 18$, where additional $n_{i2} = 16$ and 15 observations, respectively, can be taken for the first two variables at stage 2. All the proposed UGSS MEWMA charts considered in the tables allow no additional observations collected on the inexpensive variables at their second stage. Tables 5.15-5.18 have the same structure as Tables 5.13-5.14 except that different correlation coefficients $\rho = 0.3$ and 0.6 are considered.

Tables 5.13-5.18 show that the proposed UGSS MEWMA chart has better SSATS performance than the Shewhart chart in detecting small-to-moderate shifts for a selected set of group sizes vectors for the $p = 4$ case. Also when the UGSS MEWMA chart is compared to the standard MEWMA chart, it shows the same patterns as in the $p = 2$ case considered previously, i.e., the UGSS MEWMA chart has uniformly better SSATS performance over all ranges of the shift size δ when ρ is not high. In terms of good overall performance, a maximum total sample size (τ_i) having the largest value gives the best performance for all ranges of the shift size δ, which seems to be intuitively reasonable. In practical applications, it appears that it is best to choose τ_i to be as large as feasible.

Tables 5.19-5.24 have the same structure as Tables 5.13-5.18, except that Tables 5.19 -5.24 give total expected measurement costs for the proposed UGSS MEWMA chart.

Tables 5.19-5.24 show that for the independent case (ρ=0) or the small correlation coefficient ($\rho = 0.3$), the UGSS MEWMA chart has the lower total expected measurement cost for each shift direction than the cost of the standard MEWMA chart. However, even for the relatively higher correlation coefficient ($\rho = 0.6$), the UGSS MEWMA chart has lower total expected measurement cost than the standard MEWMA chart except for a small range of intermediate shifts. These comparisons of the total expected measurement cost could be considered in practical applications along with the SSATS performance when group sizes are chosen. Also, the choice of group sizes and a maximum total sample size may be affected by sampling constraints, so these constraints need to be considered in designing the UGSS MEWMA chart.

Table 5.25 shows SSATS values for the case that the correlation matrix has unequal off-diagonal components. For the $p = 4$ case, the group size vectors of $\{\boldsymbol{n}_1, \boldsymbol{n}_2\} = \{(3, 10, 10, 10), (7, 0, 0, 0)\}$ are chosen for further investigation of the effect of different correlation matrices. A total of 6 correlation matrices are selected and compared to the correlation matrices having all off-diagonal components equal to ρ. Rows 1-2 indicate how off-diagonal components are chosen for each correlation matrix, where the value of $\rho_{ii'}$ indicates the correlation coefficient between variables i and i'. Since the $p = 4$ case is considered, a total of 6 correlation coefficients are chosen for each correlation matrix. Columns 3 and 4 contain SSATS values for correlation matrices having $\rho = 0.3$ and 0.6, respectively. In columns 5-8, correlation matrices are chosen so that the first variable having the smaller number of observations at the first stage are equally correlated with the other three variables, and the other three variables also are equally correlated with each other. In column 5, the correlation coefficients $\rho_{1i'} = 0.1$, for $i' = 2, 3, 4$, $\rho_{2i'} = 0.6$, for $i' = 3, 4$, and $\rho_{34} = 0.6$ are chosen. Columns 6-8 have the same structure as column 5 except that columns 6-8 have a different set of correlation coefficients. Correlation matrices in columns 9-10 are selected so that two of the correlation coefficients between the first variable and the other three variables, and one of the correlation coefficients between the other three variables have an equal value. The rest of the three correlation coefficients have also an equal value.

Table 5.25 shows that as the correlation coefficient between the first variable and the other three variables increases the SSATS performance gets worse. This is mainly caused by the fact that the $(1, i')$ element of $\mathbf{\Sigma}_{V_j}$ is $\sqrt{n_{1j}/n_{i'j}}\rho_{1i} = \sqrt{3/10}\rho_{1i}$, for $i' = 2, 3, 4$, where the higher the correlation coefficient (ρ_{1i}) the greater the loss of information. The same pattern applies to the case where two of the correlation coefficients between the first variable and the other three variables are high. In this case, the SSATS values increase when it is compared to cases having lower correlation coefficients.

Table 5.3: SSATS Values of the UGSS MEWMA Chart when $\rho = 0$ and $p = 2$

		Shewhart	MEWMA	UGSS MEWMA							
$\boldsymbol{n}_1$		(5,5)	(5,5)	(2,10)	(3,10)	(4,10)	(2,12)	(3,12)	(4,12)	(2,18)	(3,18)
$\boldsymbol{n}_2$		—	—	(8,0)	(7,0)	(6,0)	(10,0)	(9,0)	(8,0)	(16,0)	(15,0)
τ_i		5	5	10	10	10	12	12	12	18	18
r_{ij}		—	0.1	0.1	0.1	0.1	0.1	0.1	0.1	0.1	0.1
δ	0.0	200.0	200.0	200.0	200.0	200.0	200.0	200.0	200.0	200.0	200.0
	0.1	175.7	87.5	70.2	69.1	69.6	64.8	64.0	65.4	55.3	55.6
	0.15	151.9	50.6	38.0	37.3	38.0	34.7	34.3	35.6	29.4	29.9
	0.2	126.6	32.3	23.4	23.0	23.5	21.4	21.2	22.2	18.4	18.7
	0.25	102.8	22.5	16.0	15.8	16.2	14.8	14.6	15.4	12.9	13.1
	0.3	82.3	16.9	12.0	11.8	12.1	11.1	11.0	11.5	9.8	9.9
	0.4	51.7	10.9	7.8	7.7	7.8	7.3	7.2	7.5	6.5	6.5
	0.5	32.4	8.0	5.7	5.6	5.7	5.4	5.3	5.5	4.8	4.8
	0.75	11.0	4.7	3.4	3.3	3.4	3.2	3.1	3.2	2.9	2.9
	1.0	4.4	3.3	2.4	2.3	2.3	2.2	2.2	2.3	2.0	2.0
	1.5	1.2	2.1	1.4	1.4	1.4	1.3	1.3	1.4	1.2	1.2
	2.0	0.6	1.5	1.0	0.9	1.0	0.9	0.9	1.0	0.8	0.9
	3.0	0.5	1.0	0.6	0.6	0.6	0.6	0.6	0.6	0.6	0.6
	4.0	0.5	0.6	0.5	0.5	0.5	0.5	0.5	0.5	0.5	0.5
	5.0	0.5	0.5	0.5	0.5	0.5	0.5	0.5	0.5	0.5	0.5
h		10.597	8.786	9.312	9.216	9.063	9.235	9.142	9.002	9.095	9.017
g		—	—	1.925	2.569	4.161	2.448	3.241	5.429	3.758	5.093

Table 5.4: SSATS Values of the UGSS MEWMA Chart when $\rho = 0.3$ and $p = 2$

		Shewhart	MEWMA	UGSS MEWMA							
$\boldsymbol{n}_1$		(5,5)	(5,5)	(2,10)	(3,10)	(4,10)	(2,12)	(3,12)	(4,12)	(2,18)	(3,18)
$\boldsymbol{n}_2$		—	—	(8,0)	(7,0)	(6,0)	(10,0)	(9,0)	(8,0)	(16,0)	(15,0)
τ_i		5	5	10	10	10	12	12	12	18	18
r_{ij}		—	0.1	0.1	0.1	0.1	0.1	0.1	0.1	0.1	0.1
δ	0.0	200.0	200.0	200.0	200.0	200.0	200.0	200.0	200.0	200.0	200.0
	0.1	175.7	87.5	71.7	70.7	71.6	66.5	66.0	67.6	57.5	58.1
	0.15	151.9	50.6	39.0	38.4	39.2	35.8	35.4	37.0	30.8	31.4
	0.2	126.6	32.3	24.0	23.6	24.3	22.1	21.9	23.1	19.2	19.6
	0.25	102.8	22.5	16.5	16.2	16.7	15.2	15.1	16.0	13.4	13.7
	0.3	82.3	16.9	12.3	12.1	12.4	11.4	11.3	12.0	10.2	10.3
	0.4	51.7	10.9	8.0	7.8	8.0	7.5	7.4	7.8	6.7	6.8
	0.5	32.4	8.0	5.8	5.7	5.9	5.5	5.4	5.7	5.0	5.0
	0.75	11.0	4.7	3.5	3.4	3.4	3.3	3.2	3.3	3.0	3.0
	1.0	4.4	3.3	2.4	2.4	2.4	2.3	2.2	2.3	2.1	2.1
	1.5	1.2	2.1	1.5	1.4	1.4	1.4	1.3	1.4	1.3	1.3
	2.0	0.6	1.5	1.0	1.0	1.0	0.9	0.9	1.0	0.9	0.9
	3.0	0.5	1.0	0.6	0.6	0.6	0.6	0.6	0.6	0.6	0.6
	4.0	0.5	0.6	0.5	0.5	0.5	0.5	0.5	0.5	0.5	0.5
	5.0	0.5	0.5	0.5	0.5	0.5	0.5	0.5	0.5	0.5	0.5
h		10.597	8.786	9.282	9.178	9.016	9.198	9.098	8.961	9.058	8.977
g		—	—	1.911	2.551	4.140	2.433	3.223	5.410	3.745	5.078

Table 5.5: SSATS Values of the UGSS MEWMA Chart when $\rho = 0.6$ and $p = 2$

		Shewhart	MEWMA	UGSS MEWMA							
$\boldsymbol{n}_1$		(5,5)	(5,5)	(2,10)	(3,10)	(4,10)	(2,12)	(3,12)	(4,12)	(2,18)	(3,18)
$\boldsymbol{n}_2$		—	—	(8,0)	(7,0)	(6,0)	(10,0)	(9,0)	(8,0)	(16,0)	(15,0)
τ_i		5	5	10	10	10	12	12	12	18	18
r_{ij}		—	0.1	0.1	0.1	0.1	0.1	0.1	0.1	0.1	0.1
δ	0.0	200.0	200.0	200.0	200.0	200.0	200.0	200.0	200.0	200.0	200.0
	0.1	175.7	87.5	78.5	77.7	80.0	74.3	74.1	77.3	66.8	68.2
	0.15	151.9	50.6	43.7	43.1	45.0	41.2	41.1	43.8	37.1	38.2
	0.2	126.6	32.3	27.0	26.6	28.0	25.5	25.4	27.4	23.2	24.0
	0.25	102.8	22.5	18.5	18.2	19.1	17.5	17.4	18.8	16.1	16.6
	0.3	82.3	16.9	13.7	13.4	14.1	13.0	12.9	13.9	12.1	12.4
	0.4	51.7	10.9	8.8	8.6	8.9	8.4	8.3	8.9	7.9	8.0
	0.5	32.4	8.0	6.4	6.3	6.5	6.2	6.1	6.4	5.8	5.9
	0.75	11.0	4.7	3.8	3.7	3.8	3.7	3.6	3.7	3.5	3.4
	1.0	4.4	3.3	2.7	2.6	2.6	2.6	2.5	2.6	2.4	2.4
	1.5	1.2	2.1	1.6	1.6	1.6	1.6	1.5	1.6	1.4	1.5
	2.0	0.6	1.5	1.1	1.1	1.1	1.1	1.0	1.1	1.0	1.0
	3.0	0.5	1.0	0.7	0.6	0.7	0.6	0.6	0.7	0.7	0.7
	4.0	0.5	0.6	0.5	0.5	0.5	0.5	0.5	0.6	0.6	0.6
	5.0	0.5	0.5	0.5	0.5	0.5	0.5	0.5	0.5	0.5	0.5
h		10.597	8.786	9.168	9.030	8.837	9.069	8.938	8.813	8.929	8.858
g		—	—	1.866	2.490	4.065	2.387	3.163	5.348	3.705	5.034

Table 5.6: SSATS Values of the UGSS MEWMA Chart when $\rho = 0.7$ and $p = 2$

		Shewhart	MEWMA	UGSS MEWMA							
$\boldsymbol{n}_1$		(5,5)	(5,5)	(2,10)	(3,10)	(4,10)	(2,12)	(3,12)	(4,12)	(2,18)	(3,18)
$\boldsymbol{n}_2$		—	—	(8,0)	(7,0)	(6,0)	(10,0)	(9,0)	(8,0)	(16,0)	(15,0)
τ_i		5	5	10	10	10	12	12	12	18	18
r_{ij}		—	0.1	0.1	0.1	0.1	0.1	0.1	0.1	0.1	0.1
δ	0.0	200.0	200.0	200.0	200.0	200.0	200.0	200.0	200.0	200.0	200.0
	0.1	175.7	87.5	83.7	83.0	86.6	80.3	80.4	84.4	74.0	75.6
	0.15	151.9	50.6	47.6	47.2	49.8	45.5	45.6	49.1	42.2	43.6
	0.2	126.6	32.3	29.7	29.3	31.2	28.4	28.4	31.0	26.6	27.6
	0.25	102.8	22.5	20.2	19.9	21.3	19.5	19.4	21.3	18.4	19.1
	0.3	82.3	16.9	14.9	14.7	15.6	14.4	14.3	15.7	13.7	14.2
	0.4	51.7	10.9	9.5	9.3	9.8	9.2	9.1	9.9	8.9	9.1
	0.5	32.4	8.0	6.9	6.7	7.0	6.7	6.6	7.1	6.5	6.6
	0.75	11.0	4.7	4.1	4.0	4.0	4.0	3.9	4.1	3.8	3.8
	1.0	4.4	3.3	2.9	2.8	2.8	2.8	2.7	2.8	2.7	2.6
	1.5	1.2	2.1	1.8	1.7	1.7	1.7	1.6	1.7	1.6	1.6
	2.0	0.6	1.5	1.2	1.1	1.2	1.2	1.1	1.2	1.1	1.2
	3.0	0.5	1.0	0.7	0.7	0.7	0.7	0.7	0.8	0.7	0.7
	4.0	0.5	0.6	0.5	0.5	0.5	0.6	0.5	0.6	0.6	0.6
	5.0	0.5	0.5	0.5	0.5	0.5	0.5	0.5	0.5	0.5	0.5
h		10.597	8.786	9.095	8.933	8.722	8.990	8.843	8.725	8.860	8.788
g		—	—	1.842	2.457	4.022	2.362	3.130	5.313	3.684	5.010

Table 5.7: SSATS Values of the UGSS MEWMA Chart when $\rho = 0.8$ and $p = 2$

		Shewhart	MEWMA	UGSS MEWMA							
$\boldsymbol{n}_1$		(5,5)	(5,5)	(2,10)	(3,10)	(4,10)	(2,12)	(3,12)	(4,12)	(2,18)	(3,18)
$\boldsymbol{n}_2$		—	—	(8,0)	(7,0)	(6,0)	(10,0)	(9,0)	(8,0)	(16,0)	(15,0)
τ_i		5	5	10	10	10	12	12	12	18	18
r_{ij}		—	0.1	0.1	0.1	0.1	0.1	0.1	0.1	0.1	0.1
	0.0	200.0	200.0	200.0	200.0	200.0	200.0	200.0	200.0	200.0	200.0
	0.1	175.7	87.5	92.9	93.0	97.7	90.7	91.4	96.7	85.9	88.0
	0.15	151.9	50.6	55.1	54.9	59.3	53.8	54.2	59.2	51.5	53.5
	0.2	126.6	32.3	34.9	34.7	37.7	34.2	34.5	38.2	33.1	34.7
	0.25	102.8	22.5	23.9	23.6	25.8	23.4	23.5	26.4	23.0	24.1
	0.3	82.3	16.9	17.5	17.3	18.7	17.3	17.2	19.3	17.0	17.8
	0.4	51.7	10.9	11.0	10.8	11.5	10.9	10.8	12.0	10.8	11.2
δ	0.5	32.4	8.0	7.9	7.7	8.1	7.9	7.7	8.4	7.8	8.0
	0.75	11.0	4.7	4.6	4.5	4.6	4.6	4.5	4.7	4.5	4.6
	1.0	4.4	3.3	3.2	3.1	3.2	3.2	3.1	3.3	3.2	3.1
	1.5	1.2	2.1	2.0	1.9	1.9	2.0	1.9	2.0	1.9	1.9
	2.0	0.6	1.5	1.4	1.3	1.3	1.4	1.3	1.4	1.3	1.3
	3.0	0.5	1.0	0.8	0.8	0.8	0.8	0.8	0.9	0.8	0.9
	4.0	0.5	0.6	0.6	0.6	0.6	0.6	0.6	0.6	0.7	0.7
	5.0	0.5	0.5	0.5	0.5	0.5	0.5	0.5	0.5	0.6	0.6
h		10.597	8.786	8.990	8.794	8.560	8.882	8.708	8.608	8.769	8.701
g		—	—	1.811	2.413	3.965	2.331	3.089	5.267	3.659	4.981

Table 5.8: Total Expected Measurement Costs of the UGSS MEWMA Chart when $\rho = 0$ and $p = 2$

		Shewhart	MEWMA	UGSS MEWMA							
$\boldsymbol{n}_1$		(5,5)	(5,5)	(2,10)	(3,10)	(4,10)	(2,12)	(3,12)	(4,12)	(2,18)	(3,18)
$\boldsymbol{n}_2$		—	—	(8,0)	(7,0)	(6,0)	(10,0)	(9,0)	(8,0)	(16,0)	(15,0)
τ_i		5	5	10	10	10	12	12	12	18	18
	0.0	11000	11000	11000	11000	11000	11000	11000	11000	11000	11000
	0.1	9662	4810	4436	4272	4094	4231	4033	3810	3794	3507
	0.15	8357	2785	2605	2489	2350	2496	2357	2167	2262	2053
	0.2	6962	1776	1693	1618	1519	1640	1548	1407	1518	1371
	0.25	5655	1239	1197	1147	1083	1172	1108	1008	1109	1004
	0.3	4524	928	902	870	824	890	847	774	859	781
	0.4	2841	601	587	568	544	585	561	517	580	531
δ	0.5	1784	439	425	415	400	428	413	384	431	397
	0.75	607	257	244	240	235	248	242	228	258	241
	1.0	243	181	167	165	163	171	168	160	183	172
	1.5	64	113	98	99	98	103	102	98	116	107
	2.0	33	82	68	68	68	72	70	69	77	72
	3.0	28	52	36	36	38	37	37	39	41	40
	4.0	28	35	24	25	28	25	26	29	29	30
	5.0	28	28	19	21	25	20	22	26	24	26

Table 5.9: Total Expected Measurement Costs of the UGSS MEWMA Chart when $\rho = 0.3$ and $p = 2$

		Shewhart	MEWMA	UGSS MEWMA							
$\boldsymbol{n}_1$		(5,5)	(5,5)	(2,10)	(3,10)	(4,10)	(2,12)	(3,12)	(4,12)	(2,18)	(3,18)
$\boldsymbol{n}_2$		—	—	(8,0)	(7,0)	(6,0)	(10,0)	(9,0)	(8,0)	(16,0)	(15,0)
τ_i		5	5	10	10	10	12	12	12	18	18
	0.0	11000	11000	11000	11000	11000	11000	11000	11000	11000	11000
	0.1	9662	4810	4497	4344	4195	4307	4132	3926	3899	3633
	0.15	8357	2785	2650	2538	2413	2548	2412	2247	2334	2134
	0.2	6962	1776	1723	1649	1562	1673	1582	1459	1566	1423
	0.25	5655	1239	1219	1169	1111	1194	1135	1042	1142	1039
	0.3	4524	928	920	885	843	909	866	797	886	807
	0.4	2841	601	598	579	556	598	573	532	598	548
δ	0.5	1784	439	434	423	408	438	422	394	446	411
	0.75	607	257	250	245	240	255	248	234	267	249
	1.0	243	181	171	169	167	176	172	164	189	178
	1.5	64	113	101	101	100	106	104	100	120	111
	2.0	33	82	70	70	70	74	73	70	81	75
	3.0	28	52	37	37	39	38	38	40	43	41
	4.0	28	35	24	25	28	26	27	30	30	31
	5.0	28	28	19	21	25	21	23	27	24	26

Table 5.10: Total Expected Measurement Costs of the UGSS MEWMA Chart when $\rho = 0.6$ and $p = 2$

		Shewhart	MEWMA	UGSS MEWMA							
$\boldsymbol{n}_1$		(5,5)	(5,5)	(2,10)	(3,10)	(4,10)	(2,12)	(3,12)	(4,12)	(2,18)	(3,18)
$\boldsymbol{n}_2$		—	—	(8,0)	(7,0)	(6,0)	(10,0)	(9,0)	(8,0)	(16,0)	(15,0)
τ_i		5	5	10	10	10	12	12	12	18	18
	0.0	11000	11000	11000	11000	11000	11000	11000	11000	11000	11000
	0.1	9662	4810	4812	4681	4634	4667	4529	4443	4356	4163
	0.15	8357	2785	2875	2772	2722	2806	2696	2610	2665	2500
	0.2	6962	1776	1875	1800	1760	1849	1766	1693	1789	1668
	0.25	5655	1239	1325	1273	1240	1319	1258	1201	1303	1208
	0.3	4524	928	1000	961	935	1004	959	910	1009	933
	0.4	2841	601	651	628	609	661	633	599	680	629
δ	0.5	1784	439	474	459	446	486	466	441	507	470
	0.75	607	257	275	268	261	286	275	260	305	284
	1.0	243	181	190	186	182	198	192	182	215	202
	1.5	64	113	113	111	110	119	116	111	136	127
	2.0	33	82	78	77	76	83	82	79	95	88
	3.0	28	52	43	42	43	46	45	46	52	49
	4.0	28	35	28	28	30	30	30	33	36	35
	5.0	28	28	22	23	26	23	25	28	28	29

Table 5.11: Total Expected Measurement Costs of the UGSS MEWMA Chart when $\rho = 0.7$ and $p = 2$

		Shewhart	MEWMA	UGSS MEWMA							
$\boldsymbol{n}_1$		(5,5)	(5,5)	(2,10)	(3,10)	(4,10)	(2,12)	(3,12)	(4,12)	(2,18)	(3,18)
$\boldsymbol{n}_2$		—	—	(8,0)	(7,0)	(6,0)	(10,0)	(9,0)	(8,0)	(16,0)	(15,0)
τ_i		5	5	10	10	10	12	12	12	18	18
	0.0	11000	11000	11000	11000	11000	11000	11000	11000	11000	11000
	0.1	9662	4810	5056	4944	4982	4955	4847	4823	4717	4547
	0.15	8357	2785	3064	2976	2977	3023	2929	2897	2933	2790
	0.2	6962	1776	2009	1940	1934	2002	1926	1892	1981	1869
	0.25	5655	1239	1421	1368	1359	1430	1373	1340	1440	1351
	0.3	4524	928	1071	1030	1021	1087	1040	1011	1111	1041
	0.4	2841	601	696	670	659	714	684	658	748	696
δ	0.5	1784	439	507	490	479	525	503	481	557	518
	0.75	607	257	296	287	280	309	297	282	335	311
	1.0	243	181	205	199	195	215	208	197	236	221
	1.5	64	113	122	120	117	129	126	121	148	139
	2.0	33	82	84	83	82	90	89	85	105	98
	3.0	28	52	47	47	47	51	50	50	59	55
	4.0	28	35	31	31	32	34	33	35	40	39
	5.0	28	28	24	24	27	26	26	29	31	31

Table 5.12: Total Expected Measurement Costs of the UGSS MEWMA Chart when $\rho = 0.8$ and $p = 2$

		Shewhart	MEWMA	UGSS MEWMA							
$\boldsymbol{n}_1$		(5,5)	(5,5)	(2,10)	(3,10)	(4,10)	(2,12)	(3,12)	(4,12)	(2,18)	(3,18)
$\boldsymbol{n}_2$		—	—	(8,0)	(7,0)	(6,0)	(10,0)	(9,0)	(8,0)	(16,0)	(15,0)
τ_i		5	5	10	10	10	12	12	12	18	18
	0.0	11000	11000	11000	11000	11000	11000	11000	11000	11000	11000
	0.1	9662	4810	5510	5450	5573	5472	5408	5484	5322	5204
	0.15	8357	2785	3448	3373	3485	3450	3382	3445	3426	3326
	0.2	6962	1776	2284	2225	2291	2313	2254	2287	2348	2262
	0.25	5655	1239	1620	1570	1611	1652	1603	1622	1713	1638
	0.3	4524	928	1219	1178	1199	1254	1210	1215	1317	1253
	0.4	2841	601	788	760	762	819	788	780	880	829
δ	0.5	1784	439	573	552	547	600	576	562	652	611
	0.75	607	257	334	322	316	353	339	325	391	364
	1.0	243	181	232	225	219	247	237	226	276	257
	1.5	64	113	140	136	132	150	144	138	172	161
	2.0	33	82	96	94	93	104	101	98	123	115
	3.0	28	52	56	55	55	61	59	59	73	67
	4.0	28	35	36	36	37	41	39	41	49	46
	5.0	28	28	27	27	29	31	30	32	37	36

Table 5.13: SSATS Valeus of the UGSS MEWMA Chart when $\rho = 0$ and $p = 4$

		Shewhart	MEWMA	UGSS MEWMA				
$\boldsymbol{n}_1$		(5,5,5,5)	(5,5,5,5)	(2,10,10,10)	(3,10,10,10)	(2,2,10,10)	(3,3,10,10)	(4,4,10,10)
$\boldsymbol{n}_2$		—	—	(8,0,0,0)	(7,0,0,0)	(8,8,0,0)	(7,7,0,0)	(6,6,0,0)
τ_i		5	5	10	10	10	10	10
r_{ij}		—	0.1	0.1	0.1	0.1	0.1	0.1
δ	0.0	200.0	200.0	200.0	200.0	200.0	200.0	200.0
	0.1	184.1	105.0	77.4	77.9	85.1	84.2	84.6
	0.15	167.3	63.3	42.3	42.6	47.2	46.5	47.1
	0.2	147.4	40.4	26.0	26.3	28.8	28.4	28.9
	0.25	126.7	27.8	17.8	18.1	19.5	19.2	19.7
	0.3	106.9	20.6	13.3	13.5	14.3	14.1	14.5
	0.4	73.1	13.0	8.6	8.7	9.1	9.0	9.2
	0.5	48.7	9.4	6.3	6.4	6.6	6.5	6.7
	0.75	17.6	5.4	3.8	3.8	3.9	3.8	3.9
	1.0	7.0	3.8	2.6	2.7	2.7	2.7	2.7
	1.5	1.6	2.3	1.6	1.6	1.7	1.6	1.6
	2.0	0.7	1.7	1.2	1.2	1.1	1.1	1.1
	3.0	0.5	1.1	0.7	0.7	0.6	0.6	0.7
	4.0	0.5	0.7	0.5	0.5	0.5	0.5	0.5
	5.0	0.5	0.5	0.5	0.5	0.5	0.5	0.5
h		14.860	12.913	13.327	13.231	13.588	13.479	13.295
g		—	—	5.612	7.737	4.177	5.104	7.238

Table 5.14: SSATS Values of the UGSS MEWMA Chart when $\rho = 0$ and $p = 4$ (Continued)

		Shewhart	MEWMA	UGSS MEWMA				
$\boldsymbol{n}_1$		(5,5,5,5)	(5,5,5,5)	(2,2,12,12)	(3,3,12,12)	(4,4,12,12)	(2,2,18,18)	(3,3,18,18)
$\boldsymbol{n}_2$		—	—	(10,10,0,0)	(9,9,0,0)	(8,8,0,0)	(16,16,0,0)	(15,15,0,0)
τ_i		5	5	12	12	12	18	18
r_{ij}		—	0.1	0.1	0.1	0.1	0.1	0.1
δ	0.0	200.0	200.0	200.0	200.0	200.0	200.0	200.0
	0.1	184.1	105.0	78.5	77.9	79.4	65.6	66.2
	0.15	167.3	63.3	42.7	42.2	43.7	34.8	35.4
	0.2	147.4	40.4	26.0	25.8	26.9	21.3	21.8
	0.25	126.7	27.8	17.6	17.5	18.4	14.7	15.0
	0.3	106.9	20.6	13.1	13.0	13.6	11.0	11.2
	0.4	73.1	13.0	8.4	8.3	8.7	7.2	7.3
	0.5	48.7	9.4	6.1	6.1	6.4	5.4	5.4
	0.75	17.6	5.4	3.6	3.6	3.7	3.2	3.2
	1.0	7.0	3.8	2.5	2.5	2.6	2.2	2.2
	1.5	1.6	2.3	1.5	1.5	1.6	1.3	1.4
	2.0	0.7	1.7	1.0	1.0	1.1	0.9	1.0
	3.0	0.5	1.1	0.6	0.6	0.7	0.6	0.6
	4.0	0.5	0.7	0.5	0.5	0.5	0.5	0.5
	5.0	0.5	0.5	0.5	0.5	0.5	0.5	0.5
h		14.860	12.913	13.498	13.388	13.224	13.335	13.237
g		—	—	4.934	6.025	8.846	6.713	8.424

Table 5.15: SSATS Values of the UGSS MEWMA Chart when $\rho = 0.3$ and $p = 4$

		Shewhart	MEWMA	UGSS MEWMA				
$\boldsymbol{n}_1$		(5,5,5,5)	(5,5,5,5)	(2,10,10,10)	(3,10,10,10)	(2,2,10,10)	(3,3,10,10)	(4,4,10,10)
$\boldsymbol{n}_2$		—	—	(8,0,0,0)	(7,0,0,0)	(8,8,0,0)	(7,7,0,0)	(6,6,0,0)
τ_i		5	5	10	10	10	10	10
r_{ij}		—	0.1	0.1	0.1	0.1	0.1	0.1
δ	0.0	200.0	200.0	200.0	200.0	200.0	200.0	200.0
	0.1	184.1	105.0	78.9	79.4	87.2	86.4	87.2
	0.15	167.3	63.3	43.3	43.8	48.7	47.9	49.0
	0.2	147.4	40.4	26.7	27.1	29.8	29.4	30.1
	0.25	126.7	27.8	18.3	18.6	20.1	19.8	20.5
	0.3	106.9	20.6	13.6	13.8	14.7	14.6	15.0
	0.4	73.1	13.0	8.8	8.9	9.4	9.2	9.5
	0.5	48.7	9.4	6.5	6.5	6.8	6.7	6.9
	0.75	17.6	5.4	3.8	3.9	4.0	3.9	4.0
	1.0	7.0	3.8	2.7	2.7	2.8	2.7	2.8
	1.5	1.6	2.3	1.7	1.7	1.7	1.7	1.7
	2.0	0.7	1.7	1.2	1.2	1.2	1.1	1.2
	3.0	0.5	1.1	0.7	0.7	0.7	0.6	0.7
	4.0	0.5	0.7	0.5	0.5	0.5	0.5	0.5
	5.0	0.5	0.5	0.5	0.5	0.5	0.5	0.5
h		14.860	12.913	13.290	13.185	13.548	13.426	13.229
g		—	—	5.592	7.714	4.152	5.073	7.203

Table 5.16: SSATS Values of the UGSS MEWMA Chart when $\rho = 0.3$ and $p = 4$ (Continued)

		Shewhart	MEWMA	UGSS MEWMA				
$\boldsymbol{n}_1$		(5,5,5,5)	(5,5,5,5)	(2,2,12,12)	(3,3,12,12)	(4,4,12,12)	(2,2,18,18)	(3,3,18,18)
$\boldsymbol{n}_2$		—	—	(10,10,0,0)	(9,9,0,0)	(8,8,0,0)	(16,16,0,0)	(15,15,0,0)
τ_i		5	5	12	12	12	18	18
r_{ij}		—	0.1	0.1	0.1	0.1	0.1	0.1
δ	0.0	200.0	200.0	200.0	200.0	200.0	200.0	200.0
	0.1	184.1	105.0	80.9	80.4	82.2	68.7	69.5
	0.15	167.3	63.3	44.3	44.0	45.7	36.8	37.5
	0.2	147.4	40.4	27.1	26.8	28.2	22.6	23.1
	0.25	126.7	27.8	18.4	18.2	19.3	15.5	15.9
	0.3	106.9	20.6	13.5	13.4	14.2	11.6	11.9
	0.4	73.1	13.0	8.7	8.6	9.1	7.6	7.7
	0.5	48.7	9.4	6.4	6.3	6.6	5.6	5.7
	0.75	17.6	5.4	3.8	3.7	3.8	3.3	3.3
	1.0	7.0	3.8	2.6	2.6	2.7	2.3	2.3
	1.5	1.6	2.3	1.6	1.5	1.6	1.4	1.4
	2.0	0.7	1.7	1.1	1.1	1.1	1.0	1.0
	3.0	0.5	1.1	0.6	0.6	0.7	0.6	0.6
	4.0	0.5	0.7	0.5	0.5	0.5	0.5	0.5
	5.0	0.5	0.5	0.5	0.5	0.5	0.5	0.5
h		14.860	12.913	13.450	13.329	13.164	13.281	13.185
g		—	—	4.909	5.996	8.818	6.693	8.403

Table 5.17: SSATS Values of the UGSS MEWMA Chart when $\rho = 0.6$ and $p = 4$

		Shewhart	MEWMA	UGSS MEWMA				
$\boldsymbol{n}_1$		(5,5,5,5)	(5,5,5,5)	(2,10,10,10)	(3,10,10,10)	(2,2,10,10)	(3,3,10,10)	(4,4,10,10)
$\boldsymbol{n}_2$		—	—	(8,0,0,0)	(7,0,0,0)	(8,8,0,0)	(7,7,0,0)	(6,6,0,0)
τ_i		5	5	10	10	10	10	10
r_{ij}		—	0.1	0.1	0.1	0.1	0.1	0.1
δ	0.0	200.0	200.0	200.0	200.0	200.0	200.0	200.0
	0.1	184.1	105.0	82.3	83.2	92.1	91.2	93.1
	0.15	167.3	63.3	46.1	47.0	52.6	52.0	53.7
	0.2	147.4	40.4	28.6	29.2	32.4	32.0	33.3
	0.25	126.7	27.8	19.6	20.1	21.9	21.6	22.6
	0.3	106.9	20.6	14.6	14.9	16.0	15.8	16.5
	0.4	73.1	13.0	9.4	9.6	10.1	10.0	10.3
	0.5	48.7	9.4	6.8	6.9	7.3	7.2	7.4
	0.75	17.6	5.4	4.1	4.1	4.3	4.2	4.3
	1.0	7.0	3.8	2.9	2.9	3.0	2.9	3.0
	1.5	1.6	2.3	1.8	1.8	1.8	1.8	1.8
	2.0	0.7	1.7	1.3	1.3	1.3	1.2	1.2
	3.0	0.5	1.1	0.7	0.7	0.7	0.7	0.7
	4.0	0.5	0.7	0.5	0.5	0.5	0.5	0.5
	5.0	0.5	0.5	0.5	0.5	0.5	0.5	0.5
h		14.860	12.913	13.199	13.073	13.456	13.302	13.071
g		—	—	5.546	7.662	4.102	5.010	7.131

Table 5.18: SSATS Values of the UGSS MEWMA Chart when $\rho = 0.6$ and $p = 4$ (Continued)

		Shewhart	MEWMA	UGSS MEWMA				
$\boldsymbol{n}_1$		(5,5,5,5)	(5,5,5,5)	(2,2,12,12)	(3,3,12,12)	(4,4,12,12)	(2,2,18,18)	(3,3,18,18)
$\boldsymbol{n}_2$		—	—	(10,10,0,0)	(9,9,0,0)	(8,8,0,0)	(16,16,0,0)	(15,15,0,0)
τ_i		5	5	12	12	12	18	18
r_{ij}		—	0.1	0.1	0.1	0.1	0.1	0.1
δ	0.0	200.0	200.0	200.0	200.0	200.0	200.0	200.0
	0.1	184.1	105.0	86.5	86.3	89.0	75.4	76.6
	0.15	167.3	63.3	48.7	48.5	51.0	41.7	42.7
	0.2	147.4	40.4	29.9	29.8	31.8	25.7	26.5
	0.25	126.7	27.8	20.3	20.2	21.7	17.6	18.2
	0.3	106.9	20.6	14.9	14.8	16.0	13.1	13.4
	0.4	73.1	13.0	9.5	9.4	10.1	8.5	8.7
	0.5	48.7	9.4	6.9	6.8	7.2	6.2	6.3
	0.75	17.6	5.4	4.1	4.0	4.2	3.7	3.7
	1.0	7.0	3.8	2.8	2.8	2.9	2.6	2.5
	1.5	1.6	2.3	1.7	1.7	1.7	1.5	1.6
	2.0	0.7	1.7	1.2	1.2	1.2	1.1	1.1
	3.0	0.5	1.1	0.7	0.7	0.8	0.7	0.7
	4.0	0.5	0.7	0.5	0.5	0.6	0.6	0.6
	5.0	0.5	0.5	0.5	0.5	0.5	0.5	0.5
h		14.860	12.913	13.347	13.200	13.037	13.180	13.086
g		—	—	4.862	5.938	8.761	6.656	8.365

Table 5.19: Total Expected Measurement Costs of the UGSS MEWMA Chart when $\rho = 0$ and $p = 4$

		Shewhart		MEWMA		UGSS MEWMA				
$\boldsymbol{n}_1$		(5,5,5,5)		(5,5,5,5)		(2,10,10,10)	(3,10,10,10)	(2,2,10,10)	(3,3,10,10)	(4,4,10,10)
$\boldsymbol{n}_2$		—		—		(8,0,0,0)	(7,0,0,0)	(8,8,0,0)	(7,7,0,0)	(6,6,0,0)
τ_i		5		5		10	10	10	10	10
	0.0	13000	22000	13000	22000	13000	13000	22000	22000	22000
	0.1	11967	20252	6824	11548	5612	5357	10581	10241	9822
	0.15	10875	18403	4117	6967	3312	3076	6393	6096	5740
	0.2	9583	16218	2624	4441	2155	1983	4143	3947	3684
	0.25	8238	13940	1810	3062	1530	1406	2907	2770	2594
	0.3	6946	11754	1338	2264	1160	1069	2171	2079	1951
	0.4	4752	8041	847	1433	758	707	1385	1340	1271
δ	0.5	3165	5356	609	1031	554	521	995	969	927
	0.75	1142	1933	352	596	320	306	565	555	540
	1.0	452	765	246	416	221	213	385	381	374
	1.5	106	180	152	257	132	129	227	228	224
	2.0	45	76	110	186	92	91	158	158	155
	3.0	33	55	71	121	46	49	84	84	87
	4.0	33	55	48	81	29	33	51	54	59
	5.0	33	55	36	60	26	30	38	44	51

Table 5.20: Total Expected Measurement Costs of the UGSS MEWMA Chart when $\rho = 0$ and $p = 4$ (Continued)

		Shewhart	MEWMA	UGSS MEWMA				
$\boldsymbol{n}_1$		(5,5,5,5)	(5,5,5,5)	(2,2,12,12)	(3,3,12,12)	(4,4,12,12)	(2,2,18,18)	(3,3,18,18)
$\boldsymbol{n}_2$		—	—	(10,10,0,0)	(9,9,0,0)	(8,8,0,0)	(16,16,0,0)	(15,15,0,0)
τ_i		5	5	12	12	12	18	18
δ	0.0	22000	22000	22000	22000	22000	22000	22000
	0.1	20252	11548	10057	9634	9140	8813	8183
	0.15	18403	6967	6049	5687	5244	5275	4773
	0.2	16218	4441	3948	3710	3361	3522	3157
	0.25	13940	3062	2794	2633	2377	2551	2288
	0.3	11754	2264	2111	1994	1805	1968	1768
	0.4	8041	1433	1367	1307	1193	1319	1195
	0.5	5356	1031	993	953	880	977	892
	0.75	1933	596	572	555	519	579	536
	1.0	765	416	392	384	362	407	379
	1.5	180	257	235	232	219	252	233
	2.0	76	186	164	161	154	173	161
	3.0	55	121	85	85	88	85	84
	4.0	55	81	52	55	61	56	59
	5.0	55	60	40	45	53	45	51

Table 5.21: Total Expected Measurement Costs of the UGSS MEWMA Chart when $\rho = 0.3$ and $p = 4$

		Shewhart		MEWMA		UGSS MEWMA				
$\boldsymbol{n}_1$		(5,5,5,5)		(5,5,5,5)		(2,10,10,10)	(3,10,10,10)	(2,2,10,10)	(3,3,10,10)	(4,4,10,10)
$\boldsymbol{n}_2$		—		—		(8,0,0,0)	(7,0,0,0)	(8,8,0,0)	(7,7,0,0)	(6,6,0,0)
τ_i		5		5		10	10	10	10	10
	0.0	13000	22000	13000	22000	13000	13000	22000	22000	22000
	0.1	11967	20252	6824	11548	5694	5455	10766	10432	10090
	0.15	10875	18403	4117	6967	3372	3152	6525	6229	5937
	0.2	9583	16218	2624	4441	2196	2034	4241	4043	3809
	0.25	8238	13940	1810	3062	1560	1441	2973	2833	2674
	0.3	6946	11754	1338	2264	1182	1094	2216	2125	2009
	0.4	4752	8041	847	1433	774	723	1420	1368	1305
δ	0.5	3165	5356	609	1031	565	531	1021	991	951
	0.75	1142	1933	352	596	328	313	582	570	554
	1.0	452	765	246	416	226	218	398	392	384
	1.5	106	180	152	257	136	132	235	235	231
	2.0	45	76	110	186	94	93	163	163	160
	3.0	33	55	71	121	48	51	88	88	90
	4.0	33	55	48	81	30	34	54	56	60
	5.0	33	55	36	60	26	31	40	45	52

Table 5.22: Total Expected Measurement Costs of the UGSS MEWMA Chart when $\rho = 0.3$ and $p = 4$ (Continued)

		Shewhart	MEWMA	UGSS MEWMA				
$\boldsymbol{n}_1$		(5,5,5,5)	(5,5,5,5)	(2,2,12,12)	(3,3,12,12)	(4,4,12,12)	(2,2,18,18)	(3,3,18,18)
$\boldsymbol{n}_2$		—	—	(10,10,0,0)	(9,9,0,0)	(8,8,0,0)	(16,16,0,0)	(15,15,0,0)
τ_i		5	5	12	12	12	18	18
δ	0.0	22000	22000	22000	22000	22000	22000	22000
	0.1	20252	11548	10261	9861	9433	9100	8529
	0.15	18403	6967	6193	5860	5463	5480	4996
	0.2	16218	4441	4054	3817	3510	3656	3298
	0.25	13940	3062	2870	2710	2475	2648	2388
	0.3	11754	2264	2165	2049	1875	2041	1844
	0.4	8041	1433	1408	1342	1234	1368	1243
	0.5	5356	1031	1023	981	909	1014	927
	0.75	1933	596	591	572	536	603	557
	1.0	765	416	406	397	374	424	394
	1.5	180	257	244	240	226	263	242
	2.0	76	186	170	167	160	182	169
	3.0	55	121	90	89	92	92	90
	4.0	55	81	55	58	63	60	62
	5.0	55	60	42	46	54	47	52

Table 5.23: Total Expected Measurement Costs of the UGSS MEWMA Chart when $\rho = 0.6$ and $p = 4$

		Shewhart		MEWMA		UGSS MEWMA				
$\boldsymbol{n}_1$		(5,5,5,5)		(5,5,5,5)		(2,10,10,10)	(3,10,10,10)	(2,2,10,10)	(3,3,10,10)	(4,4,10,10)
$\boldsymbol{n}_2$		—		—		(8,0,0,0)	(7,0,0,0)	(8,8,0,0)	(7,7,0,0)	(6,6,0,0)
τ_i		5		5		10	10	10	10	10
	0.0	13000	22000	13000	22000	13000	13000	22000	22000	22000
	0.1	11967	20252	6824	11548	5897	5691	11214	10904	10708
	0.15	10875	18403	4117	6967	3540	3354	6898	6631	6427
	0.2	9583	16218	2624	4441	2320	2172	4510	4312	4154
	0.25	8238	13940	1810	3062	1648	1541	3165	3023	2908
	0.3	6946	11754	1338	2264	1248	1167	2365	2263	2173
	0.4	4752	8041	847	1433	817	767	1513	1456	1402
δ	0.5	3165	5356	609	1031	596	562	1091	1054	1018
	0.75	1142	1933	352	596	347	330	624	608	591
	1.0	452	765	246	416	240	230	428	420	410
	1.5	106	180	152	257	144	140	254	252	247
	2.0	45	76	110	186	101	98	176	175	172
	3.0	33	55	71	121	53	55	98	97	98
	4.0	33	55	48	81	32	36	60	61	65
	5.0	33	55	36	60	27	32	44	47	54

Table 5.24: Total Expected Measurement Costs of the UGSS MEWMA Chart when $\rho = 0.6$ and $p = 4$ (Continued)

		Shewhart	MEWMA	UGSS MEWMA				
$\boldsymbol{n}_1$		(5,5,5,5)	(5,5,5,5)	(2,2,12,12)	(3,3,12,12)	(4,4,12,12)	(2,2,18,18)	(3,3,18,18)
$\boldsymbol{n}_2$		—	—	(10,10,0,0)	(9,9,0,0)	(8,8,0,0)	(16,16,0,0)	(15,15,0,0)
τ_i		5	5	12	12	12	18	18
δ	0.0	22000	22000	22000	22000	22000	22000	22000
	0.1	20252	11548	10783	10439	10158	9757	9256
	0.15	18403	6967	6618	6322	6029	5993	5558
	0.2	16218	4441	4353	4133	3900	4011	3678
	0.25	13940	3062	3085	2931	2742	2902	2651
	0.3	11754	2264	2331	2211	2069	2236	2036
	0.4	8041	1433	1514	1443	1348	1494	1367
	0.5	5356	1031	1102	1054	985	1109	1016
	0.75	1933	596	638	616	578	660	609
	1.0	765	416	441	428	403	464	431
	1.5	180	257	265	259	245	288	266
	2.0	76	186	186	181	173	202	187
	3.0	55	121	101	99	101	106	102
	4.0	55	81	63	64	68	68	69
	5.0	55	60	46	50	56	52	56

Table 5.25: SSATS Values of the UGSS MEWMA Chart for Unequal $\rho_{ii'}$

		MEWMA	UGSS MEWMA with $\{\boldsymbol{n}_1,\boldsymbol{n}_2\}$ ={(3,10,10,10),(7,0,0,0)}							
$(\rho_{12},\rho_{13},\rho_{14})$		(0,0,0)	(.3,.3,.3)	(.6,.6,.6)	(.1,.1,.1)	(.6,.6,.6)	(.3,.3,.3)	(.6,.6,.6)	(.1,.6,.1)	(.6,.1,.6)
$(\rho_{23},\rho_{24},\rho_{34})$		(0,0,0)	(.3,.3,.3)	(.6,.6,.6)	(.6,.6,.6)	(.1,.1,.1)	(.6,.6,.6)	(.3,.3,.3)	(.1,.6,.6)	(.6,.1,.1)
	0.0	200.0	200.0	200.0	200.0	200.0	200.0	200.0	200.0	200.0
	0.1	105.0	79.4	83.2	75.6	129.7	76.7	96.2	93.3	108.8
	0.15	63.3	43.8	47.0	41.1	93.1	41.9	57.9	54.6	69.4
	0.2	40.4	27.1	29.2	25.4	67.8	25.9	37.0	34.4	46.0
	0.25	27.8	18.6	20.1	17.5	50.4	17.8	25.6	23.6	32.1
	0.3	20.6	13.8	14.9	13.1	38.4	13.3	18.8	17.3	23.7
	0.4	13.0	8.9	9.6	8.5	24.0	8.6	11.8	10.9	14.6
δ	0.5	9.4	6.5	6.9	6.3	16.5	6.3	8.4	7.9	10.2
	0.75	5.4	3.9	4.1	3.7	8.6	3.8	4.8	4.6	5.7
	1.0	3.8	2.7	2.9	2.6	5.7	2.7	3.3	3.2	3.9
	1.5	2.3	1.7	1.8	1.6	3.4	1.6	2.0	2.0	2.4
	2.0	1.7	1.2	1.3	1.2	2.4	1.2	1.4	1.4	1.7
	3.0	1.1	0.7	0.7	0.7	1.4	0.7	0.9	0.8	1.0
	4.0	0.7	0.5	0.5	0.5	1.0	0.5	0.6	0.6	0.7
	5.0	0.5	0.5	0.5	0.5	0.8	0.5	0.5	0.5	0.6
h		12.913	13.185	13.073	13.226	12.841	13.199	12.984	13.028	12.924
g		—	7.714	7.662	7.736	7.574	7.721	7.626	7.644	7.603

5.5 Two Measurement Systems

Steiner (2000) proposed a control chart for monitoring a production process using two measurement systems, which is based on the double sampling $\bar{X}$ chart proposed by Croasdale (1974) and Daudin(1992). However, the method proposed by Steiner (2000) has different assumptions from the assumptions of Croasdale (1974) and Daudin(1992) since in the two-measurement system problem the same sample is measured possibly twice for a single quality characteristic using two different measurement devices, whereas with the double sampling $\bar{X}$ chart one assumes that all samples are measured for a quality characteristic using a single measurement device.

The two-measurement system problem assumes that two measurement devices are available for measuring a single quality dimension; that is, a measurement device which is frequently inexpensive, fast, and less accurate being used at the first stage and a measurement device which is expensive, slow, and more accurate being used at the second stage. It is also assumed that testing items using the first measurement device is not destructive or intrusive. After measuring the items using the first measurement device, which is inexpensive and easy to apply, if there is an indication of a problem in the process mean then the more accurate and expensive second measurement device is used to measure the same items again. As in the double sampling control chart, the warning limits are applied at the first stage to decide whether the second measurement device is needed to reach a conclusion about the process.

For the two-measurement system problem, Steiner (2000) formulated the model

$$Y_{kil} = X_{kl} + e_{kil}, \quad i = 1, 2, \text{ and } l = 1, 2, \cdots, n, \tag{5.6}$$

where Y_{kil} is the l^{th} observation using the i^{th} measurement device at sampling point k, X_{kl} is the true dimension of the item l at sampling point k, and e_{kil} is the measurement error. The true dimension of the quality characteristic X_{kl} is assumed to be a normal random variable with mean $\mu_k = \mu$, for $k = 1, 2, \cdots$, and known variance σ_0^2. The e_{kil}'s are independent, identically distributed (i.i.d) normal random variables with mean zero and variance σ_{0i}^2, for

$i = 1, 2$, and it is assumed that X_{kl} and e_{kil} are independent. Let μ_0 represent the in-control value for μ. The variances of the two measurement devices $(\sigma_{01}^2, \sigma_{02}^2)$, where the second measurement device is assumed to be more accurate than the first measurement device so that $\sigma_{02}^2 < \sigma_{01}^2$, are also assumed to be well known or at least estimated during an initial phase with large enough data set so that any error associated with estimating μ_0 and $(\sigma_{01}^2, \sigma_{02}^2)$ can be neglected. First define the terms in which two measurement devices are used to monitor the process. Let $\bar{Y}_{ki} (= \Sigma_{l=1}^{n} Y_{kil}/n)$ be the average of n observations using the i^{th} measurement device taken at each sampling point. It can be shown when the process is in-control that

$$\mathrm{E}(\bar{Y}_{ki}) = \mu_0, \quad \mathrm{Var}(\bar{Y}_{ki}) = \frac{\sigma_0^2 + \sigma_{0i}^2}{n}, \quad \mathrm{Cov}(\bar{Y}_{k1}, \bar{Y}_{k2}) = \frac{\sigma_0^2}{n},$$

$$\text{and} \quad \mathrm{Corr}(Y_{k1l}, Y_{k2l}) = \frac{\sigma_0^2}{\sqrt{(\sigma_0^2 + \sigma_{01}^2)(\sigma_0^2 + \sigma_{02}^2)}}.$$

Steiner (2000) did not formulate the two-measurement system problem as a multivariate monitoring problem. However, this problem can be considered as a special case of multivariate monitoring since the two variables happen to be measuring the same quality characteristic but we still have two correlated variables providing information about the process. In this special case a mean shift of the single quality characteristic being measured is not affected by which measurement device is used, and results in specific mean shifts in the two measurement variables. The details of this issue are discussed later in this section.

Steiner's (2000) basic idea for monitoring in the two-measurement system problem is similar to the idea of the sequential sampling scheme used to define the SS_1 MEWMA chart discussed in Section 3.1, except that Steiner (2000) investigated the case using a univariate $\bar{X}$ chart, where if there is an indication of a problem after measuring the items using the first measurement device $(\bar{Y}_{k1})$, then the second measurement device is used to measure the same items $(\bar{Y}_{k2})$. Define $\bar{w}_k$ to be a weighted average of $\bar{Y}_{k1}$ and $\bar{Y}_{k2}$, where

$$\bar{w}_k = K\bar{Y}_{k1} + (1 - K)\bar{Y}_{k2}.$$

The value K is chosen to minimize $\text{Var}(\bar{w}_k)$, where $K = \sigma_{02}^2/(\sigma_{01}^2 + \sigma_{02}^2)$. The decision after measuring the items using the second measurement device is based on the weighted average $\bar{w}_k$. Steiner (2000) proposed an optimization procedure to find n and the control limits, where the measurement costs are minimized while maintaining the desired in-control ATS and the minimum ATS of a specific shift size in the mean of the quality characteristic (μ).

The decision rule for the $\bar{X}$ chart proposed by Steiner (2000) requires the specification of two control limits (c_1 and c_2) and one warning limit (b_1), satisfying $0 < b_1 < c_1$. Then the decision rule is defined as follows. If the current sampling point is k,

1. Observe a sample of n observations using the first measurement device.
2. Compute $\bar{Y}_{k1}$ based on n observations.
   (a) If $\bar{Y}_{k1} \in [-b_1, b_1]$, then stop sampling at sampling point k and wait until sampling point $k+1$ to sample again.
   (b) If $|\bar{Y}_{k1}| \in [b_1, c_1]$, then go to Step 3.
   (c) If $\bar{Y}_{k1} \notin [-c_1, c_1]$, then signal that there has been a change in the mean μ.
3. Observe the same sample of n observations using the second measurement device.
4. Compute $\bar{Y}_{k2}$ based on n observations.
5. Compute $\bar{w}_k = K\bar{Y}_{k1} + (1-K)\bar{Y}_{k2}$, where $K = \sigma_{02}^2/(\sigma_{01}^2 + \sigma_{02}^2)$.
   (a) If $\bar{w}_k \in [-c_2, c_2]$, then stop sampling at sampling point k and wait until sampling point $k+1$ to sample again.
   (b) If $\bar{w}_k \notin [-c_2, c_2]$, then signal that there has been a change in the mean μ.

In this section, the UGSS MEWMA chart is applied to monitor a production process using two measurement systems. In the two-measurement system problem, since only two different measurement devices are considered to monitor a single quality characteristic, the

proposed UGSS MEWMA chart for $p = 2$ case is applied. Following the notation in Section 5.1, it is assumed that the first variable corresponds to measuring an item with a more accurate and expensive device, which is the second measurement device of Steiner (2000), and the second variable corresponds to using an inexpensive and easy to apply measurement device, which is the first measurement device of Steiner (2000). Additionally it is assumed that all items tested using the first and second measurement devices are not destructive or intrusive.

In the two-measurement system problem, since two variables are measuring the same quality characteristic, the two variables would be highly correlated and a shift in the distribution of X_{kl} in Equation (5.6) corresponds to the same shift in both Y_{k1l} and Y_{k2l}. The basic idea of applying the UGSS MEWMA chart to the two-measurement system problem is that it would be advantageous to use the UGSS MEWMA chart since the UGSS MEWMA chart performs well when a specific shift direction is considered as shown in Section 5.4, where the shift direction with the best performance mostly depends on the correlation coefficient considered.

When the UGSS MEWMA chart is applied to the two-measurement system problem, some modifications are made to the notation given in Equation (5.6), since the group sizes do not need to be n. For example, suppose that a sample of 3 items is measured using two measurement systems proposed by Steiner (2000). His method is to measure 3 items at the first stage using the inexpensive and easy to apply measurement device and, if needed, measure the same 3 items again at the second stage using the more accurate and expensive measurement device. If we apply the UGSS MEWMA chart to this example, then at the first stage we can select 5 items to measure using the inexpensive measurement device, but only 2 items are measured using the expensive measurement device. If the data at the first stage shows some indication of a problem, then the second stage of sampling is used in which the remaining 3 items are measured using the expensive measurement device.

An alternative form of the model obtained for the UGSS MEWMA chart is

$$Y_{kijl} = X_{kjl} + e_{kijl}, \quad i = 1, 2, \;\; j = 1, 2, \;\; \text{and} \;\; l = 1, 2, \cdots, n, \tag{5.7}$$

where Y_{kijl} is the l^{th} observation of the i^{th} variable at the j^{th} stage and sampling point k. Let $\bar{Y}_{kij} (= \Sigma_{l=1}^{n} Y_{kijl}/n)$ be the average of n observations using the i^{th} variable at the j^{th} stage. Then the standardized sample mean vector is defined to be

$$\boldsymbol{V}_{kj} = (V_{k1j}, V_{k2j})^T,$$

where V_{kij} is the standardized sample mean of the i^{th} variable at the j^{th} stage and sampling point k, and is given by

$$V_{kij} = \frac{\sqrt{n_{ij}}(\bar{Y}_{kij} - \mu_0)}{\sqrt{\sigma_0^2 + \sigma_{0i}^2}}.$$

The same procedures of the UGSS MEWMA chart proposed in Section 5.1 are used for the decision rule of the two-measurement system problem based on the statistic T_{kj}^2. The covariance matrix of the standardized sample mean vector $\boldsymbol{V}_{kj}$, $\boldsymbol{\Sigma}_{V_j}$ is given, for $j = 1, 2$, by

$$\boldsymbol{\Sigma}_{V_j} = \begin{pmatrix} 1 & \sqrt{\frac{n_{1j}}{n_{2j}}}\rho \\ \sqrt{\frac{n_{1j}}{n_{2j}}}\rho & 1 \end{pmatrix},$$

where $\rho = \text{Corr}(Y_{k1jl}, Y_{k2jl})$.

Steiner (2000) considered a shift in the mean of the quality characteristic X_{kjl} in Equation (5.7), not directly in the variable being measured, which is Y_{kijl} in Equation (5.7), so that we compare the SSATS performance of the proposed UGSS MEWMA chart with his method later in this section in terms of the shift size in the mean of the quality characteristic (μ) instead of units of the noncentrality parameter (δ) used in previous chapters. The assumption used by Steiner (2000) that the quality characteristic X_{kjl} has mean zero and standard variation equal to 1 is applied. We define the sustained standardized mean shift for the i^{th} variable to be

$$\nu_i = \frac{\mu}{\sqrt{\sigma_0^2 + \sigma_{0i}^2}}, \quad i = 1, 2.$$

In the proposed UGSS MEWMA chart, the standardized sample mean shift for the i^{th} variable at stage j can be obtained as

$$\begin{aligned}\nu'_{ij} &= \mathrm{E}(V_{kij}) \\ &= \sqrt{n_{ij}}\frac{\mu}{\sqrt{\sigma_0^2+\sigma_{0i}^2}} \\ &= \sqrt{n_{ij}}\nu_i, \quad i=1,2.\end{aligned}$$

When the UGSS MEWMA chart is considered, the shift direction is determined by the variance of each measurement device and the group sizes used at each stage. The direction of shift θ at the j^{th} stage for $n_{1j}(\neq 0)$ and n_{2j} can be obtained as

$$\theta = \tan^{-1}\left(\sqrt{\frac{n_{2j}(1+\sigma_1^2)}{n_{1j}(1+\sigma_2^2)}}\right), \quad j=1,2.$$

Steiner (2000) gave an example in the manufacture of engine front covers to apply a control chart using two measurement systems. The quality characteristic of interest in this example is the distance between two bolt holes in the engine cover used to attach the cover to the engine block. Two measurement devices considered are a fixture gauge and a coordinate measurement machine (CMM). The fixture gauge that clamps the engine cover in a fixed position while measuring hole diameters and relative distances is a less accurate and easy to use measurement device and the CMM is a time consuming and expensive but more accurate measurement device. When the UGSS MEWMA chart is applied to this example, the CMM is used as the first variable and the fixture gauge is used as the second variable. It is assumed in this example that $\sigma_1 = 0.05$ and $\sigma_2 = 0.5$, which values are determined from previous measurement-system studies, and the fixed measurement cost for using the CMM is six times as expensive as the fixture gauge, where the vector representing the fixed measurement cost is obtained as $\boldsymbol{f} = (6,1)^T$. Steiner (2000) gave an optimal solution for this example from solving the optimization procedure described previously, where the minimum ATS of a specific shift size in the mean of the variable $\mu = \pm 2$ is chosen to match with a Shewhart $\bar{X}$ chart with a sample size of $n = 5$. The values for the optimal solution are given

by

$$b_1\sqrt{n} = c_2\sqrt{n} = 2.89 \quad \text{and} \quad n = 5.36,$$

with a corresponding measurement cost of 5.67, where c_1 is set to be ∞ for simplification and he recommended to use the sample size of 5 for practical implementation. The proposed $\bar{X}$ chart by Steiner (2000) based on the above optimal solution will be compared next to the UGSS MEWMA chart having the sample size vector matched with his solution.

The SSATS performance of the UGSS MEWMA chart applied to the two-measurement system problem is compared to that of the $\bar{X}$ chart proposed by Steiner (2000), and is given in Tables 5.26-5.28. A total of 1,000,000 runs were used in simulation studies to estimate g, h, and compute SSATS values. Shift sizes in the mean of the quality characteristic (μ) considered in the tables are 0.1, 0.15, 0.2, 0.25, 0.3, 0.4, 0.5, 0.75, 1.0, 1.5, 2.0, 3.0, 4.0, and 5.0. Table 5.26 shows SSATS values and total expected measurement costs for the $\bar{X}$ chart proposed by Steiner (2000) based on the optimal solution and the UGSS MEWMA chart. Columns 2 and 4 contain SSATS values and total expected measurement costs, respectively, based on the $\bar{X}$ chart proposed by Steiner (2000), and Columns 3 and 5 contain SSATS values and total expected measurement costs calculated based on the UGSS MEWMA chart. Examining Table 5.26 shows that the UGSS MEWMA chart performs much better than the $\bar{X}$ chart proposed by Steiner (2000) in detecting mean shifts except for moderate sizes of mean shift considered. However, the difference is relatively small compared with the reductions in STATS values for other mean shifts considered. When the total expected measurement cost is considered, we can see that the UGSS MEWMA chart has the uniformly lower total expected measurement cost.

Now a different example is considered for the purpose of comparing the standard MEWMA chart to both the $\bar{X}$ chart proposed by Steiner (2000) and the UGSS MEWMA chart. Since the corresponding measurement cost of 5.67 is obtained by solving the optimization procedure in the above example with the vector representing the fixed measurement cost of $\boldsymbol{f} = (6, 1)^T$, the sample size of the proposed $\bar{X}$ chart by Steiner (2000) has no cor-

responding sample size for the standard MEWMA chart, where the minimum measurement cost that can be obtained for the standard MEWMA chart is 7 with the sample size of $n = 1$. Here the sample size of $n = 3$ is assumed for the standard MEWMA chart and then the sample size for the $\bar{X}$ chart proposed by Steiner (2000) is chosen by solving the optimization procedure. All charts considered in Tables 5.27-5.28 have an in-control ATS of 200 and an expected in-control measurement cost of 21, where the vector representing the fixed measurement cost $\boldsymbol{f} = (6, 1)^T$ is assumed as in the first example given above. Table 5.27 shows SSATS values for UGSS MEWMA charts for a selected set of group size vectors. Column 3 contains the reference chart of the standard MEWMA chart with the sample size of $n = 3$ having the weight of $r(n) = 0.1$. The $\bar{X}$ chart proposed by Steiner (2000) is given in column 2, where the sample size of 19 and the control limits are chosen based on the optimal solution. Columns 4-9 contain SSATS values of UGSS MEWMA charts having a maximum sample size of $\tau_i = (6, 8, 10, 12, 14, 19)$, respectively. The UGSS MEWMA chart is designed so that all items are measured for both variables either at the first stage or second stage. Table 5.28 has the same structure as Table 5.27 except that Table 5.28 gives total expected measurement costs. From Tables 5.27-5.28, we see that as τ_i increases the UGSS MEWMA chart performs much better than the other charts in terms of both the SSATS performance and the total expected measurement cost. The best performance is achieved when a group size vector of $\boldsymbol{n}_1 = (0, 19)$ and $\boldsymbol{n}_2 = (19, 0)$ are used (i.e., $\tau_i = 19$). The SSATS performance of the standard MEWMA chart is comparable to that of the $\bar{X}$ chart proposed by Steiner (2000), however, the standard MEWMA chart does not work quite as well as the proposed UGSS MEWMA chart having a relatively large value of τ_i. In practical applications, if any additional administrative cost is not that high, it appears that it is best to choose the group size vector having as large value of τ_i as is feasible.

Table 5.26: SSATS Values and Total Expected Measurement Costs of the UGSS MEWMA Chart

		SSATS		Total Expected Measurement Costs	
		Steiner	UGSS MEWMA	Steiner	UGSS MEWMA
$\boldsymbol{n}_1$		(0,5)	(0,5)	(0,5)	(0,5)
$\boldsymbol{n}_2$		(5,0)	(5,0)	(5,0)	(5,0)
τ_i		5	5	5	5
r_{ij}		—	0.1	—	0.1
μ	0.0	370.4	370.4	1960	1960
	0.1	297.5	112.9	1588	651
	0.15	236.5	62.8	1276	390
	0.2	181.0	39.4	991	266
	0.25	136.4	27.2	762	197
	0.3	102.4	20.2	587	156
	0.4	58.6	12.8	359	108
	0.5	34.7	9.2	232	82
	0.75	11.0	5.2	101	49
	1.0	4.3	3.5	58	34
	1.5	1.2	2.1	29	20
	2.0	0.6	1.5	20	14
	3.0	0.5	0.9	18	9
	4.0	0.5	0.6	18	5
	5.0	0.5	0.5	18	3
h		—	8.705	—	8.705
g		—	6.231	—	6.231
c_1		∞	—	∞	—
c_2		1.292	—	1.292	—
b_1		1.292	—	1.292	—

Table 5.27: SSATS Values of the UGSS MEWMA Chart

		Steiner	MEWMA	UGSS MEWMA					
$\boldsymbol{n}_1$		(0,19)	(3,3)	(2,6)	(2,8)	(1,10)	(1,12)	(1,14)	(0,19)
$\boldsymbol{n}_2$		(19,0)	—	(4,0)	(6,0)	(9,0)	(11,0)	(13,0)	(19,0)
τ_i		19	3	6	8	10	12	14	19
r_{ij}		—	0.1	0.1	0.1	0.1	0.1	0.1	0.1
μ	0.0	200.0	200.0	200.0	200.0	200.0	200.0	200.0	200.0
	0.1	107.3	83.6	79.7	70.1	59.9	53.7	49.4	31.8
	0.15	64.3	47.9	45.5	38.7	32.3	28.6	26.0	17.3
	0.2	38.7	30.4	29.0	24.4	20.5	18.1	16.5	11.3
	0.25	23.9	21.2	20.4	17.1	14.4	12.8	11.7	8.2
	0.3	15.3	15.9	15.3	13.0	11.0	9.8	9.0	6.4
	0.4	6.9	10.4	9.9	8.5	7.3	6.5	6.1	4.3
	0.5	3.5	7.6	7.2	6.2	5.4	4.9	4.5	3.2
	0.75	1.1	4.5	4.1	3.7	3.2	2.9	2.7	1.9
	1.0	0.6	3.1	2.8	2.5	2.2	2.0	1.9	1.4
	1.5	0.5	2.0	1.7	1.5	1.2	1.2	1.2	0.8
	2.0	0.5	1.4	1.1	1.1	0.8	0.8	0.8	0.6
	3.0	0.5	0.9	0.6	0.6	0.5	0.5	0.5	0.5
	4.0	0.5	0.6	0.5	0.5	0.5	0.5	0.5	0.5
	5.0	0.5	0.5	0.5	0.5	0.5	0.5	0.5	0.5
h		—	8.783	8.435	8.580	8.666	8.707	8.813	7.415
g		—	—	3.248	5.706	3.868	5.039	6.839	5.058
c_1		∞	—	—	—	—	—	—	—
c_2		0.618	—	—	—	—	—	—	—
b_1		0.618	—	—	—	—	—	—	—

Table 5.28: Total Expected Measurement Costs of the UGSS MEWMA Chart

		Steiner	MEWMA	UGSS MEWMA					
$\boldsymbol{n}_1$		(0,19)	(3,3)	(2,6)	(2,8)	(1,10)	(1,12)	(1,14)	(0,19)
$\boldsymbol{n}_2$		(19,0)	—	(4,0)	(6,0)	(9,0)	(11,0)	(13,0)	(19,0)
τ_i		19	3	6	8	10	12	14	19
μ	0.0	4165	4200	4200	4200	4200	4200	4200	4200
	0.1	2337	1756	1804	1548	1540	1352	1140	868
	0.15	1482	1005	1095	895	949	816	647	542
	0.2	966	638	736	591	658	565	437	388
	0.25	662	445	537	430	492	425	326	298
	0.3	479	334	414	334	386	336	258	239
	0.4	287	217	275	227	261	231	180	168
	0.5	197	159	200	169	192	172	136	127
	0.75	104	94	114	100	110	100	81	76
	1.0	74	66	78	69	75	68	56	52
	1.5	67	41	45	40	42	39	33	31
	2.0	67	30	30	28	27	26	23	19
	3.0	67	19	16	16	13	12	12	10
	4.0	67	13	11	11	8	9	10	10
	5.0	67	11	9	10	8	9	10	10

5.6 Conclusions and Recommendations for Applications

In this chapter, it is shown that the UGSS MEWMA chart performs well when a specific direction of shift is considered. When the SSATS values averaged over randomly generated shift directions are considered for both the $p = 2$ and $p = 4$ cases, the UGSS MEWMA chart has moderately better SSATS performance than the standard MEWMA chart unless the variables are highly correlated. The correlation coefficient is another factor to be considered before designing the UGSS MEWMA chart. In practical applications, we do not recommend using the UGSS MEWMA chart when most variables are highly correlated ($\rho > 0.7$) unless the shift is likely to be in directions where performance is good.

When the UGSS MEWMA chart is applied to the two-measurement system problem investigated by Steiner (2000), the UGSS MEWMA chart performs better than the $\bar{X}$ chart procedure proposed by Steiner (2000). The best performance of the UGSS MEWMA chart can be achieved using a large value of τ_i. In practical applications, it appears that it is best to choose τ_i as large as is feasible but τ_i does not need to be extremely large to give significant reductions in SSATS compared to the $\bar{X}$ chart proposed by Steiner (2000).

Chapter 6

Monitoring Linear Profiles

6.1 Phase II Methods

It is assumed that for the j^{th} random sample collected over time we have the observations (x_i, y_{ij}), $i = 1, 2, \cdots, n$. It is assumed that when the process is in statistical control, the underlying model is

$$Y_{ij} = A_0 + A_1 X_i + \epsilon_{ij}, \quad i = 1, 2, \cdots, n, \tag{6.1}$$

where the ϵ_{ij}'s are independent, identically distributed (i.i.d.) normal random variables with mean zero and variance σ^2. For simplicity, the case for which the X-values are fixed and take the same set of values for each sample is considered. In this section the Phase II case is considered, in which the in-control values of the parameters A_0, A_1, and σ^2 in Equation (6.1) are assumed to be known.

6.1.1 Bivariate Approach in Phase II Methods

Kang and Albin (2000) proposed two strategies to monitor a process when the regression parameters are all known. Their first strategy is to use a bivariate T^2 chart to monitor the

regression coefficients. This chart is based on the fact that the least squares estimators of A_0 and A_1 have a bivariate normal distribution. The least squares estimators of A_0 and A_1 for sample j are given by the following formulas:

$$a_{0j} = \bar{y}_j - a_{1j}\bar{x} \text{ and } a_{1j} = \frac{S_{xy(j)}}{S_{xx}} \tag{6.2}$$

where $\bar{y}_j = \frac{1}{n}\sum_{i=1}^{n} y_{ij}$, $\bar{x} = \frac{1}{n}\sum_{i=1}^{n} x_i$, $S_{xy(j)} = \sum_{i=1}^{n}(x_i - \bar{x})y_{ij}$, and $S_{xx} = \sum_{i=1}^{n}(x_i - \bar{x})^2$. The least squares estimators a_{0j} and a_{1j} have a bivariate normal distribution with the mean vector

$$\boldsymbol{\mu} = (A_0, A_1)^T \tag{6.3}$$

and the variance-covariance matrix

$$\boldsymbol{\Sigma} = \begin{pmatrix} \sigma_0^2 & \sigma_{01}^2 \\ \sigma_{01}^2 & \sigma_1^2 \end{pmatrix} \tag{6.4}$$

where $\sigma_0^2 = \sigma^2(\frac{1}{n} + \frac{\bar{x}^2}{S_{xx}})$, $\sigma_1^2 = \sigma^2\frac{1}{S_{xx}}$ and $\sigma_{01}^2 = -\sigma^2\frac{\bar{x}}{S_{xx}}$ are the variance of a_{0j}, the variance of a_{1j} and the covariance between a_{0j} and a_{1j}, respectively.

In their first monitoring strategy one computes the vector of sample estimates $\boldsymbol{Z}_j = (a_{0j}, a_{1j})^T$ for sample j, where a_{0j} and a_{1j} are the sample intercept and the sample slope as defined in Equation (6.2). Then one calculates the T^2 statistic given by

$$T_j^2 = (\boldsymbol{Z}_j - \boldsymbol{\mu})^T\boldsymbol{\Sigma}^{-1}(\boldsymbol{Z}_j - \boldsymbol{\mu}), \tag{6.5}$$

where $\boldsymbol{\mu}$ and $\boldsymbol{\Sigma}$ are defined as in Equations (6.3) and (6.4), respectively. When the process is in-control, T_j^2 follows a central chi-square distribution with 2 degrees of freedom. Therefore, the recommended upper control limit for the chart is UCL $= \chi_{2,\alpha}^2$, where $\chi_{2,\alpha}^2$ is the $100(1-\alpha)$ percentile of the chi-square distribution with 2 degrees of freedom. When there are shifts from the in-control parameter values, Kang and Albin (2000) pointed out that T_j^2 in Equation (6.5) follows a non-central chi-square distribution with a non-centrality parameter

$$\tau = n(\lambda + \beta\bar{x})^2 + \beta^2 S_{xx},$$

where λ is the shift in the intercept A_0 and β is the shift in the slope A_1. Both λ and β are measured in units of σ by Kang and Albin (2000), so the actual shifts in this case are $\lambda\sigma$ and $\beta\sigma$ from A_0 and A_1, respectively.

Kang and Albin (2000) studied the average run length (ARL) performance of their T^2 control chart using a simulation study. However, since T_j^2 has a non-central chi-square distribution, one can evaluate the exact ARL of the T^2 chart using the following formula:

$$\text{ARL} = \frac{1}{\Pr(T_j^2 > \chi^2_{2,\alpha})}.$$

6.1.2 Residual Control Charts in Phase II Methods

Their second strategy is to apply some standard control chart schemes to the regression "residuals" obtained at sample j using

$$e_{ij} = y_{ij} - A_0 - A_1 x_i, \quad i = 1, 2, \cdots, n.$$

They applied an EWMA chart to monitor the average value of these deviations. They suggested an R-chart be used in combination with the EWMA chart.

The average of the residuals for the j^{th} sample is denoted by $\bar{e}_j$, calculated using

$$\bar{e}_j = \frac{\sum_{i=1}^{n} e_{ij}}{n}.$$

The EWMA control chart statistics, denoted by $z_j, j = 1, 2, \cdots$, are given by

$$z_j = \theta \bar{e}_j + (1 - \theta) z_{j-1},$$

with $\theta (0 < \theta \leq 1)$ a smoothing constant and $z_0 = 0$. An out-of-control signal is given as soon as z_j is less than the LCL or z_j is greater than the UCL, where

$$\text{LCL} = -L\sigma\sqrt{\frac{r}{(2-r)n}}, \text{ UCL} = L\sigma\sqrt{\frac{r}{(2-r)n}}. \tag{6.6}$$

and $L(> 0)$ is a constant selected to give a specified in-control ARL. Kang and Albin (2000) proposed an R-chart to be used in conjunction with this EWMA chart for two reasons. The first reason is to detect shifts in the process variance σ^2 since the EWMA chart is not sensitive to shifts in the process variation. The other reason is that the EWMA chart based on the average residual is not sensitive to some shifts in A_0 and A_1 for which the magnitudes of the residuals tend to be large, but the average residual tends to be very small. This can occur, for example, when the slope of the line changes, but the average value of Y does not.

For the R-chart, Kang and Albin (2000) recommended that one calculate and plot the sample ranges $R_j = \max_i(e_{ij}) - \min_i(e_{ij}), j = 1, 2, \cdots$. The lower and upper control limits for the R-chart are

$$\text{LCL} = \sigma(d_2 - Ld_3) \text{ and } \text{UCL} = \sigma(d_2 + Ld_3), \tag{6.7}$$

respectively, where $L(> 0)$ is a constant chosen to give a specified in-control ARL. The values of d_2 and d_3 are commonly-used constants that depend on the sample size n. These values can be found, for example, in tables in Montgomery (2001) or Ryan (2000). One disadvantage of this approach, however, is that if $n < 7$ there is no lower control limit and one cannot detect decreases in variation about the regression line.

6.2 Transformation

In this proposed alternative approach, the X-values are coded first so that the average coded value is zero. This simplifies the resulting analysis and removes much of the need for a T^2 approach since, in this situation, the least squares estimators of the Y-intercept and slope for each sample are independent random variables. See, for example, Myers (1990, pp. 11-15) and Ryan (1997, pp. 38-39).

After transforming the X-values, an alternative form of the underlying model in

Equation (6.1) is obtained as

$$Y_{ij} = B_0 + B_1 X_i' + \epsilon_{ij}, \quad i = 1, 2, \cdots, n, \tag{6.8}$$

where $B_0 = A_0 + A_1\bar{X}$, $B_1 = A_1$, and $X_i' = (X_i - \bar{X})$.

For the j^{th} sample, the least squares estimator of B_0 is $b_{0j} = \bar{y}_j$ while the least squares estimator of B_1 is the same as that for A_1 in Equation (6.2). Both b_{0j} and b_{1j} are normally distributed with means B_0 and B_1 and variances $\frac{\sigma^2}{n}$ and $\frac{\sigma^2}{S_{xx}}$, respectively. Also the covariance between b_{0j} and b_{1j} is zero in Equation (6.4). Thus, a separate control chart can be applied for each sequence of random variables without the problems that would result if the estimators were highly correlated.

6.3 The Proposed Control Charts

The proposed method in Phase II to detect sustained shifts in the underlying parameters is to use three separate univariate control charts. EWMA charts are used to monitor the Y-intercept, the slope and the error variance, respectively, although one could use other types of charts, such as the cumulative sum and Shewhart charts, if desired. The three EWMA charts are used jointly, with the combination of charts signaling with the first chart to signal. The basic motivation for this proposed method comes from the fact that when assignable causes are present in a process for which the output of a product is characterized by a linear profile, it seems reasonable that at least one of three parameters, the Y-intercept, the slope and the error variance, would be directly affected. Thus, use of the three EWMA charts should result in at least one signal when there has been a sustained change in the process. Also, having a control chart corresponding to each parameter leads to an easier diagnosis of any process change than the omnibus methods of Kang and Albin (2000).

As an example, once the parameters are established in a baseline calibration study, one would want to detect any change in the Y-intercept or slope and any increase in the

variation about the regression line since such shifts correspond to greater inaccuracies in the measurement process. A change in the Y-intercept corresponds to the introduction of bias and a change in the slope could lead to a dilation or contraction of the measurement scale. A decrease in the variation about the line would correspond to an improvement in the measurement process, as long as the other parameters do not change. The effect of assignable causes, however, will vary from application to application. Sometimes, for example, one may wish to detect isolated outliers.

In this proposed method, the technique proposed by Crowder and Hamilton (1992) is first incorporated, where an EWMA chart based on the logarithmic transformation of the sample variance was used to monitor for increases in process variability. Crowder and Hamilton (1992) showed, as expected, that their EWMA chart is superior to the usual R-chart in detecting small and moderate-sized increases in a process variance. If one wishes to detect decreases in variation, as will frequently be the case, then appropriate methods are discussed by Acosta-Mejia, Pignatiello, and Rao (1999) and Lowry, Champ, and Woodall (1995).

6.3.1 Monitoring the Intercept

For the EWMA chart for monitoring the Y-intercept (B_0), the estimates of the Y-intercept, b_{0j}, is used to compute the EWMA statistics

$$\text{EWMA}_\text{I}(j) = rb_{0j} + (1-r)\text{EWMA}_\text{I}(j-1), \tag{6.9}$$

$j = 1, 2, \cdots$, with $r(0 < r \leq 1)$ a smoothing constant and $\text{EWMA}_\text{I}(0) = B_0$. An out-of-control signal is given as soon as $\text{EWMA}_\text{I}(j) < \text{LCL}$ or $\text{EWMA}_\text{I}(j) > \text{UCL}$, where

$$\text{LCL} = B_0 - L_I\sigma\sqrt{\frac{r}{(2-r)n}} \text{ and } \text{UCL} = B_0 + L_I\sigma\sqrt{\frac{r}{(2-r)n}}. \tag{6.10}$$

In Equation (6.10), $L_I(> 0)$ is chosen to give a specified in-control ARL.

6.3.2 Monitoring the Slope

The estimates of the slope B_1, b_{1j}, are used in the EWMA chart for monitoring the slope. The EWMA statistics are given by

$$\text{EWMA}_{\text{S}}(j) = rb_{1j} + (1-r)\text{EWMA}_{\text{S}}(j-1), \tag{6.11}$$

$j = 1, 2, \cdots$, with $r(0 < r \leq 1)$ a smoothing constant and $\text{EWMA}_S(0) = B_1$. The lower and upper control limits for the chart are given by

$$\text{LCL} = B_1 - L_S\sigma\sqrt{\frac{r}{(2-r)S_{xx}}} \text{ and UCL} = B_1 + L_S\sigma\sqrt{\frac{r}{(2-r)S_{xx}}}. \tag{6.12}$$

respectively, where $L_S(> 0)$ is chosen to give a specified in-control ARL.

6.3.3 Monitoring the Error Variance

Finally, the EWMA chart for monitoring the error variance (σ^2) is considered based on the approach of Crowder and Hamilton (1992). In this proposed method, the values of MSE_j, i.e., the usual estimator of σ^2 based on the residuals corresponding to the fitted line at sample j, are applied to obtain the EWMA statistics instead of their use of sample variances. In contrast to the two EWMA charts described above, this chart is a one-sided EWMA scheme to detect only increases in process variability. We have the EWMA statistics

$$\text{EWMA}_{\text{E}}(j) = \max\{rln(MSE_j) + (1-r)\text{EWMA}_{\text{E}}(j-1), ln(\sigma_0^2)\} \tag{6.13}$$

for $j = 1, 2, \cdots$, with $r(0 < r \leq 1)$ again a smoothing constant and $\text{EWMA}_{\text{E}}(0) = ln(\sigma_0^2)$. In this proposed method, the assumption that σ_0^2, the in-control value of σ^2, is 1 is made without loss of generality, so we have $\text{EWMA}_{\text{E}}(0) = 0$. Lawless (1980, pp 21-23) provided an exact expression for $\text{Var}[ln(MSE_j)]$ using the log-gamma distribution, but for convenience the following approximation that is very similar to a result derived by Crowder and Hamilton

(1992) is used:

$$\text{Var}[ln(MSE_j)] \approx \frac{2}{n-2} + \frac{2}{(n-2)^2} + \frac{4}{3(n-2)^3} - \frac{16}{15(n-2)^5}.$$

The procedure signals when $\text{EWMA}_\text{E}(j)$ is greater than an upper control limit given by

$$\text{UCL} = L_E\sqrt{\frac{r}{(2-r)}\text{Var}[ln(MSE_j)]} \tag{6.14}$$

and the multiplier $L_E(> 0)$ is again chosen to give a specified in-control ARL. One could, of course, use a two-sided procedure if detecting decreases in the error variance was also considered to be important, as will frequently be the case in applications.

6.4 ARL Comparisons

In this section the ARL performance of the proposed EWMA-based method in Phase II is compared to the performance of the methods proposed by Kang and Albin (2000). The same example used in their simulation study is considered. All chart combinations studied are designed to have the same overall in-control ARL of 200. The smoothing constants r in Equations (6.9), (6.11), and (6.13) are set equal to 0.2 as in the EWMA chart used by Kang and Albin (2000). One could, of course, use different smoothing constants for each chart. In general, smaller smoothing constants lead to quicker detection of smaller shifts, as shown by Lucas and Saccucci (1990). A total of 10,000 replications were used in this simulation study to estimate each ARL value. Exact ARL values, however, are given for the T^2 chart method.

The underlying in-control linear profile model used by Kang and Albin (2000) is $Y_{ij} = 3 + 2X_i + \epsilon_{ij}$, where the ϵ_{ij}'s are i.i.d. normal random variables with mean zero and variance one. The fixed X_i-values of 2, 4, 6, and 8 (with $\bar{x} = 5$) were used in their simulation study. In this proposed method, we transform these X_i-values using the alternate form of the model in Equation (6.8) and obtain the new linear function $Y_{ij} = 13 + 2X'_i + \epsilon_{ij}$, where the ϵ_{ij}'s are i.i.d. N(0,1) random variables. The X_i'-values are -3, -1, 1, and 3 with $\bar{x}' = 0$.

The combination of the three EWMA charts is denoted by EWMA_3. In EWMA_3, each of the three EWMA charts is designed to have the same in-control ARL when considered individually. For the EWMA chart for monitoring the Y-intercept, L_I in Equation (6.10) is chosen as 3.0156 to give the in-control ARL of 584.7. For the EWMA chart for monitoring the slope, L_S in Equation (6.12) is set equal to 3.0109 to have an in-control ARL of 584.6. Finally, L_E in Equation (6.14) is chosen as 1.3723 to achieve the in-control ARL of 584.4 for the EWMA chart for monitoring the error variance. The combination of all three EWMA charts has an overall in-control ARL of roughly 200.

The EWMA and R charts used by Kang and Albin (2000) in their simulation study have the same multiplier L in Equations (6.6) and (6.7). We found that the value $L = 3.1151$ yields an in-control ARL of approximately 802 for the EWMA chart for monitoring the average deviation and an in-control ARL of approximately 261 for the R chart, which has no lower control limit with $n = 4$. These ARL estimates were each obtained using 10,000 simulations. The in-control ARL of their combined procedure is close to 200, as they claim.

Four different types of shifts are considered in the simulation study. These are intercept shifts and slope shifts under the model in Equation (6.1), error variance increases, and slope shifts under the model in Equation (6.8) for which the average value of the independent variable is coded to be zero. The plots in each of the figures are based on ARL values for 200 equally spaced shifts within each range of shifts considered.

Table 6.1 and Figure 6.1 give the ARL values for shifts in A_0 (or equivalently in B_0) in units of σ. (Kang and Albin (2000) measure the sizes of the shifts in these units, although use of units of $\sigma/n^{1/2}$ would lead to greater generality.) This proposed method, EWMA_3 performs a little better than the EWMA/R chart and much better than the T^2 chart in detecting small-to-moderate shifts in the intercept. The T^2 chart works better than this proposed method for large shifts. For improved performance for the EWMA_3 method in detecting large shifts, one could incorporate Shewhart limits into each of the three EWMA charts in a manner discussed by Lucas and Saccucci (1990). Our use of the

constant asymptotic control limits instead of the "exact" limits discussed by Steiner (1999) also results in a slight delay in detecting shifts occurring with the first sample as is assumed in our simulations.

Table 6.1: ARL Comparisons Under Intercept Shifts From A_0 To $A_0 + \lambda\sigma$
(In-control ARL = 200)

	λ									
Chart	0.2	0.4	0.6	0.8	1.0	1.2	1.4	1.6	1.8	2.0
EWMA/R	66.5	17.7	8.4	5.4	3.9	3.2	2.7	2.3	2.1	1.9
T^2	137.7	63.5	28.0	13.2	6.9	4.0	2.6	1.8	1.5	1.2
EWMA_3	59.1	16.2	7.9	5.1	3.8	3.1	2.6	2.3	2.1	1.9

In Table 6.2 and Figure 6.2, the case when there are shifts in the slope parameter A_1 in model (6.1) in units of σ is considered. The proposed method performs uniformly slightly better than the EWMA/R chart over the entire range of shifts considered. It has much better performance than the T^2 chart except for the largest shift considered. The difference here, however, is relatively small. The use of a multivariate EWMA control chart, as proposed by Lowry et al. (1992), would result in better statistical performance than that of the T^2 chart, but the interpretation of an out-of-control signal would still not be straightforward.

Table 6.2: ARL Comparisons Under Slope Shifts in Model (6.1) From A_1 To $A_1 + \beta\sigma$
(In-control ARL = 200)

	β									
Chart	0.025	0.050	0.075	0.100	0.125	0.150	0.175	0.200	0.225	0.250
EWMA/R	119.0	43.9	19.8	11.3	7.7	5.8	4.7	3.9	3.4	3.0
T^2	166.0	105.6	60.7	34.5	20.1	12.2	7.8	5.2	3.7	2.7
EWMA_3	101.6	36.5	17.0	10.3	7.2	5.5	4.5	3.8	3.3	2.9

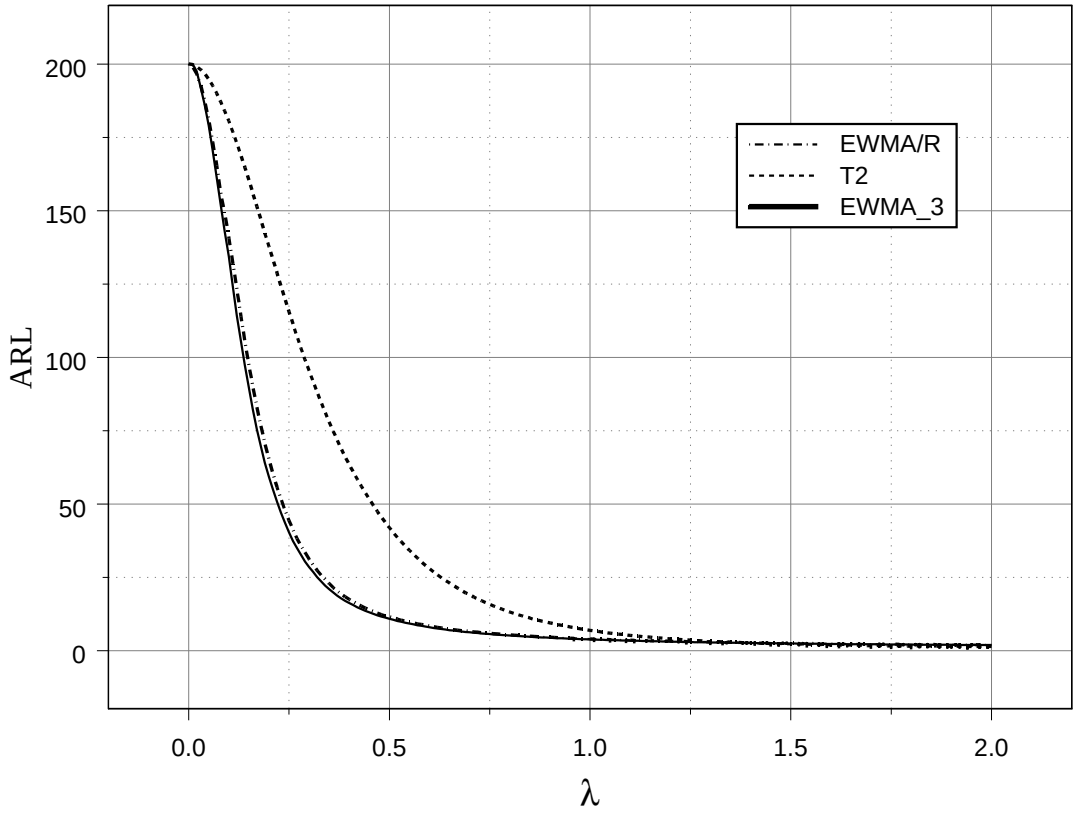

Figure 6.1: ARL Comparisons Under Intercept Shifts λ

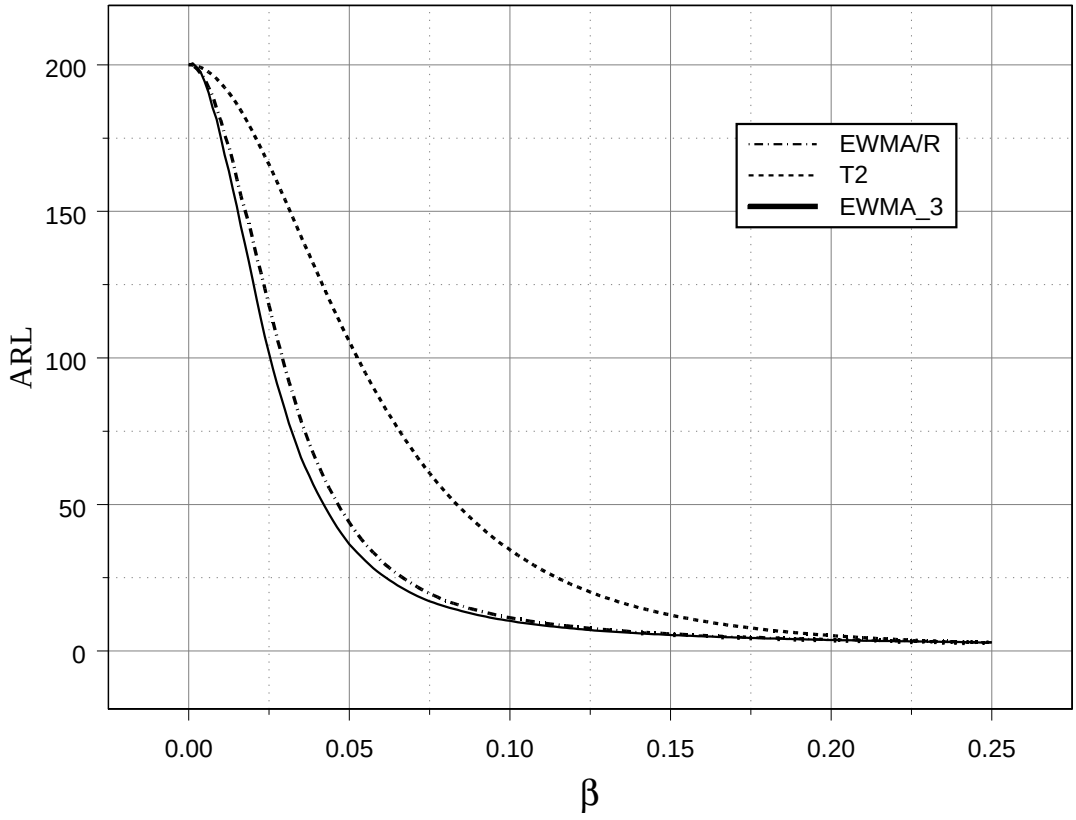

Figure 6.2: ARL Comparisons Under Slope Shifts β

Table 6.3 and Figure 6.3 show that the ARL performance of this proposed method is comparable to that of the T^2 chart for detecting increases in σ. This proposed method does not work quite as well as the EWMA/R method because the standard deviation shifts are mainly detected by the R-chart. The in-control ARL value of 261 for the R-chart is much lower than the in-control ARL value of 584.4 for the EWMA chart designed to detect shifts in the standard deviation. It was surprising to us that the T^2 chart worked so well given that no information is accumulated over time as with the EWMA charts. Since an increase in the standard deviation increases the variance of the estimators of the Y-intercept and slope, smoothing these estimators over time with EWMAs does not appear to be helpful.

Table 6.3: ARL Comparisons Under Standard Deviation Shifts From σ To $\gamma\sigma$
(In-control ARL = 200)

	γ									
Chart	1.2	1.4	1.6	1.8	2.0	2.2	2.4	2.6	2.8	3.0
EWMA/R	34.3	12.0	6.1	3.9	2.9	2.3	1.9	1.7	1.5	1.4
T^2	39.6	14.9	7.9	5.1	3.8	3.0	2.5	2.2	2.0	1.8
EWMA_3	33.5	12.7	7.2	5.1	3.9	3.2	2.8	2.5	2.3	2.1

An EWMA chart based on the natural units, instead of the logarithmic scale, would provide improved performance in detecting increases in the variation about the line. To investigate this issue, the ARL performance of EWMA_3 was compared with the EWMA chart of Crowder and Hamilton (1992) replaced by an EWMA chart with EWMA statistics

$$\text{EWMA}_{\text{N}}(j) = \max\{r(MSE_j - 1) + (1-r)\text{EWMA}_{\text{N}}(j-1), 0\}$$

for $j = 1, 2, \cdots$, with $r(0 < r \leq 1)$ a smoothing constant and $\text{EWMA}_{\text{N}}(0) = 0$. The procedure signals when $\text{EWMA}_{\text{N}}(j)$ is greater than an upper control limit given by

$$\text{UCL} = L_N\sqrt{\frac{r}{(2-r)}\text{Var}[MSE_j]}.$$

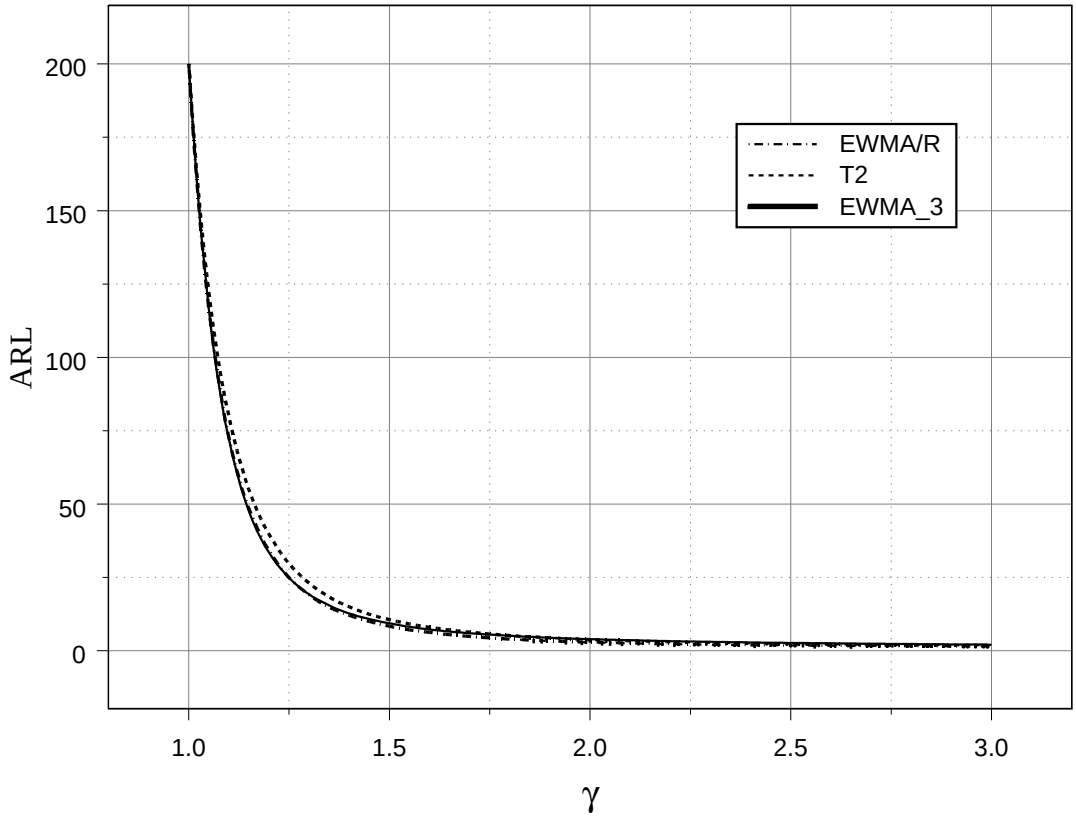

Figure 6.3: ARL Comparisons Under Standard Deviation Shifts γ

The multiplier $L_N(> 0)$ is again chosen to give a specified in-control ARL. We used $L_N = 4.0734$ to achieve the in-control ARL of 589.3 for this chart. The combination of all three EWMA charts has an overall in-control ARL of roughly 200. The ARL comparisons in Table 6.4 show, indeed, that use of the natural units does result in slightly better performance. The substitution of this EWMA chart in place of that of Crowder and Hamilton (1992) did not affect any of the other reported ARL values of our proposed method for shifts in any of the other parameters.

Table 6.4: ARL Comparisons Between the Natural-scale and Log-scale EWMA_3 Under Standard Deviation Shifts (In-control ARL = 200)

	γ									
Chart	1.2	1.4	1.6	1.8	2.0	2.2	2.4	2.6	2.8	3.0
Log-Scale	33.5	12.7	7.2	5.1	3.9	3.2	2.8	2.5	2.3	2.1
Natural-Scale	31.6	11.7	6.5	4.5	3.4	2.7	2.3	2.1	1.8	1.7

Kang and Albin (2000) considered the case for which the relationship between the intercept shift, λ (in units of σ) and the slope shift, β (in units of σ) is given as $\lambda + \beta\bar{x} = 0$ with $\bar{x} = 5$. However, after transforming the X_i-values (2, 4, 6, and 8) into X_i'-values (-3, -1, 1, and 3), this case corresponds to simply a change in slope for the model in Equation (6.8). In Table 6.5 and Figure 6.4, the shift in the slope (in units of σ) in Equation (6.8) is denoted by δ. (Note that use of units of $\sigma/(S_{xx})^{1/2}$ would lead to some greater generality.) Since it can be shown that the ARL values for shifts δ are symmetric around $\delta = 0$, positive shifts are used in Figure 6.4. When the slope B_1 in Equation (6.8) shifts a small-to-moderate amount, one can observe that the proposed EWMA_3 method has much better ARL performance.

As the shift sizes increase, we see slightly higher out-of-control ARL values compared with the T^2 chart, again a situation that could be remedied to some extent by the use of Shewhart limits with the EWMA charts or control limits based on the exact variances of the EWMA statistics.

Table 6.5: ARL Comparisons Under Slope Shifts in Model (6.8) From B_1 To $B_1 + \delta\sigma$ (In-control ARL = 200)

	δ								
Chart	-0.2	-0.3	-0.4	-0.5	-0.6	-0.7	-0.8	-0.9	-1.0
EWMA/R	76.7	33.7	15.3	7.5	4.2	2.6	1.8	1.4	1.2
T^2	52.2	21.2	9.6	4.9	2.9	1.9	1.5	1.2	1.1
EWMA_3	13.1	6.6	4.4	3.3	2.7	2.3	2.1	1.9	1.7

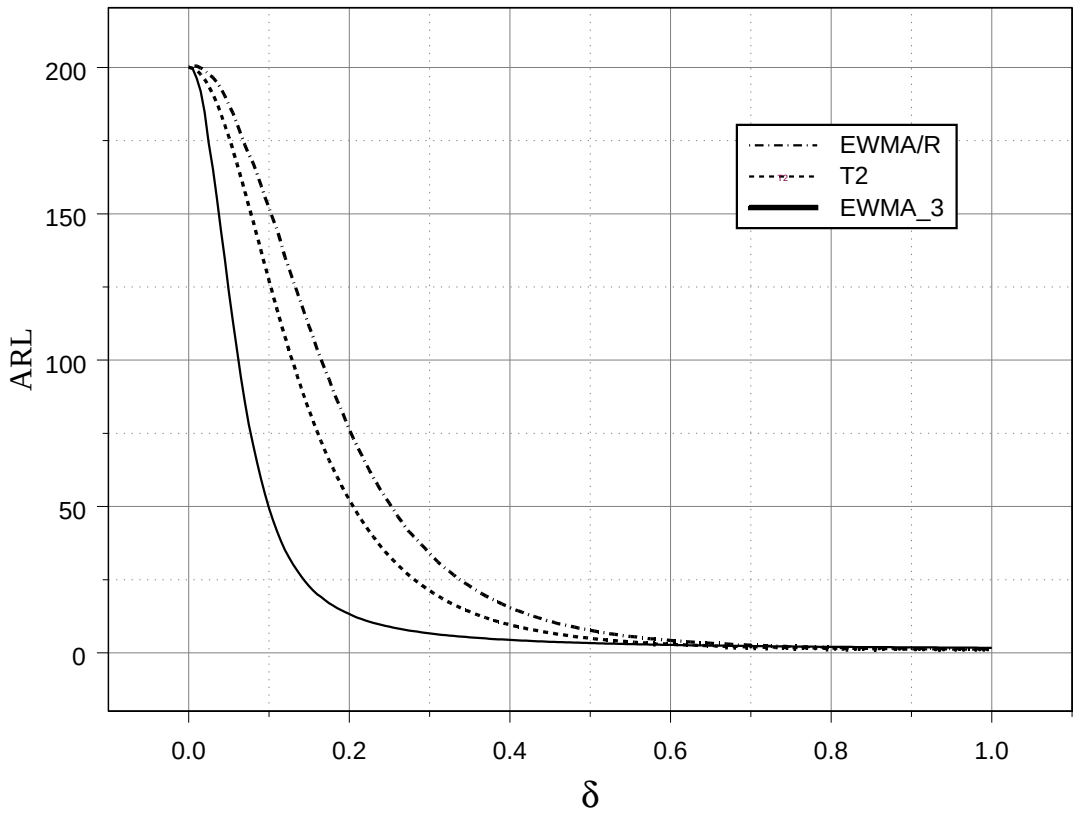

Figure 6.4: ARL Comparisons Under Slope Shifts δ

Table 6.6 gives the ARL values when simultaneous intercept shifts and slope shifts under the model in Equation (6.8) are considered. This proposed method performs uniformly better than the EWMA/R chart combination. The percentage improvement ranges from 5.8 % to 82.2 %. For example, when $\lambda = 0.45$ and $\delta = 0.025$ the ARL of the proposed method is 5.8 % lower than the ARL of the EWMA/R chart, and when $\lambda = 0.05$ and $\delta = 0.225$ the ARL of the proposed method is 82.2 % lower than the ARL of the EWMA/R chart. The percentage improvement increases as both λ decreases and δ increases.

In Table 6.7, the fixed X_i-values of 1, 2, 3, and 4 are considered to study the ARL performance for a different value of S_{xx}. In this case, we have $S_{xx} = 5$ instead of $S_{xx} = 20$ used in Tables 6.1-6.6. Only EWMA/R and EWMA_3 charts are included in the comparisons since the T^2 chart did not demonstrate good overall ARL performance. As the slope shifts δ increase, one can observe that this proposed EWMA_3 method has much better ARL performance than the EWMA/R charts. It is also observed that the ARL performance for the situations considered in Tables 6.1-6.3 and Table 6.5 has almost the same pattern as shown there. The ARL performance for larger values of S_{xx} was also considered, but the overall conclusions are the same.

Kang and Albin (2000) considered shifts in the parameters in model (6.1) corresponding to shifts in B_1 in model (6.8) as "unusual", although their view is unsupported. In general, we find the model in Equation (6.8) to be more useful in some applications than the one in Equation (6.1) since it can be used to focus attention more clearly on changes in the regression line within presumably the most important region of values of the independent variable. The types of parameter shifts of interest, however, will depend on the particular application.

Table 6.6: ARL Comparisons of EWMA/R Charts and EWMA_3 Under Combinations of Intercept and Slope Shifts in Model (6.8) (In-control ARL = 200)

EWMA/R ARL		δ									
EWMA_3 ARL		0.025	0.050	0.075	0.100	0.125	0.150	0.175	0.200	0.225	0.250
λ	0.05	179.1	169.9	156.6	140.8	123.2	105.1	88.8	73.4	60.2	49.6
		157.6	114.7	74.8	48.3	32.2	22.5	16.9	13.2	10.7	8.9
	0.10	139.5	133.6	125.4	115.5	103.5	90.4	78.3	65.7	55.6	46.3
		122.1	94.6	66.4	44.9	30.7	21.9	16.6	13.1	10.6	8.9
	0.15	96.8	94.2	90.3	85.1	78.5	70.9	63.0	55.3	47.7	40.9
		84.6	70.8	54.5	39.6	28.5	20.9	16.1	12.8	10.4	8.8
	0.20	64.8	63.8	62.1	59.7	56.6	52.9	48.5	44.0	39.2	34.6
		57.1	51.1	42.4	33.3	25.4	19.5	15.4	12.4	10.2	8.7
	0.25	44.3	43.8	42.9	41.8	40.3	38.4	36.1	33.6	30.8	28.1
		39.5	36.5	32.3	27.1	22.0	17.8	14.4	11.9	10.0	8.5
	0.30	31.0	30.8	30.5	29.9	29.2	28.3	27.1	25.7	24.2	22.5
		28.2	26.9	24.7	22.0	18.8	15.7	13.2	11.2	9.6	8.3
	0.35	22.9	22.8	22.6	22.2	21.9	21.4	20.7	19.9	19.1	18.0
		20.9	20.2	19.1	17.6	15.8	13.9	12.1	10.5	9.1	8.0
	0.40	17.4	17.3	17.2	17.1	16.8	16.6	16.2	15.8	15.3	14.7
		16.2	15.9	15.3	14.5	13.5	12.1	10.9	9.7	8.6	7.6
	0.45	13.9	13.9	13.9	13.8	13.6	13.5	13.3	13.0	12.6	12.2
		13.1	12.9	12.6	12.1	11.4	10.6	9.8	8.9	8.0	7.3
	0.50	11.5	11.5	11.4	11.3	11.3	11.1	11.0	10.8	10.6	10.3
		10.8	10.8	10.6	10.3	9.9	9.3	8.7	8.1	7.5	6.9

Table 6.7: ARL Comparisons Under Slope Shifts in Model (6.8) From B_1 To $B_1 + \delta\sigma$ (X_i-values are 1, 2, 3, and 4 and In-control ARL = 200)

	δ								
Chart	-0.2	-0.3	-0.4	-0.5	-0.6	-0.7	-0.8	-0.9	-1.0
EWMA/R	149.1	110.1	75.5	50.7	33.3	22.3	15.0	10.5	7.5
EWMA_3	49.1	22.8	13.1	8.9	6.6	5.3	4.4	3.8	3.3

6.5 Phase I Methods

In practical applications, the in-control values of parameters are not known and must be estimated using historical data collected from the process. It is assumed here that k samples of simple linear regression data are available in a set of historical data.

Kang and Albin (2000) recommended substituting estimates of the parameters in their control charts in Phase I. First, they estimated the regression parameters of the underlying model in Equation (6.1) based on the k samples available from historical data. They obtained the reference line, $\hat{Y} = a_0 + a_1 X$, and $\hat{\sigma}^2 = MSE$, where

$$a_0 = \frac{\sum_{j=1}^{k} a_{0j}}{k}, a_1 = \frac{\sum_{j=1}^{k} a_{1j}}{k}, \text{ and } MSE = \frac{\sum_{j=1}^{k} MSE_j}{k}. \tag{6.15}$$

Here MSE_j is the usual unbiased estimator of σ^2 from sample j.

After determining the initial estimates of the regression parameters as given in Equation (6.15), they advised using these estimates to calculate control limits and then applying their control algorithms. If any values fall outside the control limits for which assignable causes can be determined, then those samples are to be removed from the data and the control limits recalculated. Again, one checks to see if the points are within the control limits and, if not, the process of deleting samples and recalculating limits is repeated. The control limits used in Phase I for their multivariate approach and their residual approach are given below.

In the multivariate approach, under the assumption that $\boldsymbol{\mu}$ and $\boldsymbol{\Sigma}$ in Equations (6.3) and (6.4) are unknown, Kang and Albin (2000) evaluated the modified T^2 chart statistic for the j^{th} sample from Equation (6.5) as

$$T_{0j}^2 = \frac{k}{k-1}(\boldsymbol{Z}_j - \boldsymbol{Z})^T \boldsymbol{S}^{-1}(\boldsymbol{Z}_j - \boldsymbol{Z}), \tag{6.16}$$

where $\boldsymbol{Z} = (a_0, a_1)^T$ and $\boldsymbol{S}$ are unbiased estimators of $\boldsymbol{\mu}$ and $\boldsymbol{\Sigma}$, respectively. They obtained the sample variance-covariance matrix $\boldsymbol{S}$ by modifying the elements of Equation (6.4), with σ^2 estimated by MSE from Equation (6.15); that is,

$$\boldsymbol{S} = \begin{pmatrix} S_{11} & S_{12} \\ S_{12} & S_{22} \end{pmatrix},$$

where $S_{11} = MSE(\frac{1}{n} + \frac{\bar{x}^2}{S_{xx}})$, $S_{22} = MSE\frac{1}{S_{xx}}$ and $S_{12} = -MSE\frac{\bar{x}}{S_{xx}}$. Kang and Albin (2000) showed that the distribution of the modified T^2 chart statistic, T_{0j}^2, in Equation (6.16) is related to the F distribution with $(2, (n-2)k)$ degrees of freedom. Thus, they recommend the upper control limit for the chart as UCL $= 2F_{2,(n-2)k,\alpha}$, where $F_{2,(n-2)k,\alpha}$ is the $100(1-\alpha)$ percentile of the F distribution with $(2, (n-2)k)$ degrees of freedom.

For the EWMA and R charts in Phase I, Kang and Albin (2000) modified the lower and upper control limits for the EWMA chart in Equation (6.6) and the R-chart in Equation (6.7) by replacing σ by $\sqrt{MSE}$; that is, for the EWMA chart, we have

$$\text{LCL} = -L\sqrt{MSE}\sqrt{\frac{r}{(2-r)n}},\ \text{UCL} = L\sqrt{MSE}\sqrt{\frac{r}{(2-r)n}}$$

and for the R-chart we have

$$\text{LCL} = \sqrt{MSE}(d_2 - Ld_3),\ \text{UCL} = \sqrt{MSE}(d_2 + Ld_3).$$

One difficulty, however, in applying an EWMA chart in Phase I is that several samples could be contributing to any out-of-control signal. Thus, the rule for deleting samples and recalculating limits is not clearly defined. In general, use of an EWMA chart is not appropriate in Phase I.

Stover and Brill (1998) propose two methods in Phase I. One is a Hotelling's T^2 approach based on vectors containing estimates of the Y-intercept and slope. This method is similar to the T^2 method of Kang and Albin (2000), although the estimator of the variance-covariance matrix is different. Neither pair of authors acknowledge, however, the fact that successive values of their Phase I T^2 statistics are dependent. Thus, the marginal distribution of the control chart statistic cannot be used to determine the overall probability of a Phase I signal.

The other Phase I method proposed by Stover and Brill (1998) is a univariate chart based on the first principal component corresponding to the vectors containing the Y-intercept and slope estimators. The Shewhart-type T^2 chart could be used for the Y-intercept and slope, but also a Shewhart chart is recommended to monitor the error variance. If one codes the X-values, as we recommend, to yield Equation (6.8), then it also seems reasonable to use separate Shewhart-type charts for monitoring the Y-intercept and slope since the estimators of the Y-intercept and slope are independent for each sample. We advise against using the principal component chart proposed by Stover and Brill (1998), however, since it will not be able to detect combinations of shifts in the Y-intercept and the slope in the direction perpendicular to the major axis corresponding to the first principal component.

A principal component analysis as described by Jones and Rice (1992) can be very useful in summarizing and interpreting Phase I profile data with equally spaced X-values. Change-point methods can be very useful in Phase I if one suspects that instability can be modeled adequately by step shifts in the underlying parameter(s). Andrews, Lee, and Ploberger (1996) discussed change-point methods for linear regression models. Mahmoud and Woodall (2003) proposed a Phase I method and recommended a method based on using indicator variables. Williams, Woodall, and Birch (2003) investigated a Hotelling's T^2 chart to monitor the coefficients of the nonlinear regression fits to the successive sets of profile data in Phase I applications. See Woodall, Spitzner, Montgomery, and Gupta (2003) for general discussion of the topic involved in using control charts to monitor process and product quality profiles and review of the SPC literature on the topic.

6.6 Conclusions

The ARL comparisons show that this proposed methods are generally more effective than the methods of Kang and Albin (2000) in Phase II for detecting sustained shifts in either the Y-intercept or slope or increase in the error variance. The proposed methods are considerably more effective in detecting shifts in the slope of the line when the average Y-value does not change. This proposed methods also seem more interpretable. Also recommendations are made for an effective Phase I analysis, although much more work is needed on this type of application. In general, an overall strategy needs to be developed for monitoring process profiles.

Chapter 7

Conclusions and Future Research

In the dissertation, two topics has been considered. The first topic considered is the MEWMA chart with varying sample sizes and/or sequential sampling. The sequential sampling scheme with two possible stages is applied to the MEWMA chart in Chapter 3. The MEWMA chart with unequal sample sizes is considered in Chapter 4. In Chapter 5, the two procedures proposed in Chapter 3 and 4 are combined and applied to the MEWMA chart. The second topic considered is the monitoring of linear profiles presented in Chapter 6, where the quality of a product or process is characterized by a linear relationship between two variables.

The results presented in Chapter 3 show that the SS MEWMA chart gives much quicker detection of the mean shift than the standard MEWMA chart with a fixed sample size. The SS MEWMA chart works well for both of the two different ways of defining the EWMA vectors that were considered. Since no research has been done for applying the sequential sampling scheme to the univariate EWMA chart, further research can be done on the topic of the SS EWMA chart. Also this sequential sampling scheme with two possible stages can be extended to the sequential sampling scheme having more than two possible stages.

The results in Chapter 4 show that when the SSATS value averaged over randomly

generated shift directions is considered, the UG MEWMA chart works well for a small to moderate correlation between variables. Although the UG MEWMA chart does not show overall good performance for the case where variables are highly correlated, if a shift which is likely to be in directions where performance is good is considered, then the UG MEWMA chart can be used effectively in practice. In Chapter 4 the cost ratio of 10 is assumed, where the measurement cost of one variable is 10 unit times larger than the other variable. However, more work is needed when this cost ratio varies. For example, this procedure can be extended to the situation where all variables have the equal measurement costs but one variable is more important than the other variables.

In Chapter 5 it is shown that the SSATS performance of the UGSS MEWMA chart is moderately better than that of the standard MEWMA chart unless variables are highly correlated. As in the UG MEWMA chart, the UGSS chart can be applied effectively to the situation where a shift which is likely to be in directions where performance is good is considered. Also the effects of the choice of the cost ratio need to be further investigated. As an application, when the UGSS MEWMA chart is applied to the two-measurement system problem, the UGSS MEWMA chart performs better than the method previously proposed by Steiner (2000).

In Chapter 6 it has been shown that the ARL performance of the proposed methods is more effective than the previously proposed methods by Kang and Albin (2000) in Phase II. The proposed methods need to be extended to more complicated relationships between the independent and dependent variables. The simple linear regression model considered in the dissertation, for example, can be extended to profiles that can be represented by a polynomial or multiple linear regression models, as considered by Jensen, Hui, and Ghare (1984).

Bibliography

[1] Acosta-Mejia, C. A., Pignatiello, J. J., Jr., and Rao, B. V. (1999). "A Comparison of Control Charting Procedures for Monitoring Process Dispersion". *IIE Transactions* **31**, pp. 569-579.

[2] Andrews, D. W., Lee, I., and Ploberger, W. (1996). "Optimal Changepoint Tests for Normal Linear Regression". *Journal of Econometrics* **70**, pp. 9-38.

[3] Annadi, H. P., Keats, J. B., Runger, G. C., and Montgomery, D. C. (1995). "An Adaptive Sample Size CUSUM Control Chart". *International Journal of Production Research* **33**, pp. 1605-1616.

[4] Aparisi, F. (1996). "Hotelling's T^2 Control Chart with Adaptive Sample Sizes". *International Journal of Production Research* **34**, pp. 2853-2862.

[5] Aparisi, F., and Haro, C. L. (2001). "Hotelling's T^2 Control Chart with Variable Sampling Intervals". *International Journal of Production Research* **39**, pp. 3127-3140.

[6] Arnold, J. C., and Reynolds, M. R., Jr. (2001). "CUSUM Control Charts with Variable Sample Sizes and Sampling Intervals". *Journal of Quality Technology* **33**, pp. 68-81.

[7] Baxley, R. V., Jr. (1995). "An Application of Variable Sampling Interval Control Charts". *Journal of Quality Technology* **27**, pp. 275-282.

[8] Bodden, K. M., and Rigdon, S. E. (1999). "A Program for Approximating the In-Control ARL for the MEWMA Chart". *Journal of Quality Technology* **31**, pp. 120-123.

[9] Brill, R. V. (2001). "A Case Study for Control Charting a Product Quality Measure That is a Continuous Function Over Time". Presented at the 45th Annual Fall Technical Conference, Toronto, Ontario.

[10] Brook, D., and Evans, D. A. (1972). "An Approach to the Probability Distribution of CUSUM Run Length". *Biometrika* **59**, pp. 539-549.

[11] Carot, V., Jabaloyes, J. M., and Carot, T. (2002). "Combined Double Sampling and Variable Sampling Interval $\bar{X}$ Chart". *International Journal of Production Research* **40**, pp. 2175-2186.

[12] Champ, C. W., and Woodall, W. H. (1987). "Exact Results for Shewhart Control Charts with Supplementary Runs Rules". *Technometrics* **29**, pp. 393-399.

[13] Costa, A. F. (1994). "$\bar{X}$ Charts with Variable Sample Size". *Journal of Quality Technology* **26**, pp. 155-163.

[14] Costa, A. F. B. (1997). "$\bar{X}$ Charts with Variable Sample Size and Sampling Intervals". *Journal of Quality Technology* **29**, pp. 197-204.

[15] Croasdale, P. (1974). "Control Charts for a Double-Sampling Scheme Based on Average Production Run Lengths". *International Journal of Production Research* **12**, pp. 585-592.

[16] Crosier, R. B. (1988). "Multivariate Generalizations of Cumulative Sum Quality Control Schemes". *Technometrics* **30**, pp. 291-303.

[17] Crowder, S. V. (1987). "A Simple Method for Studying Run-Length Distributions of Exponentially Weighted Moving Average Charts". *Technometrics* **29**, pp. 401-407.

[18] Crowder, S. V., and Hamilton, M. D. (1992). "An EWMA for Monitoring a Process Standard Deviation". *Journal of Quality Technology* **24**, pp. 12-21.

[19] Daudin, J. J. (1992). "Double Sampling $\bar{X}$ Charts". *Journal of Quality Technology* **24**, pp. 78-87.

[20] Hauck, D. J., Runger, G. C., and Montgomery, D. C. (1999). "Multivariate Statistical Process Monitoring and Diagnosis with Grouped Regression-Adjusted Variables". *Communications in Statistics-Simulation and Computation* **28**, pp. 309-328.

[21] Hawkins, D. M. (1991). "Multivariate Quality Control Based on Regression-Adjusted Variables". *Technometrics* **33**, pp. 61-75.

[22] Hawkins, D. M. (1992). "Evaluation of Average Run Lengths of Cumulative Sum Charts for an Arbitrary Data Distribution". *Communications in Statistics-Simulation and Computation* **21**, pp. 1001-1020.

[23] Hawkins, D. M. (1993). "Regression Adjustment for Variables in Multivariate Quality Control". *Journal of Quality Technology* **25**, pp. 170-182.

[24] Hawkins, D. M., and Olwell, D. H. (1998). *Cumulative Sum Charts and Charting for Quality Improvement*. Springer, New York, NY.

[25] He, D. (2002). "Development of Multivariate Double Sampling $\bar{X}$ Control Charts". Presented at the INFORMS 2002 Annual Meeting, San Jose, CA.

[26] He, D., Grigoryan, A., and Sigh, M. (2002). "Design of Double- and Triple-Sampling $\bar{X}$ Control Charts Using Genetic Algorithms". *International Journal of Production Research* **40**, pp. 1387-1404.

[27] Healy, J. D. (1987). "A Note on Multivariate CUSUM Procedures". *Technometrics* **29**, pp. 409-412.

[28] Hotelling, H. (1947). "Multivariate Quality Control-Illustrated by the Air Testing of Sample Bombsights" in *Techniques of Statistical Analysis* edited by C. Eisenhart, M. W. Hastay, and W. A. Wallis. McGraw-Hill, New York, NY.

[29] Irianto, D., and Shinozaki, N. (1998). "An Optimal Double Sampling $\bar{X}$ Control Chart". *International Journal of Industrial Engineering-Theory Applications and Practice* **5**, pp. 226-234.

[30] Jensen, D. R., Hui, Y. V., and Ghare, P. M. (1984). "Monitoring an Input-Output Model for Production. I. The Control Charts". *Management Science* **30**, pp. 1197-1206.

[31] Jin, J. H., and Shi, J. J. (2001). "Automatic Feature Extraction of Waveform Signals for In-Process Diagnostic Performance Improvement". *Journal of Intelligent Manufacturing* **12**, pp. 257-268.

[32] Johnson, M. E. (1987). *Multivariate Statistical Simulation*. John Wiley & Sons, New York, NY.

[33] Jones, M. C., and Rice, J. A. (1992). "Displaying the Important Features of Large Collections of Similar Curves". *American Statistician* **46**, pp. 140-145.

[34] Kang, L., and Albin, S. L. (2000). "On-Line Monitoring When the Process Yields a Linear Profile". *Journal of Quality Technology* **32**, pp. 418-426.

[35] Lawless, J. F. (1980). *Statistical Models and Methods for Lifetime Data*. John Wiley & Sons. New York, NY.

[36] Lawless, J. F., MacKay, R. J., and Robinson, J. A. (1999). "Analysis of Variation Transmission in Manufacturing Processes-Part I". *Journal of Quality Technology* **31**, pp. 131-142.

[37] Lowry, C. A., Champ, C. W., and Woodall, W. H. (1995). "The Performance of Control Charts for Monitoring Process Dispersion". *Communications in Statistics-Simulation and Computation* **24**, pp. 409-437.

[38] Lowry, C. A., Woodall, W. H., Champ, C. W., and Rigdon, S. E. (1992). "A Multivariate Exponentially Weighted Moving Average Control Chart". *Technometrics* **34**, pp. 46-53.

[39] Lucas, J. M., and Saccucci, M. S. (1990). "Exponentially Weighted Moving Average Control Schemes: Properties and Enhancements". *Technometrics* **32**, pp. 1-12.

[40] Mahmoud, M., and Woodall, W. H. (2003). "Phase I Monitoring of Linear Profiles with Calibration Applications". Submitted to Technometrics.

[41] Mandel, B. J. (1969). "The Regression Control Chart". *Journal of Quality Technology* **1**, pp. 1-9.

[42] Mestek, O., Pavlik, J., and Suchanek, M. (1994). "Multivariate Control Charts: Control Charts for Calibration Curves". *Fresenius' Journal of Analytical Chemistry* **350**, pp. 344-351.

[43] Miller, A. (2002). "Analysis of Parameter Design Experiments for Signal-Response Systems". *Journal of Quality Technology* **34**, pp. 139-151.

[44] Molnau, W. E., Runger, G. C., Montgomery, D. C., Skinner, K. R., Loredo, E. N., and Prabhu, S. S. (2001). "A Program for ARL Calculation for Multivariate EWMA Charts". *Journal of Quality Technology* **33**, pp. 515-521.

[45] Montgomery, D. C. (2001). *Introduction to Statistical Quality Control*. 4th Edition, John Wiley & Sons, New York, NY.

[46] Myers, R. H. (1990). *Classical and Modern Regression with Applications*. 2nd Edition, PWS-Kent Publishing Company, Boston, MA.

[47] Nair, V. N., Taam, W., and Ye, K. Q. (2002). "Analysis of Functional Responses from Robust Design Studies". *Journal of Quality Technology* **34**, pp. 355-370.

[48] Page, E. S. (1954). "Continuous Inspection Schemes". *Biometrics* **41**, pp. 100-114.

[49] Park, C., and Reynolds, M. R., Jr. (1999). "Economic Design of a Variable Sampling Rate $\bar{X}$ Chart". *Journal of Quality Technology* **31**, pp. 427-443.

[50] Pignatiello, J. J., Jr., and Runger, G. C. (1990). "Comparisons of Multivariate CUSUM Charts". *Journal of Quality Technology* **22**, pp. 173-186.

[51] Prabhu, S. S., Montgomery, D. C., and Runger, G. C. (1994). "A Combined Adaptive Sample Size and Sampling Interval $\bar{X}$ Control Scheme". *Journal of Quality Technology* **26**, pp. 164-176.

[52] Prabhu, S. S., Runger, G. C., and Keats, J. B. (1993). "An Adaptive Sample Size $\bar{X}$ Control Scheme". *International Journal of Production Research* **31**, pp. 2895-2909.

[53] Reynolds, M. R., Jr. (1995). "Evaluating Properties of Variable Sampling Interval Control Charts". *Sequential Analysis* **14**, pp. 59-97.

[54] Reynolds, M. R., Jr. (1996a). "Shewhart and EWMA Variable Sampling Interval Control Charts with Sampling at Fixed Times". *Journal of Quality Technology* **28**, pp. 199-212.

[55] Reynolds, M. R., Jr. (1996b). "Variable Sampling Interval Control Charts with Sampling at Fixed Times". *IIE Transactions* **28**, pp. 497-510.

[56] Reynolds, M. R., Jr., Amin, R. W., and Arnold, J. C. (1990). "CUSUM Charts with Variable Sampling Intervals". *Technometrics* **32**, pp. 371-384.

[57] Reynolds, M. R., Jr., Amin, R. W., Arnold, J. C., and Nachlas, J. A. (1988). "$\bar{X}$ Charts with Variable Sampling Intervals". *Technometrics* **30**, pp. 181-192.

[58] Reynolds, M. R., Jr., and Arnold, J. C. (2001). "EWMA Control Charts with Variable Sample Sizes and Variable Sampling Intervals". *IIE Transactions* **33**, pp. 511-530.

[59] Reynolds, M. R., Jr., and Stoumbos, Z. G. (1998). "The SPRT Chart for Monitoring a Proportion". *IIE Transactions* **30**, pp. 545-561.

[60] Reynolds, M. R., Jr., and Stoumbos, Z. G. (2001). "Monitoring the Process Mean and Variance Using Individual Observations and Variable Sampling Intervals". *Journal of Quality Technology* **33**, pp. 181-205.

[61] Reynolds, M. R., Jr., and Stoumbos, Z. G. (2003). "Control Charts and the Efficient Allocation of Sampling Resources". To appear in *Technometrics*.

[62] Rigdon, S. E. (1995a). "An Integral Equation for the In-Control Average Run Length of a Multivariate Exponentially Weighted Moving Average Control Chart". *Journal of Statistical Computation and Simulation* **52**, pp. 351-365.

[63] Rigdon, S. E. (1995b). "A Double-Integral Equation for the Average Run Length of a Multivariate Exponentially Weighted Moving Average Control Chart". *Statistics and Probability Letters* **24**, pp. 365-373.

[64] Roberts, S. W. (1959). "Control Chart Tests Based on Geometric Moving Averages". *Technometrics* **1**, pp. 239-250.

[65] Runger, G. C., and Pignatiello, J. J., Jr. (1991). "Adaptive Sampling for Process Control". *Journal of Quality Technology* **23**, pp. 135-155.

[66] Runger, G. C., and Prabhu, S. S. (1996). "A Markov Chain Model for the Multivariate Exponentially Weighted Moving Averages Contol Chart". *Journal of the American Statistical Association* **91**, pp. 1701-1706.

[67] Ryan, T. P. (1997). *Modern Regression Methods*. John Wiley & Sons, New York, NY.

[68] Ryan, T. P. (2000). *Statistical Methods for Quality Improvement*. 2nd Edition, John Wiley & Sons, New York, NY.

[69] Saccucci, M. S., Amin, R. W., and Lucas, J. M. (1992). "Exponentially Weighted Moving Average Control Schemes with Variable Sampling Intervals". *Communications in Statistics-Simulation and Computation* **21**, pp. 627-657.

[70] Shewhart, W. A. (1931). *The Economic Control of Quality Manufactured Products*. Van Nostrand, New York, NY.

[71] Steiner, S. H. (1999). "EWMA Control Charts with Time-Varying Control Limits and Fast Initial Response". *Journal of Quality Technology* **31**, pp. 75-86.

[72] Stoumbos, Z. G., and Reynolds, M. R., Jr. (1996). "Control Charts Applying a General Sequential Test at Each Sampling Point". *Sequential Analysis* **15**, pp. 159-183.

[73] Stoumbos, Z. G., and Reynolds, M. R., Jr. (1997). "Control Charts Applying a Sequential Test at Fixed Sampling Intervals". *Journal of Quality Technology* **29**, pp. 21-40.

[74] Stoumbos, Z. G., and Reynolds, M. R., Jr. (2001). "The SPRT Control Chart for the Process Mean with Samples Starting at Fixed Times". *Nonlinear Analysis, Series B: Real-World Applications* **2**, pp. 1-34.

[75] Stoumbos, Z. G., and Sullivan, J. H. (2002). "Robustness to Non-normality of the Multivariate EWMA Control Chart". *Journal of Quality Technology* **34**, pp. 260-276.

[76] Stover, F. S., and Brill, R. V. (1998). "Statistical Quality Control Applied to Ion Chromatography Calibrations". *Journal of Chromatography* A **804**, pp. 37-43.

[77] Sullivan, J. H., and Woodall, W. H. (1996). "A Comparison of Multivariate Control Charts for Individual Observations". *Journal of Quality Technology* **28**, pp. 398-408.

[78] Sullivan, J. H., and Woodall, W. H. (1998). "Adapting Control Charts for the Preliminary Analysis of Multivariate Observations". *Communications In Statistics-Simulation and Computation* **27**, pp. 953-979.

[79] Tagaras, G. (1998). "A Survey of Recent Developments in the Design of Adaptive Control Charts". *Journal of Quality Technology* **30**, pp. 212-231.

[80] van Dobben de Bruyn, C. S. (1968). *Cumulative Sum Test: Theory and Practice, Griffin's Statistical Monographs & Courses*. No. 24, Hafner, New York, NY.

[81] Wade, M. R., and Woodall, W. H. (1993). "A Review and Analysis of Cause-Selecting Control Charts". *Journal of Quality Technology* **25**, pp. 161-169.

[82] Wald, A. (1947). *Sequential Analysis*, John Wiley, New York, NY.

[83] Walker, E., and Wright, S. P. (2002). "Comparing Curves Using Additive Models". *Journal of Quality Technology* **34**, pp. 118-129.

[84] Williams, J. D., Woodall, W. H., and Birch, J. B. (2003). "Phase I Monitoring of Nonlinear Profiles", Presented at the 2003 Quality and Productivity Research Conference, Yorktown Heights, New York.

[85] Woodall, W. H. (1984). "On the Markov Chain Approach to the Two-Sided CUSUM Procedure". *Technometrics* **26**, pp. 41-46.

[86] Woodall, W. H. (2000). "Controversies and Contradictions in Statistical Process Control". *Journal of Quality Technology* **32**, pp. 341-350.

[87] Woodall, W. H., and Ncube, M. M. (1985). "Multivariate CUSUM Quality Control Procedures". *Technometrics* **27**, pp. 285-292.

[88] Woodall, W. H., Spitzner, D. J., Montgomery, D. C., and Gupta, S. (2003). "Using Control Charts to Monitor Process and Product Quality Profiles". Submitted for Publication.

[89] Zhang, G. X. (1992). *Cause-Selecting Control Chart and Diagnosis, Theory and Practice*. Aarhus School of Business, Department of Total Quality Management, Aarhus, Denmark.

[90] Zimmer, L. S., Montgomery, D. C., and Runger, G. C. (1998). "Evaluation of a Three-State Adaptive Sample Size $\bar{X}$ Control Chart". *International Journal of Production Research* **36**, pp. 733-743.

Vita

Keunpyo Kim was born on November 22, 1971 in Seoul, Korea. In 1990, he graduated from Seoul High School. He attended Chung-Ang University, where he received a Bachelor of Science degree in Mathematics in 1996 and a Master of Economics degree in Statistics in 1998. He holds a Master of Science degree in Statistics from Virginia Polytechnic Institute and State University (1999).